Enhancement of the PFD to Improve Bank Angle Representation

Evaluating the effect of static monocular depth cues on attitude indicator interpretation using misleading motion cues

Chloë Van Droogenbroeck

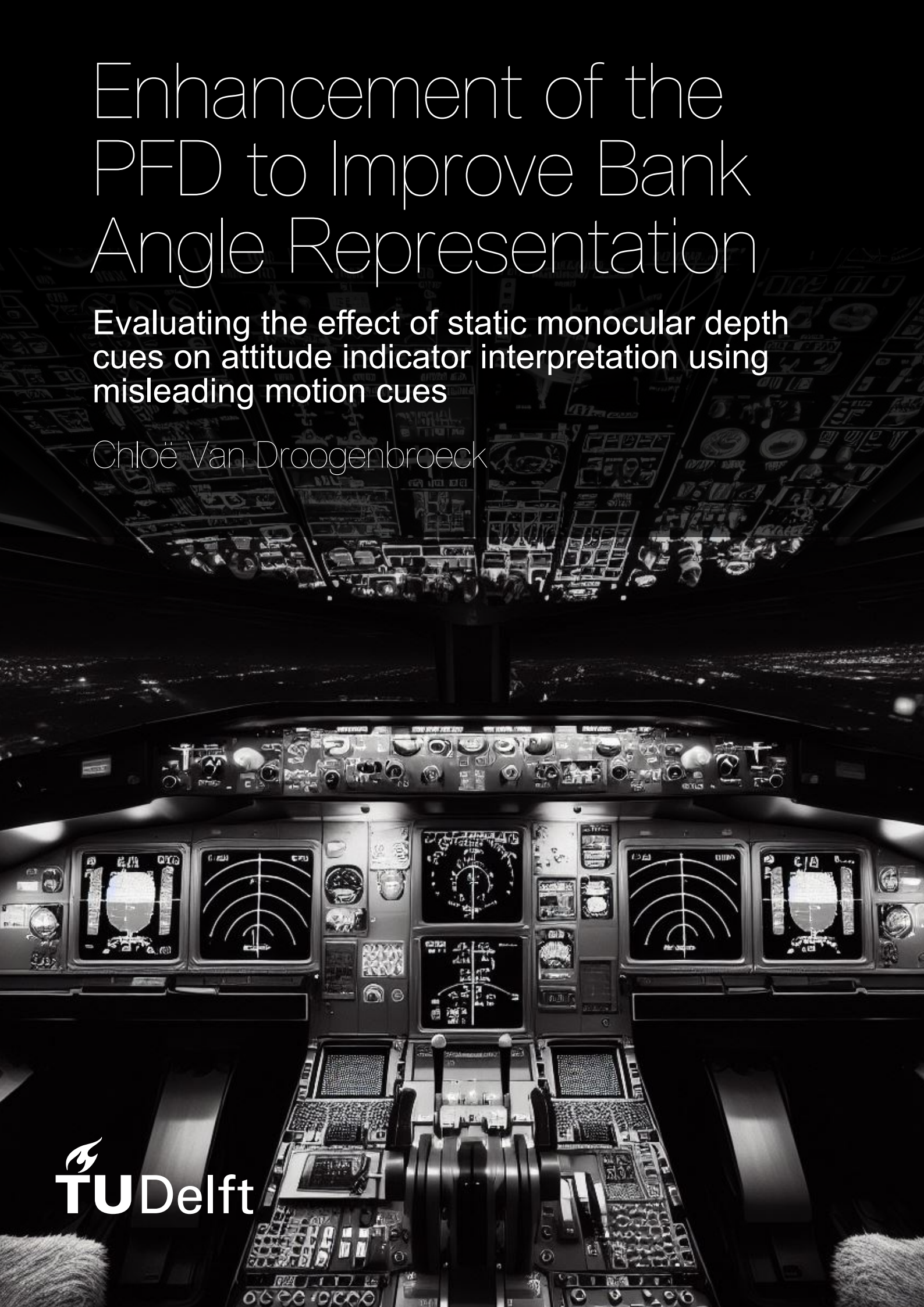

TU Delft

Enhancement of the PFD to Improve Bank Angle Representation

Evaluating the effect of static monocular depth cues on attitude indicator interpretation using misleading motion cues

Thesis report

by

Chloë Van Droogenbroeck

to obtain the degree of Master of Science
at the Delft University of Technology
to be defended publicly on February 13, 2024

Thesis committee:

Supervisors:	Prof. dr. ir. M. Mulder
	Dr. H. M. Landman
	Ir. O. Stroosma
	Dr. ir. M. M. van Paassen
Place:	Faculty of Aerospace Engineering, Delft
Project Duration:	February, 2023 - February, 2024
Student number:	4649591

An electronic version of this thesis is available at `http://repository.tudelft.nl/`.

Faculty of Aerospace Engineering · Delft University of Technology

Contents

List of Figures

List of Tables

Part I

Scientific Article

Improving Bank Angle Representation on the Primary Flight Display Using Static Monocular Depth Cues

C. Van Droogenbroeck
Faculty of Aerospace Engineering
Delft University of Technology
Delft, the Netherlands

Supervised by: H.M. Landman*, O. Stroosma†,
M.M. van Paassen†, M. Mulder†
**TNO Soesterberg*
†*Delft University of Technology*
* Soesterberg, the Netherlands
† Delft, the Netherlands

***Abstract*—Roll reversal errors, where the pilot tries to steer the aircraft back to wings-level but unintentionally *increases* the bank angle instead, have contributed to several accidents. Previous studies have shown that these errors can be caused by misinterpreting the attitude indicator (AI), with the figure-ground relations cited as contributing to this misinterpretation. A modified AI was developed, which uses several static monocular depth cues (color gradient, linear perspective lines, and shadow-light relationship) to strengthen the figure-ground relationship. The modified version of the AI was compared to a baseline AI in a two-part flight simulator experiment where pilot reaction time and error rate, severity, and duration were measured. The first part induced the leans illusion making use of physiological adaptation to roll angle, distraction, and surprise. The second part simulated the leans illusion by simply rolling the simulator to the left or right. A group of 25 experienced commercial airline pilots performed a roll-to-level task in a moving-base simulator, which also provided spatially disorienting motion cues, using both the baseline and modified versions of the AI. While the modified display had a lower error rate in the motion-opposite scenario when using the novel method (4.91% compared to 6.07%), no significant difference was found between the error rate of the two displays. The only significant difference was found in the reaction time, where the modified AI caused an increase in reaction time. The error rates and reaction times of the first part of the experiment did not match previous research. The novel disorientation method seemed to work best in a surprise scenario. While no significant differences were found between the modified AI and the baseline AI, it is still recommended to continue testing the modified AI with a new experiment setup, especially analyzing its effect in more extreme attitudes.**

I. Introduction

Loss of Control In-Flight (LOC-I) has for a long time been identified as the number one fatal accident category in commercial aviation [1]. During LOC-I, the flight crew cannot maintain control over the aircraft's flight path, which results in an unrecoverable situation.

One of the main causes of LOC-I is spatial disorientation (SD) [2], an erroneous sense of the aircraft's attitude and motion. SD can lead to an incorrect interpretation of the attitude indicator (AI), the primary source for self-orientation when the natural horizon is absent. Misinterpretation of the AI can lead to pilots incorrectly responding when trying to level the aircraft. This phenomenon is known as a control reversal error, the most common of which is a roll reversal error (RRE), where the pilot makes a roll input towards the opposite side than intended.

Confusion about the bank angle leading to RREs was implied in several recent accidents. One example is Kenya Airways flight KQA507 [3]. A combination of a slow roll to the right, inadequate instrument scanning, and a lack of external visual references caused pilots to be surprised when the aural bank angle warning sounded. The pilot flying initially rolled the aircraft even more to the right, indicating that he misinterpreted the AI. Multiple control inputs to the left and right were given but to no avail. The aircraft crashed shortly after take-off as a result of LOC-I, leaving no survivors.

This example shows that the correct interpretation of the AI is crucial for safe flying. It has been argued that the moving horizon (MH) AI is ambiguous and can cause misinterpretation [4], [5]. The MH AI adheres to the "principle of pictorial realism" [6], [7]. It is designed to mimic the outside view: the horizon line moves and the aircraft symbol remains fixed. In experiments that were intended to evaluate the AI when the previous bank angle was unknown and without the use of motion, non-pilots had an RRE rate of 15-20% [6], [8] and pilots showed a rate of 3.9-8.7% [6], [9]. In-flight, non-pilots had an RRE rate of 21.9% [10] whereas pilots had a rate of 1.5-3.1% [9], [11]. While this last number might seem low, it is still very high from a safety perspective. These outcomes indicate that there is indeed ambiguity in the AI display, even for pilots.

The first possible issue with the AI display has to do with the lack of display-control motion compatibility, i.e., it does not adhere to the "principle of the moving part". The motion direction of the moving parts of the display does not correspond with the inputs the pilot gives with the control column or side stick. That is, a rotation of the display to the right is a result of the movement of the control column or side stick to the left. This is the opposite of what one would expect [6]. The second possible issue is the figure-ground relationship. Figure-ground organization, which is part

of the Gestalt principles, is the process of how the human brain quickly distinguishes between the foreground (figure) and background (ground) of an image [6], [12], [13]. The horizon symbol does not optimally satisfy the characteristics of a background, due to it being the moving part and the display lacking depth, which makes it harder to perceive the horizon as something *behind* the aircraft symbol. Because of this, the pilot may attempt to move the horizon symbol instead of the fixed aircraft symbol. This error is known as horizon-control reversal [14].

Numerous attempts have been made to solve the issue of RREs caused by the ambiguity of the AI. Solving the display-control motion compatibility and the moving element issues would require changing the dynamics of the display which could induce errors due to pilots having to be retrained. Some attempts have been made at solving the "background characteristics" problem. An extended horizon, where the horizon symbol is extended behind the speed and altitude tapes has been applied in the Boeing 787 [15]. Increasing the display size was also attempted with mixed results [16], [17]. Finally, tests with a stereoscopic multi-layer display showed that this was ineffective when it came to self-orientation [18]. Other means of adapting the AI display to enhance the figure-ground relationship will thus have to be found. This study proposes the use of static monocular depth cues to achieve this. If successful, this could reduce the occurrence of RREs and as a result decrease the number of accidents caused by LOC-I. The results of an experiment that consisted of two parts will be discussed. The main objective of the experiment is to compare the two displays in their effectiveness in reducing RREs.

To increase the number of RREs made and to simulate spatial disorientation situations, an expectation of the bank angle will be instilled by using inertial motion cues. This will be done in two ways: The first part of the experiment will provide motion as described in Van den Hoed et. al [19], which simulates the lean illusion using a method that requires relatively more time, but which is more representative of actual leans cues. The second part of the experiment will be a novel way of simulating the leans, which is more time-effective but also less ecologically accurate. Both parts will feature two motion conditions: The motion-matching condition where the simulator's motion matches what is shown on the AI and the motion-opposite condition where the simulator's motion will go in the opposite direction of what is shown on the AI. A secondary objective of the experiment is to test the effectiveness of the novel method at inducing disorientation.

II. Background

Recent studies have shown that an incorrect expectation of the bank angle increases the likelihood of making an RRE for both pilots and non-pilots [19]–[21]. Pilots made 11.2 times more RREs when the shown bank angle was in the opposite direction of what they expected and 2.5 times more when the aircraft was shown as level but was actually in an ongoing turn. This indicates that RREs were in many cases caused by expectation-induced misinterpretation of the AI bank angle. However, experiments evaluating the AI did not take into consideration the effect an expectation of the bank angle could have on the occurrence of RREs and even prevented participants from building up an expectation [6], [10], [11], [22].

A. Vestibular Perception: the Leans

An incorrect expectation of a bank angle is the most common form of spatial disorientation, called "the leans" [23], [24]. This is an illusion that can occur due to the semicircular canals of the vestibular system, which is located in the inner ear, being unable to sense low roll accelerations or sustained roll motions. The human perception thresholds are reported to be around 0.0349 rad/s^2 for roll accelerations and 0.002 rad/s for angular velocity [25], [26]. However, it is hard to put an exact number on these thresholds as they can be raised due to a low state of mental arousal, fatigue, or just individual variation [24]. The threshold can also vary across the different degrees of freedom and with frequency. A subthreshold roll motion may cause the pilot to assume that the aircraft is still level, while it is actually banked. When this unnoticed bank angle has developed, a superthreshold roll motion back to level may cause the pilot to incorrectly assume the aircraft is banking to the *opposite* side, such as in Figure 1. Illusions like the leans often occur when the outside visibility is low, forcing pilots to rely solely on their instruments to determine the aircraft's attitude. While this illusion is unwanted in flight, it can be exploited in simulators. By tilting the simulator at sub- and superthreshold rates, an expectation of the bank angle can be instilled. If this expectation does not match the bank angle shown on the AI, the pilot can become confused and more prone to making an error. While pilots are taught to ignore vestibular cues and only rely on the AI, even experienced pilots are not immune to their expectations influencing their judgment of their attitude [20], [21].

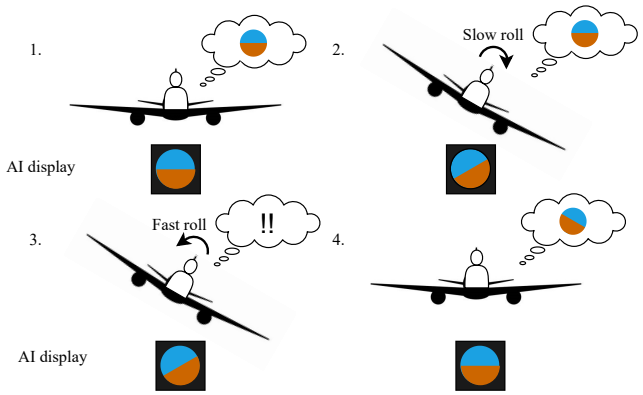

Figure 1: Illustration of the leans illusion showing the pilot's internal model compared to the AI display when in a sub-threshold (slow) roll and superthreshold (fast) roll

B. Visual Perception

The AI is the primary source of self-orientation when flying. It is crucial that pilots correctly interpret the AI as misinterpretation can have fatal consequences. Understanding human visual perception can significantly improve the quality of the information being shown on displays. To improve the AI to decrease RREs, it is thus vital to look into how humans perceive their surroundings. It should be noted that humans create a "complete picture" of their surroundings based on the stimulus world which they process through their senses. This is known as "bottom-up" processing. They also make this picture based on their knowledge, experiences, and desires, which is "top-down" processing. The following three aspects will form the base of the modifications made to the AI display in the current study, aiming to improve the figure-ground relation:

1) *Depth perception*: Depth perception is the ability to perceive the world in three dimensions and have a sense of the distance of an object. Depth information cues need to be present for depth perception to be possible. For this research, the focus will be on static monocular depth cues, a subcategory of depth cues that can be perceived with one eye only and that stay still in the field of view. Static monocular depth cues are often referred to as "pictorial depth cues", such as [24], [27], [28]:
   - Size constancy: The size of objects that are known and object sizes compared to each other. The smaller an object, the further away it will be perceived.
   - Shape constancy: The shape of an object compared to the known shape of that object.
   - Interposition: An object overlapping another object is perceived as being closer by.
   - Texture gradient: The apparent loss of detail with increased distance.
   - Linear perspective: The distance between parallel lines decreases the further away the lines are.
   - Light and shadow relation: This comes from the tendency to perceive the light source to be above an object and the association that more deeply shaded parts of an object are further away from the light source.
   - Height in plane: The more upward an object is placed in a frame, the further away it is perceived (often combined with size constancy).
   - Aerial perspective: Surfaces in the foreground appear brighter and have more saturated colors whereas distant objects appear less bright and less saturated. This is caused by the scattering of light air molecules and by particles in the air, also known as atmospheric haze.

   These cues are often combined to strengthen the idea of depth.
2) *Pre-attentive processing*: The brain differentiates between stimuli, determining which are "interesting" and which are not. The interesting stimuli have so-called "pre-attentive properties" which make them stand out and cause them to be processed before others. Typically, a task that can be performed in less than 200-250 milliseconds is considered pre-attentive [29].
3) *Figure-ground organization*: Figure-ground organization is a major process in perceptual organization, where once the brain is done with the pre-attentive processing of stimuli, it has to decide how to group these stimuli and form a pattern. Much of what is known about perceptual organization comes from Gestalt psychology. In the early days of Gestalt psychology, three key observations stood at the base of the theory [12]:
   - The perceptual experience is organized in a particular way. It consists of objects and a background.
   - Organization depends on a particular grouping, seemingly going hand in hand with segregation from the rest.
   - Perceptual organization appears definite and lawful, not arbitrary and the lawfulness does not result from an act of will.

   The early founders of Gestalt psychology investigated the underlying principles of grouping and segmentation, which have now become known as "Gestalt principles". Figure-ground organization is the process of how the brain distinguishes between a figure and a background, or "ground" for short. Which feature is the figure, and which is the ground can sometimes switch, but it can never be both at the same time. Two main mechanisms work in the segregation of figure and ground [30]–[32]: boundary detection, which is the enhancement of the borders of the figure, and region growing, which groups regions of the image with similar features together. The Gestalt principles will be taken into account when modifying the AI.

III. Improving Bank Angle Representation

Figure 2 shows the baseline AI. The modified AI can be seen in Figure 3 and will from now on be called the Pictorial Depth Cues Modified (PDCM) AI. The following modifications were made:

- Linear perspective lines: Straight lines on the ground that coincide at a point in the distance in the center of the horizon. This is based on the principle that the distance between parallel lines decreases the farther the lines are.
- Color gradient: The color of both the "sky" and "ground" parts of the display gets less saturated the closer to the horizon line. This is based on the principle of aerial perspective. The lightest color in this color gradient is made the same color as the linear perspective lines to create an apparent loss of detail with distance.
- Shadow image below the aircraft symbol: A shadow below the aircraft symbol gives the illusion that the aircraft symbol "stands out" from the background. This creates the illusion that the aircraft symbol is closer by, making the display less "flat" and causing the symbol to be pre-attentively processed.

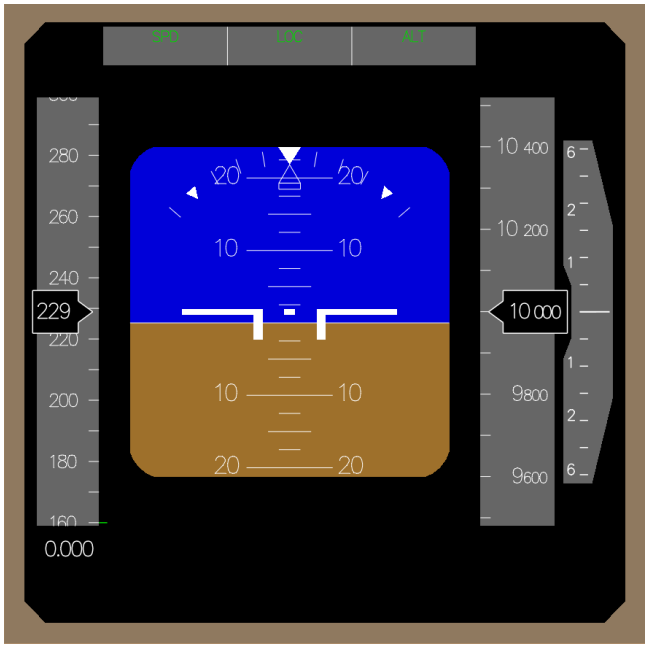

Figure 2: PFD with baseline AI

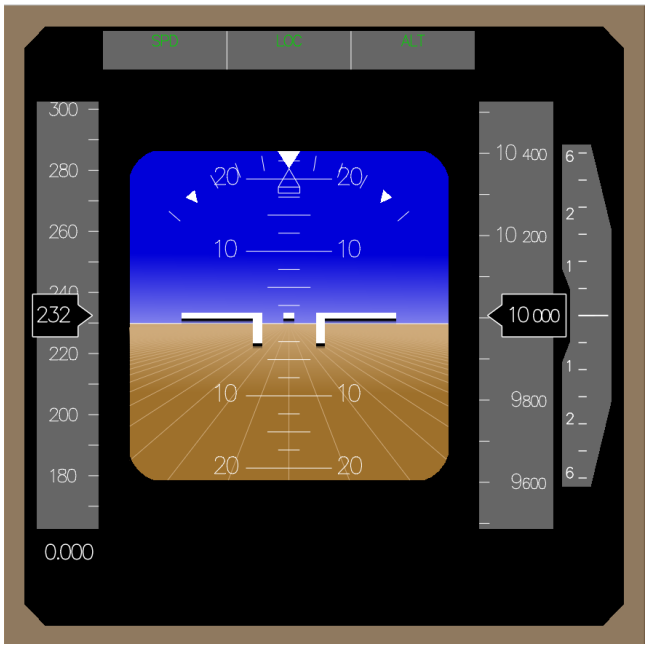

Figure 3: PFD with PDCM AI

These depth cues strengthen each other when combined and make the display adhere to several Gestalt principles:

- Principle of "good continuation" which states "*Grouping depends on the relative configuration or arrangement of elements, specifically elements forming continuous lines or curves.*" [12]: The color gradient and the linear perspective lines both continue behind the aircraft symbol.
- Principle of "common fate" which states "*Elements that undergo a particular change together are grouped together.*" [12]: The color gradient presents a continuous change of luminance.
- Principle of "uniform connectedness" which states "*The visual system initially subdivides an image into a set of mutually exclusive connected regions that have uniform (or smoothly changing) properties such as luminance, color, texture, motion, and depth.*" [12]: The color of the sky and Earth smoothly changes whereas the aircraft symbol remains the same color.

These grouping principles strengthen the figure-ground relationship as they group the background, separating it from the figure (the aircraft symbol).

IV. Method

A. Participants

A total of 25 (22 male, 3 female) commercial airline pilots participated in the study with an average age of 48.9 years (*SD* = 9.6), and an average total number of 12,436 flight hours (*SD* = 5,157). All were familiar with flying medium- to large-sized aircraft and were in possession of an ATPL. The experiment was approved by the Human Research Ethics Committee of Delft University of Technology and informed consent was obtained from each participant.

B. Apparatus

The experiment was performed in the Simona Research Simulator (SRS) at the faculty of Aerospace Engineering of Delft University of Technology [33]. The SRS is a six-degree-of-freedom full-motion simulator with a hydraulic hexapod motion system, which can realize accelerations below the human vestibular threshold [25]. The participant was seated in the left-hand seat of the cockpit in front of a collimated 180° horizontal by 40° vertical field of view screen. The outside visuals were rendered by FlightGear software and projected using three DLP projectors. Audio simulation featured a constant engine and wind noise and the autopilot disconnect alert. Pilots wore noise-canceling headphones to prevent them from hearing the simulator's motion system, however, they could hear the autopilot disconnect alert. A 9" tablet was used for a secondary distraction task.

The aircraft flight dynamics were simulated using a DLR A320 model as these flight dynamics correspond most with the aircraft the participants have experience with. Participants could only control the roll axis, using a control column with electric control loading. The control column contains a control loading model with a breakout torque of 2.0Nm, and a static and dynamic friction of 0.3Nm. Throttle was controlled by the autopilot throughout the entire experiment. The only instrument provided was a simplified digital Primary Flight Display (PFD), showing the aircraft's attitude, speed, and altitude. A modified autopilot was used to bank the internal aircraft model to the required test conditions. In this phase, the motion system was either kept still or used to provide disorientation cues to the participant, as described in subsection IV-C.

C. Experiment Procedure

The experiment consisted of two parts. The first part was performed according to the leans illusion designed by Van den Hoed et al. [19] to test the displays with more realistic leans cueing and in a situation where pilots respond after being distracted. However, in that study, a steep learning curve was found. While 38.9% of participants made an RRE the first time they encountered this leans illusion, this reduced to zero the fourth time participants encountered the same illusion. Simulating this illusion also takes a relatively long time. As two displays needed to be compared within a reasonable amount of time, and enough errors needed to be made to get statistically relevant data, the decision was made to also use shorter runs with less accurate leans cues but with the potential to induce confusion in pilots with regards to the bank angle. These short runs form the second part of the experiment.

1) Briefing and Familiarization: Participants were provided with a written experiment briefing and were informed of the main goals of the experiment and the experiment task. They were told that the goal of the experiment was to compare the PDCM AI to the baseline AI in a series of tasks where they had to roll the aircraft back to wings-level using the AI, but they were not told that confusing motion cues were going to be provided. They were instructed to respond *immediately* when the AI appeared as "an intuitive response was desired and their reaction time would be one of the outcome measures". Participants were able to familiarize themselves with the simulator and controls by flying for two minutes. More was not deemed necessary as the experimental task was very simple and performance metrics only concerned their initial response to being presented with the AI.

2) Stimuli: For both parts of the experiment, the speed remained fixed at around 230 knots and an altitude of 10,000 feet. Continuous light turbulence (using a Dryden model of turbulence with σ = 1.0, L = 2,000 m, V = 200 m/s [34]) was added to mask motion onsets. However, both parts of the experiment featured different motion stimuli.

(i) *Part 1 (long runs)* Figure 4 shows the timeline of a long run.

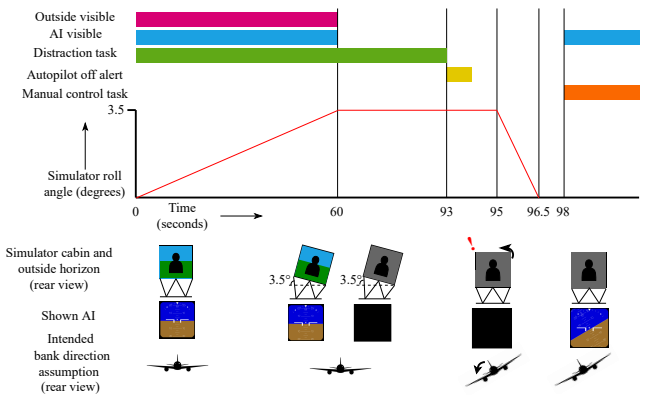

Figure 4: A timeline of the stimuli in a long run for a motion-opposite condition

The run started with straight and level flight with the autopilot engaged. Participants had to perform a distraction task, where they had to guess the next number in a sequence of numbers[1]. This task was performed on a tablet attached to the surface of the center pedestal to the participant's right-hand side, which required them to lean over and be slightly turned to the side. With the autopilot flying the aircraft and the participant performing the distraction task, the simulator cab was slowly prepositioned to 3.5° bank in 60 seconds while the AI and the outside view continued to indicate level flight. For this prepositioning of the simulator cabin, a maximum roll acceleration of 1.696 x 10^{-5} rad/s^2 and a maximum roll rate of 0.001 rad/s were used, both being *below* the human perception thresholds [25], [26].

After the prepositioning phase, the simulator cabin maintained a fixed roll angle of 3.5° for 33 seconds to induce vestibular adaptation to the roll angle. According to earlier studies [35], prolonged exposure to a roll angle can cause a subsequent roll in the opposite direction to be overestimated in that direction. This adaptation phase was also required to realistically simulate a situation where the aircraft rolled below a pilot's threshold to a new bank angle. Six seconds after the prepositioning phase, the outside visuals and the AI faded to black. At the end of the adaptation phase, the autopilot disconnect alert sounded, signaling that the participant should prepare for intervention by facing the still-black AI and by holding the control column. Two seconds after the alert, the simulator platform was tilted back to level in one and a half seconds with a maximum role rate of 0.04 rad/s and a maximum roll acceleration of 0.075 rad/s^2, both of which are *above* the human perceptual threshold [25], [26]. One and a half seconds after this super-threshold roll ended, the AI was shown again. The participant would then use the AI to roll back to wings-level.

(ii) *Part 2 (short runs)* Figure 5 shows the timeline of a short run. No outside visuals were shown during the run and each run started with a blacked-out AI.

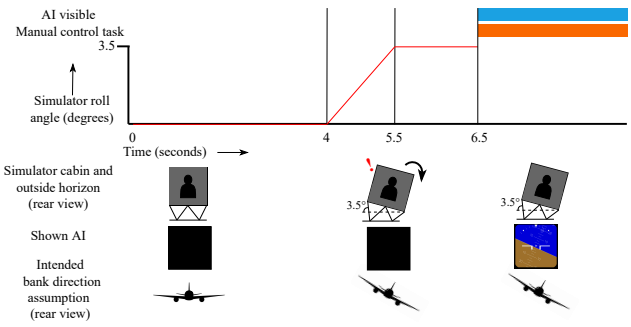

Figure 5: A timeline of the stimuli in a short run for a motion-opposite condition

[1]Test of Numerical Sequences - Nibcode, URL = https://www.nibcode.com/en/psychometric-training/test-of-numerical-sequence

Participants were instructed to keep their hands on the control column the entire time. In the first four seconds, the simulator did not move but the autopilot brought the aircraft model to the desired bank angle. The participant did not see this as the AI was blacked out. After four seconds, the simulator cabin rolled to 3.5° in 1.5 seconds, with a maximum roll rate of 0.04 rad/s and maximum roll acceleration of 0.075 rad/s^2, both above the human perceptual threshold [25], [26]. One second after this motion ended, the AI was shown, and the participant could use the AI to roll back to wings-level.

3) Conditions: Both parts of the experiment with the procedure described above were repeated for several runs with each run featuring either of the two following motion conditions:

(i) *Motion-matching*: The AI shown after the motion cues indicated a bank angle of 30° in the same direction as the super-threshold roll cue. This condition was used to get pilots to instill trust in the motion cues and to make the occurrence of runs in the other condition less predictable.

(ii) *Motion-opposite*: The AI shown after the motion cues indicated a bank angle of 30° in the *opposite* direction of the super-threshold roll cue. This condition was used to simulate the leans and possibly elicit RREs.

Additionally, each run featured the presentation of one of two display conditions: baseline AI or PDCM AI..

4) Number and Order of Runs: Figure 6 shows an example of the experiment design. The runs of each display condition were grouped in blocks. Halfway through the short runs, a break was taken to avoid fatigue and boredom. The practice runs only featured the motion-matching condition to make pilots trust the motion cues.

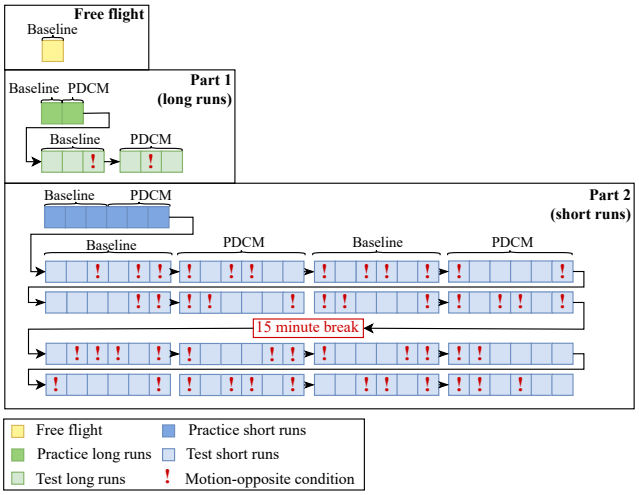

Figure 6: Example of experiment design

(i) *Part 1 (long runs)*: Participants first performed two long runs to practice, one with each display. These practice runs only featured the motion-matching condition to make pilots trust the motion cues. Six test runs were then performed, three for each display. The order of display conditions was counterbalanced between participants. For each display, one of the three runs was the motion-opposite condition with the others being the motion-matching condition. The choice to perform only two motion-opposite runs is based on the learning curve found in Van den Hoed et al. [19] where the most errors were made in the first two runs. To ensure participants could not predict when the motion-opposite condition would occur, the following measures were taken:

a) The motion-opposite condition for the second display did not occur at the same time as it did for the first display. Participants might notice at what point the motion-opposite run happened for the first display and could be inclined to believe the same will happen for the second display.

b) The last run of the second display was not a motion-opposite run. Participants most likely would have realized at this point that a motion-opposite condition would happen in one of the three runs for this second display. If it did not happen in the first two runs, they would know it would happen in the third run.

(ii) *Part 2 (short runs)*: Participants first performed six short runs to practice, three with each display. These practice runs only featured the motion-matching condition to make pilots trust the motion cues. A total of 96 test runs were performed with the short runs, 24 for each display x motion combination. Participants performed these runs in blocks of six, switching between displays every block of six. The order of display conditions was counterbalanced between participants. To generate a random order of runs for each participant, avoid them recognizing a pattern that could influence their performance as well as counteract any fatigue effects, the following steps were taken:

a) A random order of the motion-matching and -opposite conditions was generated, which adhered to the following rules: at most three consecutive runs that are *exactly* the same, an equal number of motion-matching and -opposite runs occurred, and an equal number of motion-matching and -opposite runs for each display.

b) This random order was divided into blocks of six runs.

c) A random order of these blocks was generated for Participant 1. Participant 2 had the "mirrored" version of the order of the blocks of Participant 1, i.e., the last block of Participant 1 was the first block of Participant 2, the second-to-last block of Participant 1 was the second block of Participant 2, etc. A random order of the blocks was generated for Participant 3 and Participant 4 had the "mirrored" version of Participant 3. The same was done for Participants 5 and 6, 7 and 8, 9 and 10, etc.

D. Dependent Measures

Outcomes were compared between the PDCM AI and the baseline AI to test the effectiveness of the PDCM AI. Outcomes were also compared between the motion-matching

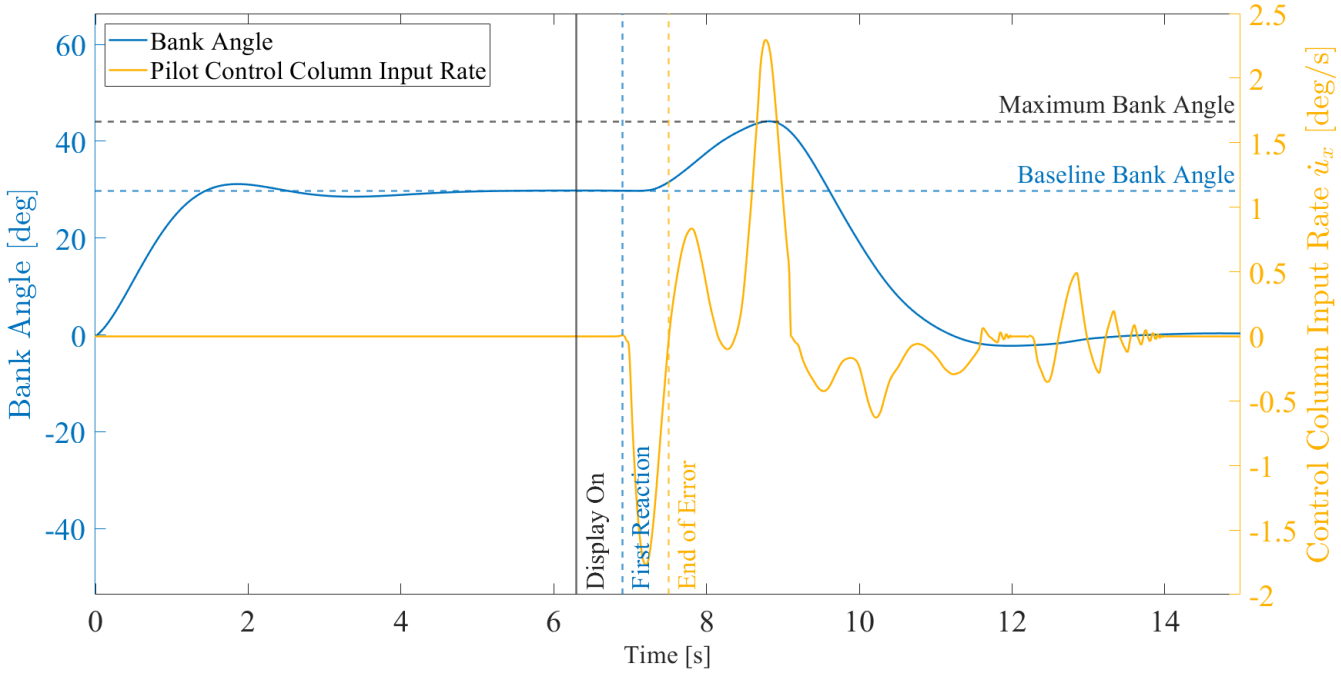

Figure 7: Example of a short run showing bank angle and pilot control column input rate when an error was recorded

and -opposite conditions of the long runs and short runs, to test the effectiveness of both cueing types in eliciting RREs. The following dependent measures were obtained:

Reaction Time - This was the time between the display presentation and the start of the first control input. The control loading model stays at zero until a torque is exerted above the breakout. The derivative of the control loading model was taken and the first instance of it being larger than 0, was seen as the first reaction. See Figure 7.

Error Rate - An error was defined as a roll input away from wings-level flight following the AI presentation that caused the control column to exceed 1° of roll deflection, consistent with previous research [19], [36].

Error Duration - This is the time it took for the participant to correct their error and start turning the control column to the correct side (i.e., column deflection rate switching signs, as is shown as "End of Error" in Figure 7). Error duration was only measured when an error was recorded. The beginning of the error duration is thus the moment of initial reaction *if* an error was detected.

Error Severity - This is the difference between the maximum bank angle reached during an error and the aircraft bank angle at the moment of the initial control input, also called "baseline bank angle" (see Figure 7). The baseline bank angle is chosen to be at the moment of the first input as the autopilot is still ever so slightly moving the aircraft bank angle the moment the display turns on. The bank angle at the moment of first input can thus be seen as the bank angle the participant interpreted before responding to it.

Post-experiment Questionnaire Answers - After the experiment was completed, participants got a questionnaire consisting of close- and open-ended questions related to the effectiveness of both the displays and experiment procedures.

E. Hypotheses

Fewer errors, less severe errors, lower reaction times, and a lower error duration were expected for the PDCM AI. These hypotheses are rooted in the idea that the modifications of the AI should cause a strengthened figure-ground relationship which in turn would make it easier to interpret the bank angle direction.

F. Data Analysis

The simulator data of two participants were corrupted and could thus not be processed and analyzed. However, they did experience the experiment as intended thus their answers to the post-experiment questionnaire were still valid and included. Statistical analysis was performed using IBM SPSS software. The data were checked for normality. For data that were normally distributed a 2x2 (display condition, motion condition) repeated measures ANOVA test was used to compare the sample means. For data that were not normally distributed the Wilcoxon signed-rank test was used to compare the sample medians. Furthermore, to compare the two displays based on the error rate of the first encounter of a motion-opposite run, a chi-square test was performed. If no statistical analysis is possible due to an insufficient number of data points raw data will be reported instead.

V. Results

Figure 8 shows the order of display conditions given to each participant as well as when they made an RRE and during

which motion condition this happened. The rectangles and squares represent blocks of three long runs and six short runs, respectively. Not all runs in these blocks were usable, some had to be removed for the following reasons:

- Extra runs due to simulator operator error: A total of seven extra runs were removed. This does not affect the total number of usable runs for the participants who performed an extra run.
- Incorrect simulator motion: A total of four (three long, one short) runs were removed due to incorrect simulator motion.
- Participant exerting force on control column above the breakout level before display turned on: A total of nine (three long, six short) runs were removed for this reason.

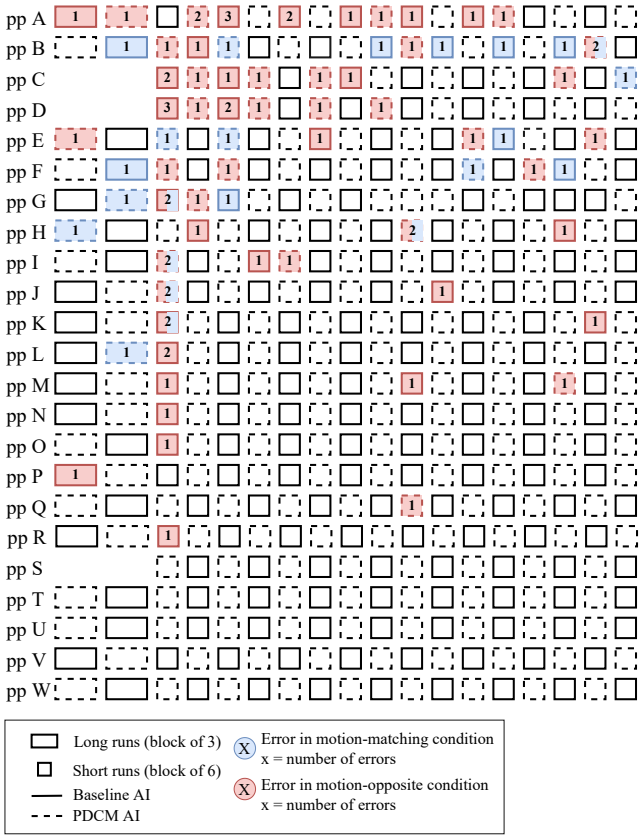

Figure 8: Overview of errors made by participants, ordered from most to least RREs

Due to the removal of some runs, three participants had missing data (i.e., no data for a certain display x motion condition) for the long runs. As this would have too big of an impact on the statistical analysis, the decision was made to remove the long runs for these participants. The total number of runs for each experiment condition is shown in Table I. A total of eighteen long runs (13%) and seven short runs (0.32%) were lost. Table II and Table III show an overview of the performance outcomes of the long runs and short runs, respectively.

Table I: Number of runs for each experiment condition

	Long Runs		**Short Runs**	
Condition	Baseline AI	PDCM AI	Baseline AI	PDCM AI
Matching Motion	40	40	550	552
Opposite Motion	20	20	548	551

A. *Long Runs*

For the data analysis of the long runs, the data of 20 participants was used.

1) Reaction time: Figure 9 and Figure 10 show the data distribution of the average reaction times for both displays in the motion-matching and motion-opposite scenarios, respectively. There was no significant difference between the displays in the matching condition (Z = -0.317 and p = 0.751) in the motion-opposite condition (Z = -0.916 and p = 0.360), nor overall (Z = -0.616 and p = 0.538). There was also no significant difference between the motion conditions (Z = -1.849 and p = 0.064), irrespective of the display conditions.

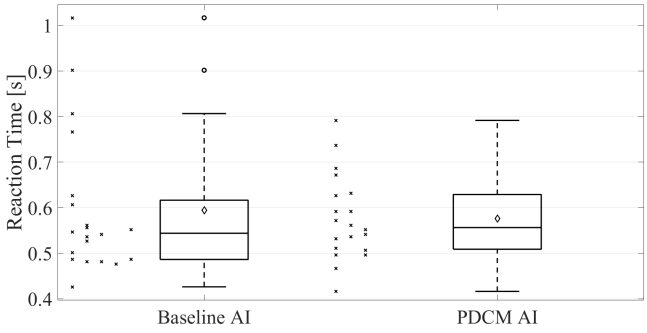

Figure 9: Box plot of average reaction time per participant per display during the long runs with motion-matching condition

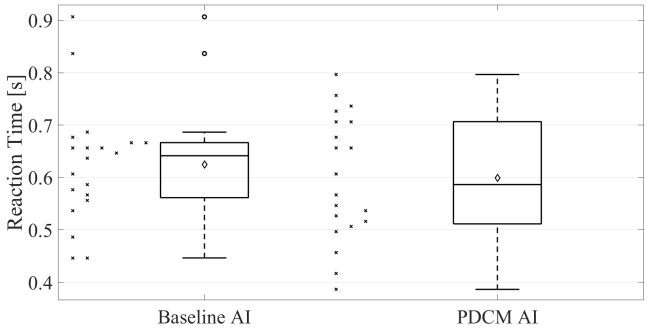

Figure 10: Box plot of average reaction time per participant per display during the long runs with motion-opposite condition

In the motion-matching condition, the median reaction time was 0.544 seconds (IQR = 0.130) for the baseline AI and 0.556 seconds (IQR = 0.120) for the PDCM AI. In the motion-opposite condition, the median reaction time was 0.642 seconds (IQR = 0.105) for the baseline AI and 0.586 seconds (IQR = 0.195) for the PDCM AI.

Table II: Overview of the performance outcomes of the long runs

Condition	Long Runs									
	Motion-matching					Motion-opposite				
	Baseline		PDCM			Baseline		PDCM		
	Median [IQR]	N	Median [IQR]	N	Δ	Median [IQR]	N	Median [IQR]	N	Δ
Reaction Time [s]	0.544 [0.130]	20	0.556 [0.120]	20	-0.012	0.642 [0.105]	20	0.586 [0.195]	20	0.056
Error Rate [%]	0.00 [0.00]	20	0.00 [0.00]	20	0.00	0.00 [0.00]	20	0.00 [0.00]	20	0.00
Error Severity [deg]	0.07 [0.18]	3	0.07 [3.77]	3	0.00	2.06 [4.06]	2	0.58 [0.99]	2	1.48
Error Duration [s]	0.242 [0.045]	3	0.280 [0.263]	3	-0.038	0.385 [0.370]	2	0.305 [0.130]	2	0.080

Table III: Overview of the performance outcomes of the short runs

Condition	Short Runs									
	Motion-matching					Motion-opposite				
	Baseline		PDCM			Baseline		PDCM		
	Mean (SD) or Median [IQR]	N	Mean (SD) or Median [IQR]	N	Δ	Mean (SD) or Median [IQR]	N	Mean (SD) or Median [IQR]	N	Δ
Reaction Time [s]	0.504 (0.067)	23	0.523 (0.076)	23	-0.019	0.539 (0.079)	23	0.548 (0.074)	23	-0.009
Error Rate [%]	0.00 [0.00]	23	0.00 [4.17]	23	0.00	4.17 [8.33]	23	4.17 [8.33]	23	0.00
Error Severity [deg]	0.04 [0.12]	9	0.04 [0.39]	9	0.00	0.19 [0.76]	33	0.32 [0.86]	27	-0.13
Error Duration [s]	0.230 [0.075]	9	0.230 [0.133]	9	0.000	0.290 [0.095]	33	0.270 [0.143]	27	0.020

2) Error Rate: Figure 11 shows the error rates for both displays as well as the error rates for each of the two motion conditions that were used for both displays.

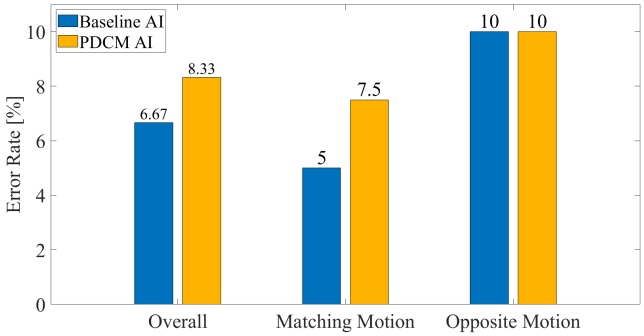

Figure 11: Error rates for each display x motion condition as well as overall error rate for each display during the long runs

There was no significant difference between matching motion (Z = -0.447, p = 0.655), opposite motion (Z = 0.000, p = 1.000), or overall (Z = -0.264, p = 0.792) error rates when comparing the displays. No significant difference was found between the two motion conditions either (Z = -0.431 and p = 0.666).

Figure 12 shows the error rate for each display for each encounter of a motion opposite run. In this case, participants only encountered two of those runs. The largest error is found in the first encounter where three out of 20 participants made an error of which two were made with the baseline AI and one with the PDCM AI. A chi-squared test was performed on this first encounter to compare the displays but showed no significant difference (χ^2 = 0.392 and p = 0.531).

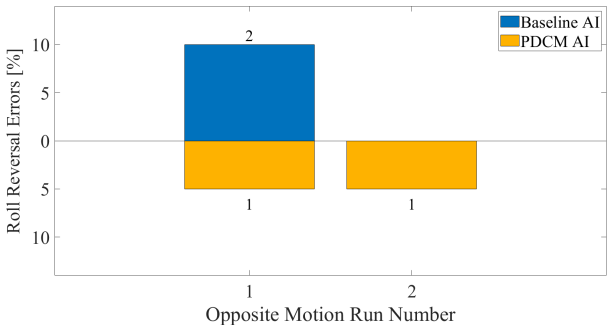

Figure 12: Percentage (as well as the actual number on top or below) of participants who made an error for each encounter of the opposite motion condition during the long runs

3) Error Severity: Figure 13 shows the severity of all errors made by participants during the long runs. Not enough participants made errors in both display conditions or both motion conditions, thus no statistical analysis could be performed.

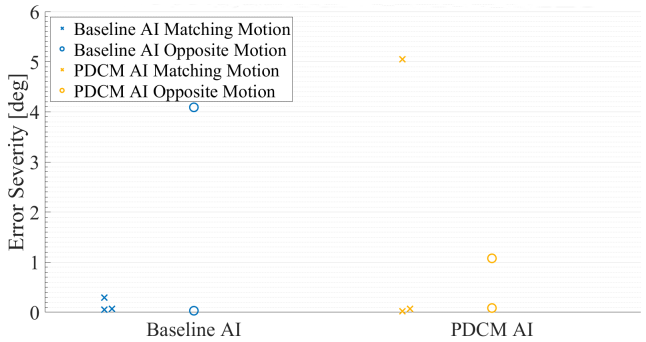

Figure 13: Error severity, in degrees exceeding the baseline bank, of each error made during the long runs

The median error severity of all errors made in the motion-matching condition was 0.07° (*IQR* = 0.18) for the baseline AI and 0.07° (*IQR* = 3.77) for the PDCM AI. In the motion-opposite condition, the median error severity was 0.58° (*IQR* = 0.99) for the PDCM AI and 2.06° (*IQR* = 4.06) for the baseline AI.

4) Error Duration: Figure 14 shows the duration of all errors made by participants during the long runs. However, as with the error severity, not enough participants made errors with both displays so no statistical analysis could be performed. The median error duration in the motion-matching condition was 0.280 seconds (*IQR* = 0.263) for the PDCM AI and 0.242 seconds (*IQR* = 0.045) for the baseline AI. In the motion-opposite condition, the median error duration was 0.305 seconds (*IQR* = 0.130) for the PDCM AI and 0.385 (*IQR* = 0.370) for the baseline AI.

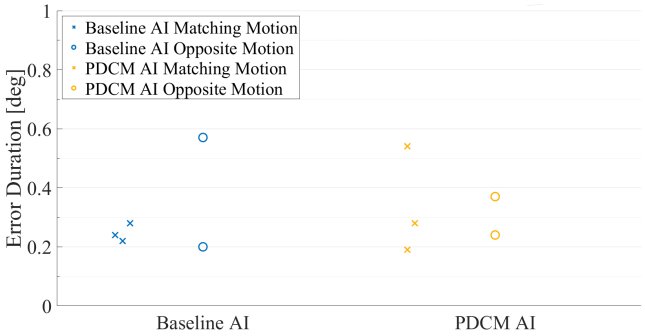

Figure 14: Error duration of each error made in the long runs

B. Short Runs

For the data analysis of the short runs, the data of 23 participants was used.

1) Reaction time: Figure 15 and Figure 16 show the data distribution of the average reaction times for both displays in the motion-matching and motion-opposite scenarios, respectively. A repeated measures ANOVA test showed a significant difference between the displays ($F(1,22) = 26.703$, $p < 0.001$ and $\eta^2_{partial} = 0.548$) with the PDCM AI causing an *increase* of 0.013 seconds (0.535 seconds compared to 0.522 seconds). A significant difference was also found between the motion conditions, irrespective of the displays ($F = 39.545$, $p < 0.001$ and $\eta^2_{partial} = 0.642$) with the motion-opposite condition causing an increase of 0.031 seconds (0.544 seconds compared to 0.513 seconds). No significant display x motion condition interaction was found ($F = 1.823$ and $p = 0.191$).

In the motion-matching condition, the mean reaction time was 0.504 seconds (*SD* = 0.067) for the baseline AI and 0.523 seconds (*SD* = 0.076) for the PDCM AI. In the motion-opposite condition, the mean reaction time was 0.539 seconds (*SD* = 0.079) for the baseline AI and 0.548 seconds (*SD* = 0.074) for the PDCM AI.

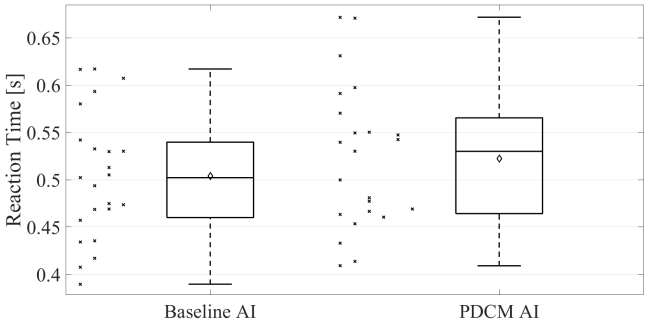

Figure 15: Box plot of average reaction time per participant per display during the short runs with motion-matching condition

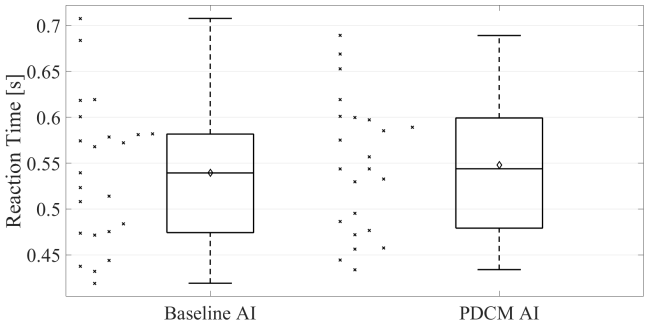

Figure 16: Box plot of average reaction time per participant per display during the short runs with motion-opposite condition

2) Error Rate: Figure 17 shows the error rates for both displays and the error rates for each of the two motion conditions used for both displays.

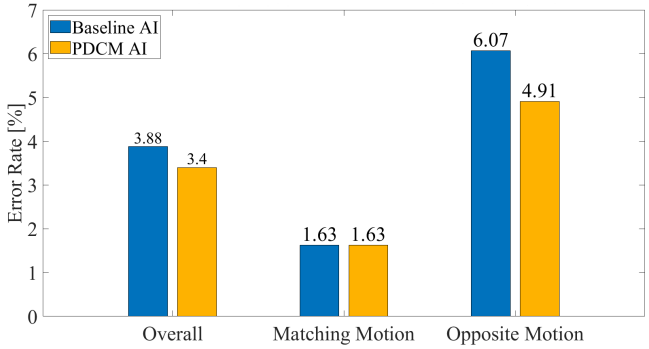

Figure 17: Error rates for each display x motion condition as well as overall error rate for each display during the short runs

There was no significant difference between the displays in either the overall (Z = -0.901, p = 0.367), matching motion (Z = -0.144, p = 0.886), or opposite motion (Z = -1.257, p = 0.209). However, a significant difference was found between the two motion conditions, irrespective of the display, (Z = -2.983 and p = 0.003) with the motion-opposite condition causing more errors than the motion-matching condition (median of 4.17% compared to 0%).

Figure 18 shows the error rate for each display for each encounter of a motion opposite run. The error rate decreases the more motion-opposite runs participants encountered, with a smaller peak at run number 25 which was on average the first motion-opposite encounter after the break. The largest error rate is found in the first encounter where twelve out of 23 participants (or 52.2%) made an error of which eight were made with the baseline AI and four with the PDCM AI. A chi-squared test was performed on this first encounter to compare the displays, but no significant difference was found (χ^2 = 2.112 and p = 0.146).

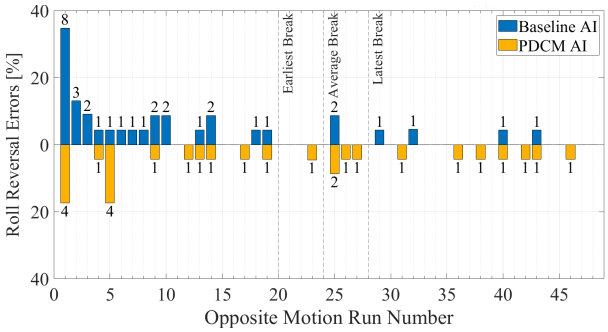

Figure 18: Percentage (as well as the actual number on top or below) of participants who made an error for each encounter of the opposite motion condition during the short runs

3) Error Severity: Figure 19 shows the severity of all errors made by participants during the short runs. Not enough participants made errors in both display conditions or both motion conditions, thus no statistical analysis could be performed on the error severity. The median error severity of all errors made in the motion-matching condition was 0.04° (*IQR* = 0.12) for the baseline AI and 0.04° (*IQR* = 0.39) for the PDCM AI. In the motion-opposite condition, the median error severity was 0.32° (*IQR* = 0.86) for the PDCM AI and 0.19° (*IQR* = 0.76) for the baseline AI.

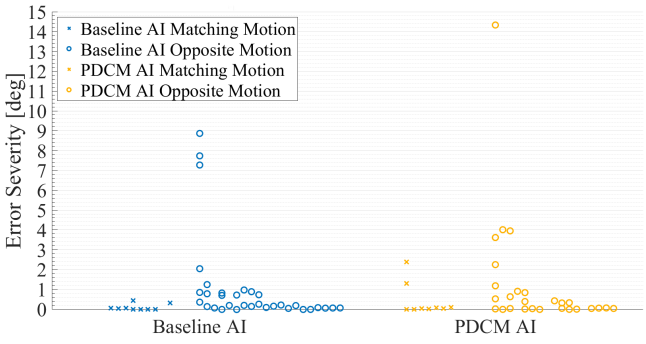

Figure 19: Error severity, in degrees exceeding the baseline bank, of each error made during the short runs

4) Error Duration: Figure 20 shows the duration of all errors made by participants during the long runs. However, as with the error severity, not enough participants made errors with both displays so no statistical analysis could be performed. The median error duration of all errors made in the motion-matching condition was 0.230 seconds (*IQR* = 0.075) for the baseline AI and 0.230 seconds (*IQR* = 0.133) for the PDCM AI. In the motion-opposite condition, the median error duration was 0.270 seconds (*IQR* = 0.143) for the PDCM AI and 0.290 (*IQR* = 0.095) for the baseline AI.

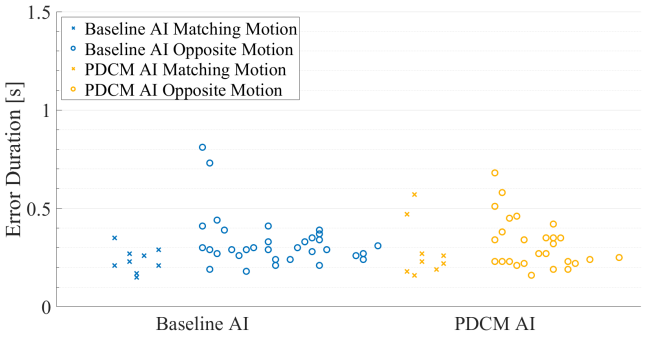

Figure 20: Error duration of each error made in the long runs

C. Questionnaire Output

Figure 21 summarizes the responses given to the close-ended questions of the post-experiment questionnaire.

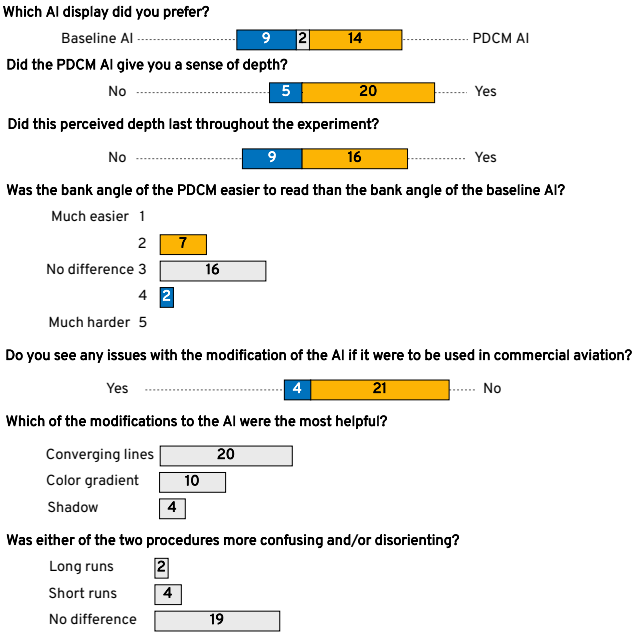

Figure 21: Answers to the close-ended questions from the post-experiment questionnaire including the answer possibilities (blue color is in favor of the baseline AI, dark yellow is in favor of the PDCM AI)

While fourteen out of 25 surveyed participants prefer the PDCM AI, only seven of them found it easier to read the bank angle and two found it harder. Most participants (sixteen out of 25) found there to be no difference in reading the bank angle. Five participants did not get a sense of depth from the modifications made to the AI. Out of the 20 that *did*

get a sense of depth, four lost it throughout the experiment. Participants were allowed to pick multiple answers when asked about which modification they thought to be the most helpful, hence the total number of "votes" being more than 25. The most preferred modification was the converging lines. When comparing the two procedures used during the experiment (long and short runs) based on how disorienting they were perceived to be, most participants did not find either to be more disorienting than the other.

VI. Discussion

No significant differences between the baseline AI and PDCM AI were found when it came to error rate, error severity, and error duration. Thus, the null hypothesis cannot be rejected. A significant difference was found in reaction time in the short runs, but the outcome was not as hypothesized: the PDCM AI caused an *increase* in reaction time of 0.013 seconds. The same significance was not found in the long runs. Different effects of the PDCM AI were found when looking at the long and short runs separately. These differences are likely caused by the difference in the number of runs for both parts of the experiment.

More accurate conclusions about the PDCM AI can be drawn from the short runs. The increase in reaction time with the PDCM AI is consistent with previous research [18] and could be due to the increased complexity of the display or participants needing some time to get used to it. In the motion-opposite condition, the error rate was 4.91% for the PDCM AI and 6.07% for the baseline AI. However, this difference was not significant. Twelve participants first encountered this motion-opposite condition when using the baseline AI with eight (or 67%) of those participants making an error. Eleven participants first encountered it with the PDCM AI and four (or 36%) of those made an error. This difference is however not significant and decreases with increasing encounters of the motion-opposite condition, but it seems that the PDCM AI possibly "protects" against errors in a surprise scenario.

Nine out of 25 participants commented that the perception of depth that was supposed to be created with the PDCM AI disappeared throughout the experiment. Five of those participants already did not report experiencing a sense of depth at the beginning of the experiment. When asked about their preference, fourteen participants responded that they prefer the PDCM AI with the main reason being that it felt more intuitive as it is a more accurate representation of the real world. Nine participants preferred the baseline AI as it is simpler, i.e., less cluttered. By far, the most appreciated modification was the converging lines (mentioned by 20 participants), it added a sense of depth and created an extra sense of awareness of the bank angle. Especially in more extreme attitudes, this could help with distinguishing better between sky and ground, and guide pilots back to straight and wings-level. While four participants appreciated the added contrast created by the shadow below the aircraft symbol, others mentioned it obscured their view of the horizon and made it harder for them to align the aircraft symbol to the horizon. Although it made little difference in the control task given to the participants in this experiment, it is still an unwanted effect. It is therefore recommended to adapt the shadow. While only ten participants indicated that they found the color gradient useful, it is still recommended to keep it as it creates an apparent loss of detail. It is also possible that only the converging lines and color gradient are enough to strengthen the figure-ground relationship, in which case the shadow around the aircraft symbol could be left out if it, even with some changes, still poses problems with pitch.

The PFD used in this experiment is also a simplified version of what is shown in an aircraft. Some participants commented that the PFD used in this experiment is far less cluttered than what they are used to, a few even indicated that they feared the PDCM AI would only add to the clutter already present. Future experiments could benefit from including all other information typically present in a commercial aviation aircraft's PFD to test if any positive impact the modifications made to the AI might have is nullified due to too much clutter. The changes to the display could also be made more subtle, e.g., making the converging lines and color gradient closer in color to the brown color already used for the ground.

The short runs show promise as a statistically significant increase in both reaction time and error rate was found between the two motion conditions. However, it should be noted that the short runs are less realistic and can cause extra confusion due to the (unrealistic) motion cues caused by gravity. The first encounter of a motion-opposite run also resulted in a peak error rate of 52.2%. There also seems to be a peak after, on average, the break. However, this peak is caused by just two participants making an error so it could be a coincidence. The large peak in the first motion-opposite encounter could indicate that these short runs with opposite motion work best in a surprise scenario. When using this method, it would be recommended to mix it up with different flight tasks to increase the number of RREs.

Multiple participants mentioned that the 30° bank angle used in the experiment is within their "comfort zone" and evokes little to no surprise or concern, even when preceded by a motion cue in the incorrect direction. More extreme bank angles would most likely show bigger differences in reaction time and would make participants have to interpret the AI under pressure. However, when using these more extreme attitudes in an experiment, it is important to pick participants carefully as the training they have received can influence the outcome. It is also important to make sure that the experiment does not get too tiring as fatigue due to repetitions can start to play a role too. One participant also noted that they knew when they were going to have to give an input due to the motion upset always happening a couple of seconds before the AI would be presented. For this reason, it is recommended to place the moment of motion upset closer to the presentation of the AI such that the simulator is still moving when the AI turns on again or to vary this timing.

While the same procedure was used for the long runs as the one described in Van den Hoed et al. [19], different

results were obtained. No significant difference in error rate or reaction time between the two motion conditions was found. During the long runs, participants responded almost four times quicker after the presentation of the AI and the error rate for the motion opposite condition was almost half compared to Van den Hoed's study. These differences were not caused by the experimental method as this was not changed. It was ensured that the participants fit the same criteria, namely in possession of an ATPL and familiar with flying medium-to-large-sized aircraft. It was also ensured that participants in this experiment did not partake in Van den Hoed's study. However, aspects such as age, experience, background, etc. could have had an effect. The reason for the difference in error rate could also be the recent increase in Upset Prevention and Recovery Training (UPRT) since Van den Hoed's study, as mentioned by participants, which could also explain why the PDCM AI had no significant effects in decreasing the error rate. Some participants even indicated that they did not notice the superthreshold roll motion and subsequently did not make any errors in the motion-opposite condition. More UPR training could also cause pilots to have an improved ability to read the AI in unexpected attitudes, resulting in a lower reaction time. One participant indicated that the AP disconnect alarm gave them a warning about when a motion upset would be occurring, giving them time to prepare for intervention. This, however, does not explain the decrease in reaction time nor the decrease in error rate as the same was done in Van den Hoed's study.

The use of the long runs in this experiment was a means of comparing it to the results found in Van den Hoed et al. [19]. If the decrease in error rate and reaction time is a result of increased UPR training, this effect is likely also present in the short runs where the error rate in the opposite-motion condition was also lower than previously found in Van den Hoed's study. Interestingly, errors were still made in the motion-matching condition in both the long and short runs. The error rate for the matching motion condition in the short runs (1.63%), is consistent with previous research with pilots, albeit in flight, where an error rate between 1.5 and 3.1% was found [9], [11] in conditions where the motion matched what was shown on the AI. In contrast, the error rate for this motion condition was almost four times as high during the long runs, which could be due to the relatively low number of runs when compared to the number of short runs. In both the long and short runs, the median error severity and median error duration were higher in the motion-opposite scenario compared to the motion-matching scenario. However, no statistical analysis could be performed on these as an insufficient number of participants made errors in all four conditions or either both displays or both motion conditions.

Even though participants were told to look at the center of the AI, two admitted later on that due to the nature of the experiment (i.e., only rolling left or right), they tended to mainly look at the roll index. This further shows that it is a good idea to mix this method of disorientation with other control tasks to ensure participants do not change their control strategy because of the repetitiveness of the control task. Previous research has also shown that the roll index used in commercial aviation is not spatially compatible [37] and can cause up to five times the number of RREs compared to the roll index used in general or military aviation, as was shown in an experiment using commercial airline pilots [22]. Participants also admitted that it was hard for them to recount their control strategy to get the aircraft back to wings-level. It might just be the case that they unconsciously also looked at the roll index. For these reasons, it could be interesting to get more insight into the control strategy using eye tracking or to remove the roll index from the experimental displays.

VII. Conclusion

Regarding roll reversal errors, the modified AI performed at the same level as the conventional AI when it comes to pilots providing a control input to roll back to wings-level from an unknown bank direction. The added static monocular depth cues did provide 20 out of 25 with a sense of depth, of which four lost this sense of depth throughout the experiment. Based on this, the modifications seemed to enhance the experienced figure-ground relationship of the AI. In this experiment, the modifications did not significantly reduce the ambiguity of the AI but there is potential. It is recommended to test the modified display in more challenging scenarios where participants need to recover from more extreme attitudes. It is also recommended to slightly change the modified AI according to the feedback given by some participants who stated that the modifications created too much clutter.

The novel way of inducing disorientation significantly increased the reaction time and error rate when the simulator motion did not match what could be seen on the AI. The effect on the error rate was the most prominent in a "surprise" scenario. A peak in roll reversal errors could be seen in the very first encounter of a motion-opposite run. The novel method is simpler yet still induces errors. However, when using this method, it would be recommended to combine it with different flight tasks to increase the number of RREs.

References

[1] International Air Transport Association, "Loss of Control In-Flight Accident Analysis Report 2019 Edition," 2019, accessed on 22/04/2023. [Online]. Available: https://www.iata.org/contentassets/b6eb2adc248c484192101edd1ed36015\/loc-i_{2019}.pdf

[2] C. M. Belcastro, J. V. Foster, G. H. Shah, I. M. Gregory, D. E. Cox, D. A. Crider, L. Groff, R. L. Newman, and D. H. Klyde, "Aircraft Loss of Control Problem Analysis and Research Toward a Holistic Solution," *Journal of Guidance, Control, and Dynamics*, vol. 40, no. 4, April 2017.

[3] Cameroon Civil Aviation Authority, "Technical Investigation into the Accident of the B737-800 Registration 5Y-KYA Operated by Kenya Airways that Occured on the 5th of May 2007 in Douala," 2010, (Accessed on 22/04/2023). [Online]. Available: https://reports.aviation-safety.net/2007/20070505-0_B738_5Y-KYA.pdf

[4] S. L. Johnson and S. N. Roscoe, "What Moves, the Airplane or the World?" *Human Factors*, vol. 14, no. 2, pp. 107–129, April 1972.

[5] S. N. Roscoe, "Airborne Displays for Flight and Navigation," *Human Factors*, vol. 10, no. 4, pp. 321–332, August 1968.

[6] S. Müller, V. Sadovitch, and D. Manzey, "Attitude Indicator Design in Primary Flight Display: Revisiting an Old Issue With Current Technology," *The International Journal of Aerospace Psychology*, vol. 28, pp. 1–16, July 2018.

[7] R. M. Taylor, "Aircraft Attitude Awareness from Visual Displays," *Displays*, vol. 8, no. 2, pp. 65–75, April 1988.

[8] F. Ince, R. C. Williges, and S. N. Roscoe, "Aircraft Simulator Motion and the Order of Merit of Flight Attitude and Steering Guidance Displays," *Human Factors*, vol. 17, no. 4, pp. 388–400, August 1975.

[9] D. B. Beringer, R. C. Williges, and S. N. Roscoe, "The Transition of Experienced Pilots to a Frequency-Separated Aircraft Attitude Display: A Flight Experiment," *Proceedings of the Human Factors Society Annual Meeting*, vol. 18, no. 1, pp. 62–70, October 1974.

[10] S. N. Roscoe and R. C. Williges, "Motion Relationships in Aircraft Attitude and Guidance Displays: A Flight Experiment," *Human Factors*, vol. 17, no. 4, pp. 374–387, August 1975.

[11] A. H. Hasbrook and P. G. Rasmussen, *In-flight Performance of Civilian Pilots using Moving-Aircraft and Moving-Horizon Attitude Indicators*. Oklahoma City (OK), USA: Federal Aviation Administration, June 1973.

[12] J. Wagemans, *Perceptual Organization*. John Wiley & Sons, February 2018, ch. 18, pp. 1–70.

[13] W. Grether, *A Discussion of Pictorial versus Symbolic Aircraft Instrument Displays (Memo. Rep. No. TSEAA-694-8B)*. Wright-Patterson Air Force Base (OH), USA: Air Material Command, August 1947.

[14] S. N. Roscoe, "Moving Horizons, Control Reversals, and Graveyard Spirals," *Ergonomics in Design*, vol. 12, no. 4, pp. 15–19, October 2004.

[15] J. R. Comstock., L. C. Jones, and A. T. Pope, "The Effectiveness of Various Attitude Indicator Display Sizes and Extended Horizon Lines on Attitude Maintenance in a Part-Task Simulation," in *Proceedings of the Human Factors and Ergonomics Society Annual Meeting*, vol. 47, no. 1, October 2003, pp. 144–148.

[16] V. Hiremath, R. W. Proctor, R. O. Fanjoy, R. G. Feyen, and J. P. Young, "Comparison of Pilot Recovery and Response Times in Two Types of Cockpits," in *Human Interface and the Management of Information. Information and Interaction*, G. Salvendy and M. J. Smith, Eds. Heidelberg, Germany: Springer Berlin Heidelberg, July 2009, pp. 766–775.

[17] C. R. Kelley, S. de Groot, and H. M. Bowen, "Relative Motion III. Some Relative Motion Problems in Aviation," no. AD256346, Port Washington (NY), USA, May 1961.

[18] D.-A. Arrundell, A. Landman, O. Stroosma, M. M. Van Paassen, E. Groen, and M. Mulder, "Stereoscopic Depth Cues for Enhancing Pilot Interpretation of the Artificial Horizon," in *22nd International Symposium on Aviation Psychology*, May 2023.

[19] A. van den Hoed, A. Landman, D. V. Baelen, O. Stroosma, M. M. van Paassen, E. L. Groen, and M. Mulder, "Leans Illusion in Hexapod Simulator Facilitates Erroneous Responses to Artificial Horizon in Airline Pilots," *Human Factors*, vol. 64, no. 6, pp. 962–972, December 2020.

[20] A. Landman, E. L. Groen, M. M. van Paassen, A. W. Bronkhorst, and M. Mulder, "Expectation Causes Misperception of the Attitude Indicator in Nonpilots: A Fixed-Base Simulator Experiment," *Perception*, vol. 49, no. 2, pp. 155–168, January 2020.

[21] A. Landman, S. Davies, E. L. Groen, M. M. van Paassen, N. J. Lawson, A. W. Bronkhorst, and M. Mulder, "In-flight Spatial Disorientation Induces Roll Reversal Errors when Using the Attitude Indicator," *Applied Ergonomics*, vol. 81, p. 102905, November 2019.

[22] G. Singer and S. Dekker, "The Effect of the Roll Index (Sky Pointer) on Roll Reversal Errors," *Journal of Human Factors and Aerospace Safety*, vol. 2, pp. 33–43, January 2002.

[23] H. Pennings, E. Oprins, H. Wittenberg, M. Houben, and E. Groen, "Spatial Disorientation Survey Among Military Pilots," *Aerospace Medicine and Human Performance*, vol. 91, pp. 4–10, January 2020.

[24] K. K. Gillingham and F. H. Previc, "Spatial Orientation in Flight," Armstrong Laboratory, Brooks Airforce Base (TX), USA, Tech. Rep., November 1993.

[25] H. Heerspink, W. Berkouwer, O. Stroosma, M. M. Van Paassen, M. Mulder, and B. Mulder, "Evaluation of Vestibular Thresholds for Motion Detection in the SIMONA Research Simulator," in *AIAA Modelling and Simulation Technologies Conference and Exhibit*, August 2005, p. 6502.

[26] A. J. Gundry, "Thresholds to Roll Motion in a Flight Simulator," *Journal of Aircraft*, vol. 14, no. 77, pp. 624–631, July 1977.

[27] J. J. Gibson, *The Perception of the Visual World*. Boston (MA), USA: Houghton Mifflin, 1950.

[28] R. N. Haber, "How We Perceive Depth from Flat Pictures," *American Scientist*, vol. 68, no. 4, pp. 370–380, July 1980.

[29] C. Healey and J. Enns, "Attention and Visual Memory in Visualization and Computer Graphics," *IEEE Transactions on Visualization and Computer Graphics*, vol. 18, pp. 1170–1188, July 2011.

[30] V. A. Lamme, "The neurophysiology of figure-ground segregation in primary visual cortex," *The Journal of Neuroscience*, vol. 15, no. 2, February 1995.

[31] D. Mumford, S. Kosslyn, L. Hillger, and R. Herrnstein, "Discriminating Figure from Ground: The Role of Edge Detection and Region Growing," *Proceedings of the National Academy of Sciences of the United States of America*, vol. 84, no. 20, p. 7354—7358, October 1987. [Online]. Available: https://europepmc.org/articles/PMC299291

[32] S. Wolfson and M. S. Landy, "Examining Edge- and Region-based Texture Analysis Mechanisms," *Vision Research*, vol. 38, no. 3, pp. 439–446, 1998.

[33] O. Stroosma, M. M. Van Paassen, and M. Mulder, "Using the SIMONA Research Simulator for Human-machine Interaction Research," in *Proceedings of the AIAA Modeling and Simulation Technologies Conference*, no. AIAA 2003-5525, Austin (TX), USA, August 2003, pp. 1–8.

[34] H. W. Liepmann, "On the Application of statistical concepts to the Buffeting Problem," *The International Journal of Aerospace Psychology*, vol. 19, no. 11, pp. 793–800, December 1952.

[35] B. T. Crane, "Roll Aftereffects: Influence of Tilt and Interstimulus Interval," *Experimental Brain Research*, vol. 223, pp. 89–98, September 2012.

[36] R. Lewkowicz, B. Bałaj, and P. Francuz, "Susceptibility to Flight Simulator-Induced Spatial Disorientation in Pilots and Non-Pilots," *The International Journal of Aerospace Psychology*, vol. 30, no. 1-2, pp. 25–37, January 2020.

[37] D. Ding and R. W. Proctor, "Interactions between the Design Factors of Airplane Artificial Horizon Displays," *Proceedings of the Human Factors and Ergonomics Society Annual Meeting*, vol. 61, no. 1, pp. 84–88, September 2017.

Part II

Preliminary Report

*This part has been assessed for the course AE4020 Literature Study.

1 Introduction

May 4^{th} 2007 shortly before midnight, Kenya Airways flight KQA 507 took off from Abidjan International Airport with destination Jomo Kenyatta Airport Nairobi, carrying eight crew members and 108 passengers. Shortly after take-off, at about 1,000 ft, the aircraft entered a slow right roll. This roll went unnoticed by the cockpit crew due to inadequate instrument scanning and the lack of external visual references in the dark. Only when the aural bank angle warning sounded, was the crew informed of the potential dangers of their bank angle. This warning was met with surprise. The control wheel was immediately turned to the right, indicating that the pilot flying had misinterpreted the attitude indicator display, aggravating the bank angle. The captain did not comprehend the reactions of the aircraft and made several confused attempts at getting the wings level but to no avail. The aircraft crashed shortly after midnight as a consequence of spatial disorientation (Cameroon Civil Aviation Authority, 2010).

This case is an example of an accident caused by loss of control in-flight (LOC-I) as a consequence of spatial disorientation. LOC-I has shown to be one of the most significant contributors to fatal accidents, with spatial disorientation, or loss of attitude awareness, being the leading cause of fatalities when it comes to crew (in)action (International Air Transport Association, 2019). Spatial disorientation often goes hand in hand with surprise: Pilots do not always realize they are disoriented so a sudden warning or movement by the aircraft's autopilot can take them by surprise.

Misinterpretation of the attitude indicator (AI), as in the example of the Kenya Airways flight, has also been linked to spatial disorientation and LOC-I (Roscoe & Williges, 1975). In moments of surprise, pilots must intuitively understand the AI. If they misinterpret the AI, it could lead to control reversal errors, of which the most common type is roll reversal errors where the pilot tries to steer the aircraft back to wings-level but unintentionally *increases* the bank angle. Aircraft in the West use a moving horizon (MH) AI where the aircraft symbol stays still, and the horizon line moves. The moving aircraft (MA) AI that is used in Russia, works the opposite way: The horizon line stays still, and the aircraft symbol moves. The MH and MA displays are often compared to determine which one is the easiest to interpret. However, the focus of this report will be on the MH AI as it is the most used display. Research will be done into how the MH AI display can be improved to decrease the occurrence of spatial disorientation and LOC-I as a consequence of misinterpretation.

Research Question

The research question for this literature study is as follows:

"Can the moving horizon attitude indicator display be improved to reduce the occurrence of spatial disorientation and loss of control in-flight?"

To answer this research question, the current issues with the MH AI that lead to spatial disorientation and LOC-I need to be investigated as well as how others have attempted to solve these issues. A new way of improving the MH AI will be identified, which will lead to a more detailed research question for the thesis project. In a later stage of the thesis project, an experiment will be performed to fully answer this research question.

Report Structure

To successfully design an adapted AI display and give an answer to the research question, knowledge must be gained into various aspects of this research. Chapter 2 will first provide some context to the research by analyzing LOC-I accidents and presenting background information on their main causes. This research heavily focuses on a pilot's interaction with their environment, thus Chapter 3 will elaborate on the physiological and psychological processes involved in spatial orientation. In Chapter 4 a review is done on current literature and previous research into roll reversal errors and how these can be mitigated by adapting the AI. This chapter will be concluded with the research gap and the research question that will have to be answered. Previous research has highlighted the importance of human visual perception, which includes depth perception and grouping principles. This will be elaborated on in Chapter 5. Chapter 6 will then propose some adaptations to the AI to decrease the occurrence of roll reversal errors. To answer the research question, an experiment will need to be conducted. Chapter 7 will discuss a preliminary experiment plan.

2
Research Context

It is known that roll reversal errors (RREs) can occur with the moving horizon (MH) representation of the attitude indicator (AI) in the primary flight display (Beringer, Williges, & Roscoe, 1974; Hasbrook & Rasmussen, 1973; Singer & Dekker, 2002; Müller, Sadovitch, & Manzey, 2018). RREs are a consequence of spatial disorientation where pilots in some cases provide a roll input, which unintentionally *increases* the bank angle error. Spatial disorientation is one of the main causes of loss of control in-flight (LOC-I) accidents (Belcastro et al., 2017). This current research will look into improving the MH AI to decrease the occurrence of spatial disorientation and LOC-I. This chapter will explain the context behind the research. Section 2.1 will first illustrate the need for this research by looking at LOC-I accidents in the last two decades. One of the leading causes of fatal LOC-I accidents, spatial disorientation, will be explained in Section 2.2 including a description of the most common vestibular illusion, the leans. Spatial disorientation often goes hand in hand with startle and surprise which will be elaborated on in Section 2.3. Section 2.4 briefly describes the ambiguity of the attitude indicator (AI), which has been linked to spatial disorientation. Lastly, Section 2.5 briefly summarizes this chapter and describes the issue that this literature study seeks to address.

2.1. Loss of Control In-flight Accident Analysis

LOC-I refers to accidents in which the flight crew was unable to maintain control of the aircraft in flight, resulting in an unrecoverable deviation from the intended flight path (International Air Transport Association, 2019). While LOC-I only accounts for 8% of all commercial aircraft accidents between the years of 2009 and 2018, as can be seen in Figure 2.1, it is the number one fatal accident category. As is shown in Figure 2.2, about 94% of LOC-I accidents involved fatalities to passengers and/or crew.

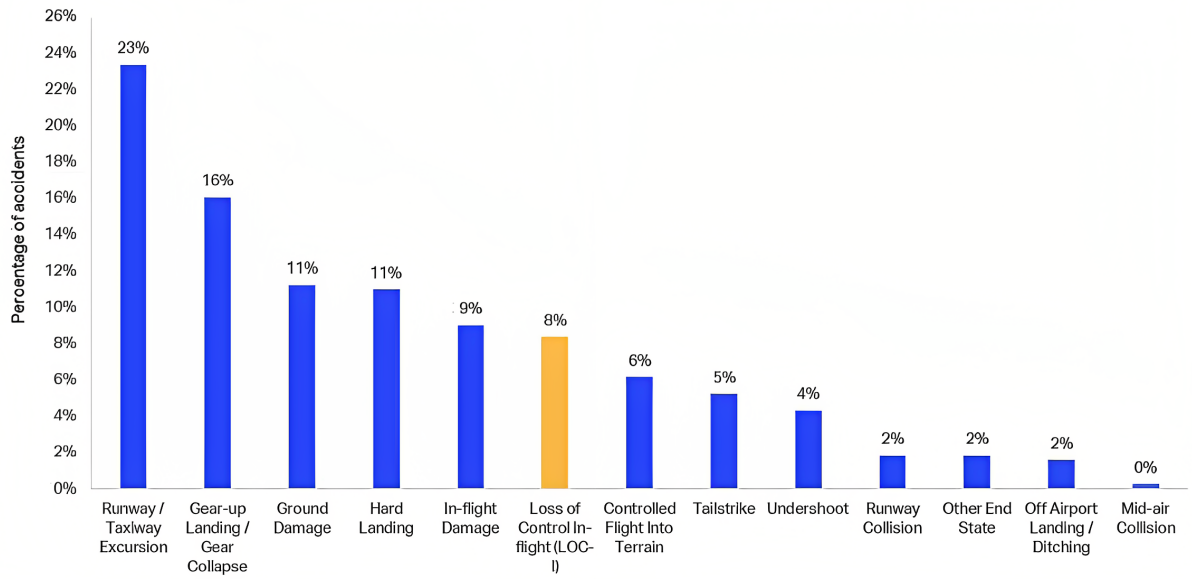

Figure 2.1: Percentage of commercial accident categories in relation to total accidents (International Air Transport Association, 2019)

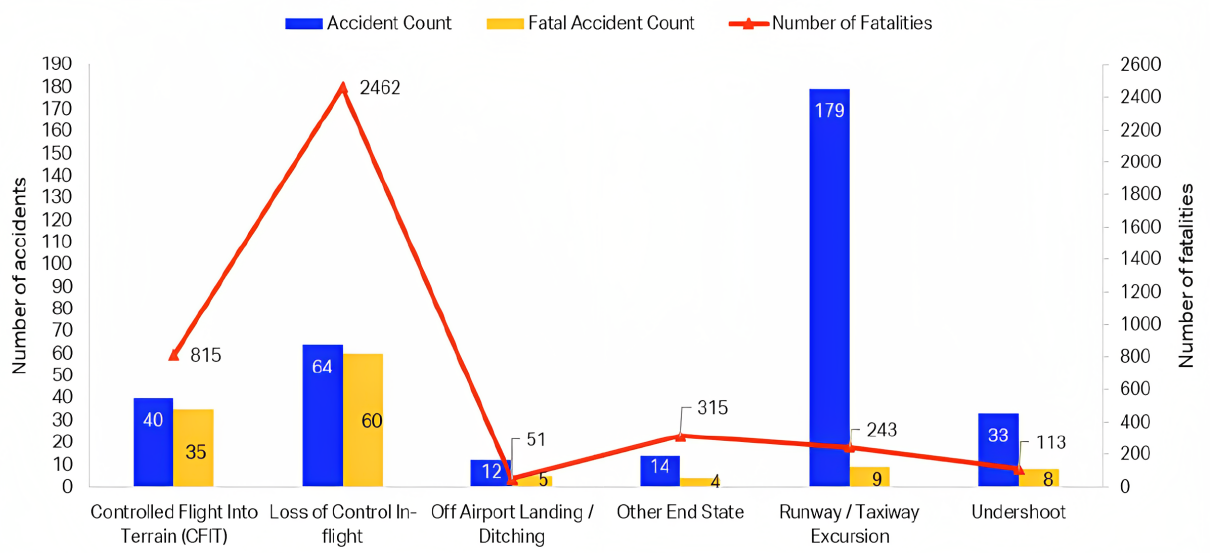

Figure 2.2: Fatality rate of the top six of fatal accident categories (International Air Transport Association, 2019)

The current research concerns spatial disorientation, which has been found as the main cause of fatal LOC-I accidents when it comes to crew (in)action. As can be seen in Figure 2.3, it accounts for 26% of LOC-I fatalities.

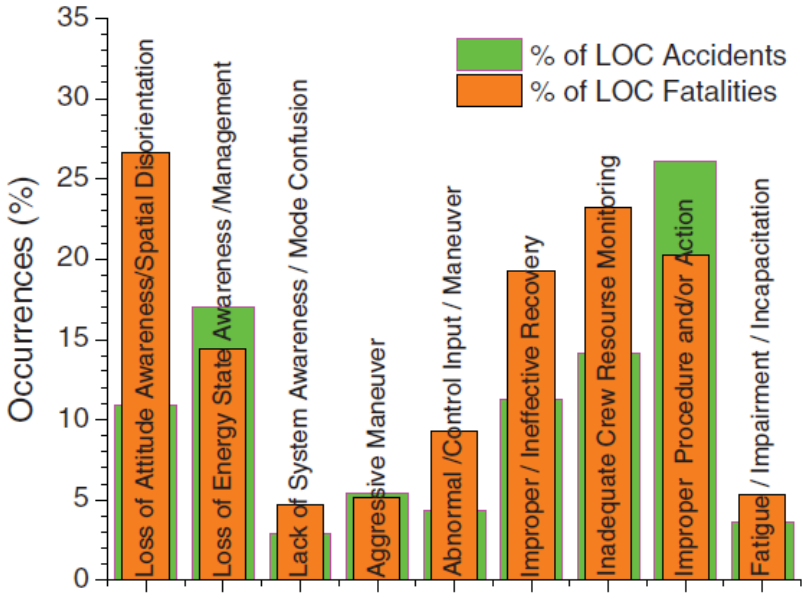

Figure 2.3: LOC-I accident occurrence related to crew (in)action (Belcastro et al., 2017)

2.2. Spatial Disorientation

As mentioned in the previous section, spatial disorientation is one of the leading causes of fatal LOC-I accidents. It can be defined as "*an erroneous sense of one's position and motion relative to the plane of the Earth's surface*" (Gillingham & Previc, 1993, page 77). Three types of spatial disorientation in flight can be distinguished (Gillingham & Previc, 1993):

- Type I (unrecognized): The pilot has no conscious perception of any of the manifestations of disorientation, also called 'misorientation'.
- Type II (recognized): While this type is labeled 'recognized', it does not mean that the pilot *realizes* they are disoriented. They may realize that there is a problem in controlling the aircraft, while not knowing that the source of the problem is spatial disorientation.
- Type III (incapacitating): The pilot is disoriented and most likely realizes this, but cannot do anything about it.

While people combine inputs from various systems such as the vestibular, proprioceptive, and visual system, which will be elaborated on in Chapter 3, to orient themselves, the visual system is by far the most effective and overpowers all others. This phenomenon is known as "visual dominance" (Gillingham & Previc, 1993). Spatial disorientation often occurs during the transition from Visual Flight Rules to Instrument Flight Rules. Humans use ambient cues to orient themselves. When these ambient cues are reduced and the familiar ambient cues are rapidly changed or when there is a period of distraction and inattention when flying according to Instrument Flight Rules without ambient cues, disorientation can happen (Taylor, 1988).

A person can be provided with a false perception of their orientation, in which case they experience orientational illusions or have spatial disorientation. Pilots who have become disoriented in flight commonly fluctuate between control inputs as they alternate between responding to one orientational perception and then to the other (Gillingham & Previc, 1993). Illusions can be beneficial in the sense that they can be exploited in simulators, however, in-flight illusions are very much unwanted. A great number of in-flight illusions exist, some examples are the leans, the Coriolis effect, and the somatogravic illusion. The leans illusion, a Type I spatial disorientation, is one of the most common in-flight illusions (Gillingham & Previc, 1993; Pennings, Oprins, Wittenberg, Houben, & Groen, 2020). It will thus be explained in more detail.

The leans

The leans is the most common vestibular illusion. In the leans, a pilot has a false perception of the angular displacement about the roll axis, i.e., an illusion of bank. There is no single explanation for the leans, but it is known that it is invoked due to the shortcomings of the otolith organ and the semicircular canals. The otolith organ responds to gravity and acceleration combined, not to gravity alone. It is thus an unreliable source of information on whether a person is exactly upright as it cannot discriminate between acceleration and head tilt. The semicircular canals in the inner ear of a human only register a roll when the roll acceleration is above a certain threshold. The semicircular canals do not sense a low roll acceleration or a sustained roll motion. In the absence of visual input, these shortcomings could lead to a pilot believing they are flying straight when this is not the case (Gillingham & Previc, 1993). An abrupt correction (i.e., above the threshold) of this bank angle, makes the pilot think they are leaning in the opposite direction, see Figure 2.4. The pilot believes they need to correct this by rolling the aircraft back to what they believe is straight flight. However, in reality, they will make the initial bank angle worse, which is what is known as a roll reversal error.

It has been shown that an incorrect expectation, due to spatial disorientation, of the bank angle, induces RREs in-flight (Landman, Groen, van Paassen, Bronkhorst, & Mulder, 2020). It has also been demonstrated that it is possible to produce the leans illusion in a hexapod simulator (van den Hoed et al., 2020) where pilots make RREs due to spatial disorientation.

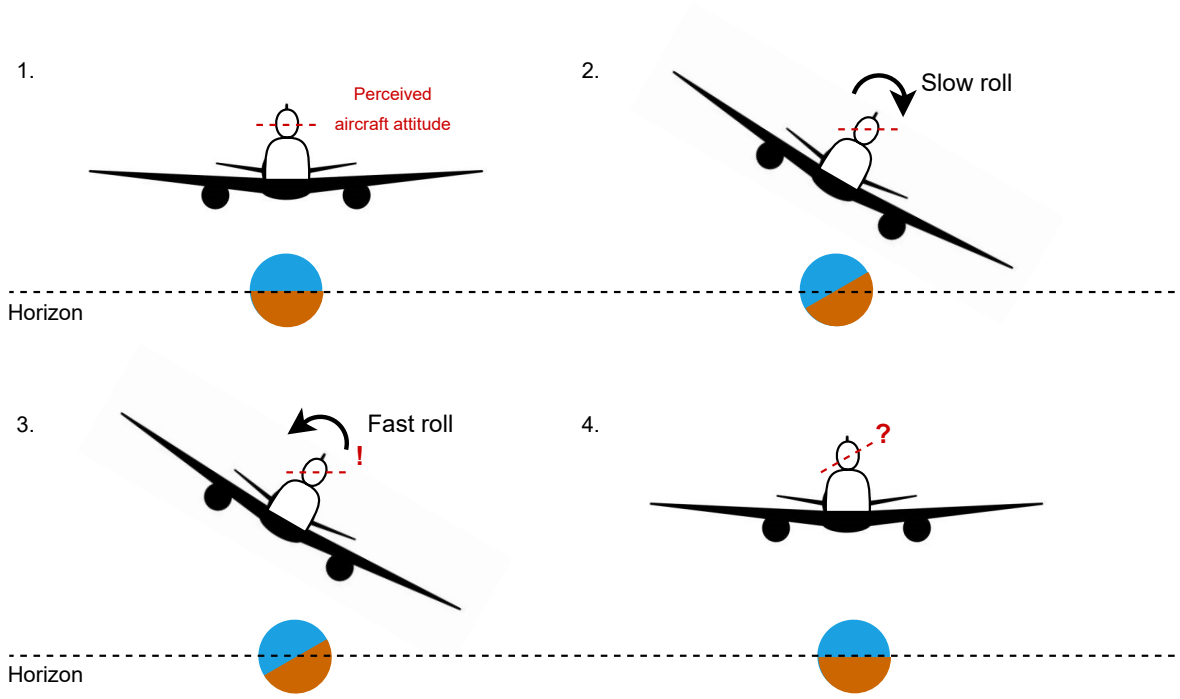

Figure 2.4: Illustration of the leans illusion

Commonly, when talking about ”the leans”, the vestibular leans illusion is meant. However, the leans illusion can also be induced by false horizons (Gillingham & Previc, 1993) by, for example, a sloping cloud deck. If it extends for a great distance into the pilot's visual field, it would be very hard not to see it as horizontal. This is known as ”cloud leans”. Pilots get the impression that the wings of their aircraft are not level and will start flying parallel to the clouds, as shown in Figure 2.5, to get their aircraft back to what they perceive as ”level”. Several other phenomena can also create a false horizon: uniformly sloping terrain, lights of a city built on a sloping terrain at night, a distant rain shower obscuring the real horizon and creating the impression of a horizon at the base of the rainfall, etc.

Figure 2.5: Cloud leans induced by a sloping cloud deck (Bednarek et al., 2019)

2.3. Startle & Surprise

Spatial disorientation often goes hand in hand with startle and surprise, which are often voiced as potentially contributing factors to aircraft incidents due to their possible negative side effects on flight crew performance (Rivera, Talone, Boesser, Jentsch, & Yeh, 2014). The terms ”startle” and ”surprise” are often used interchangeably but their effect on the human operator is vastly different (Landman, Groen, van Paassen, Bronkhorst, & Mulder, 2017; Rivera et al., 2014).

Startle is a brief, fast, and highly physiological reaction to a sudden intense, or threatening stimulus and can be measured, for example, in terms of eye blinks, contraction of facial and neck muscles, suspension of ongoing behavior, etc. While the unexpectedness of the stimuli increases the response, anticipated stimuli are still startling. The startle reflex is increased when arousal or stress level is at extremes, meaning both when an individual has a very high arousal level (e.g., when stressed, anxious, threatened, or operating intensely) and when an individual has a very low arousal level (e.g., when resting, drowsy, or close to falling asleep). Startle may induce brief disorientation and short-term psycho-motor impairment, which likely leads to task interruptions or brief confusion but can also significantly impair decision-making (Rivera et al., 2014). An example of a startling but not very surprising event in aviation is a lightning strike when flying in stormy weather.

Surprise is an emotional, cognitive, and behavioral response to an unexpected event that is, momentarily, difficult to explain and forces a person to change their understanding of the situation, i.e., a mismatch between the mental expectation and the perception of the environment. Surprise can be evoked by an unexpected stimulus or the absence of an expected stimulus. It can be experienced without a startle reflex and can disappear in anticipation of a stimulus. The main concern with surprise is that it generally interrupts an ongoing task. In a study investigating the effects of surprise on action interruption, it was found that a surprising stimulus interrupted the ongoing action of 78% of participants (Horstmann, 2006). Surprise has been considered to be a factor in LOC-I accidents and automation has been identified as one of the major causes of flight deck surprises. An example of a surprising stimulus is the aircraft flying back to level, thus sensing a roll motion, while the pilot thought they were flying level, like what happens in the leans illusion.

2.4. Ambiguity in the Attitude Indicator

During instrument flying, pilots are consistently taught to trust the instruments, as these are deemed the most reliable, and distrust any other sources (Singer & Dekker, 2002). To evaluate their attitude, pilots are fully relying on their attitude indicator (AI). It is thus vital that the AI can quickly be (correctly) interpreted to avoid any dangerous situations.

Currently, two types of AI displays are being used in commercial aviation:

1. Moving horizon (MH) where the aircraft coordinates are used as the reference system (Johnson & Roscoe, 1972), depicted in Figure 2.6. Also called inside-out AI.
2. Moving aircraft (MA) where the Earth coordinates are used as the reference system (Johnson & Roscoe, 1972), depicted in Figure 2.7. Also called outside-in AI.

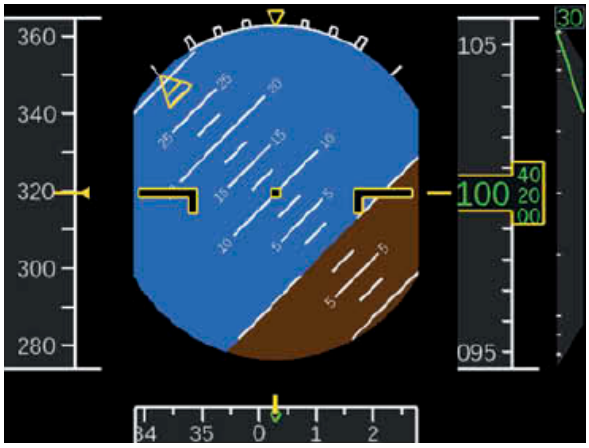

Figure 2.6: Moving horizon attitude indicator display (Müller et al., 2018)

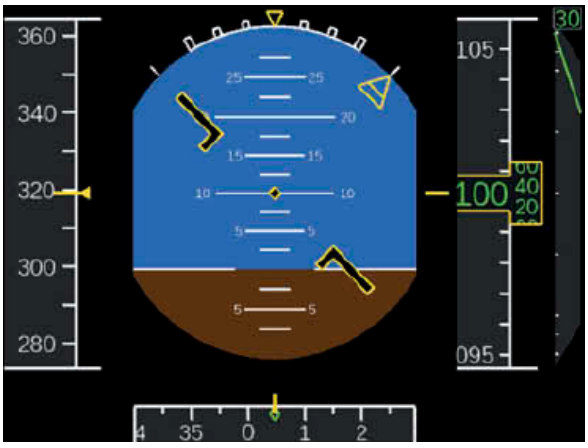

Figure 2.7: Moving aircraft attitude indicator display (Müller et al., 2018)

The MH display is used throughout the West while the MA display is mainly used in Russia. The difference between these displays lies in their dynamics: In the MA display, the horizon line stays still while the aircraft moves, complying with the principle of the moving part. In the MH display, the aircraft stays still while the horizon line moves, complying with the principle of pictorial realism (Müller et al., 2018). These two principles are defined as follows:

- Principle of moving part: The moving elements in a display should move in a pattern and direction compatible with the user's mental model (Roscoe, 1968).
- Principle of pictorial realism: Images on a visual display should match the user's mental model (Roscoe, 1968).

Discussion on which of these displays is "the best" has been going on for decades. Studies done in the 1950s-1970s had a clear preference for MA, however, these studies were mostly done with novices (Roscoe & Williges, 1975) whereas studies done with more experienced pilots were inconsistent (Browne, 1594; Gardner, Lacey, & Seeger, 1954). Many recent studies comparing MA and MH could not replicate earlier findings, possibly due to using only continuous tracking tasks and an AI display that was much larger than the real one. If the modern AI is accurately presented during the experiment, meaning with the correct dimensions, and recovery tasks are used, there seems to be no difference in whether experiments were done with the old electromechanical instruments versus the modern AIs (Müller et al., 2018). This suggests that specific display design in itself might be a key factor.

Motion cues can also affect the outcome of display evaluation. According to Roscoe and Williges (1975), outcomes of experiments in fixed-base simulators or ones providing highly distorted motion cues should be taken with a grain of salt if spatial orientation is a central consideration, as is the case for this research. One could argue that pilots are taught to ignore vestibular cues and to rely solely on their instruments, however, vestibular cues cannot be completely ignored, and they can be used to induce an expectation that would increase the likelihood of an RRE occurring (Landman et al., 2020).

All in all, switching to the MA display is not possible due to enormous efforts in terms of investments and new certifications (Müller et al., 2018). It would also mean retraining pilots, which poses a risk in itself as it is likely that they revert to their old habits when in a stressful situation.

2.5. Problem Statement

LOC-I is the leading cause of fatal aviation accidents while only comprising a relatively small percentage of aviation accidents. The industry has recognized this and is attempting to reduce the occurrence of this type of accident. When looking at the causes of LOC-I, spatial disorientation is the leading cause of fatalities when it comes to crew (in)action. Spatial disorientation can have multiple causes, but when it occurs it is highly important that pilots can quickly and correctly interpret the instruments they use for self-orientation, like the attitude indicator. Misinterpreting the AI can lead to erroneous control inputs. It is important to figure out why this misinterpretation happens and how to solve this issue to decrease the number of LOC-I accidents. The following chapters will dive deeper into human self-orientation and how the AI display can be improved.

3
The Human Operator

The human pilot plays a central role in this study. How they interact with their surroundings and how they spatially orient themselves is of great importance in understanding the occurrence of roll reversal errors and designing a display that could prevent these errors. Section 3.1 will explain the basic biology and the function of the orientational senses. Section 3.2 will explain the multitasking environment in which the pilot has to work while flying and monitoring an aircraft.

3.1. The Orientational Senses

The three main orientational senses are the vestibular system, the visual system, and the proprioceptive system. When two components of these are absent or heavily compromised, spatial orientation becomes strongly impaired. For example, in the absence of both vision and a working vestibular system, the proprioceptive system does not suffice to maintain spatial orientation and postural equilibrium, at least on Earth (Gillingham & Previc, 1993). As the previous example already alluded, these systems are made for and adapted to ground-based movement, not for three-dimensional movement in flight. This can cause mismatches between different stimuli and lead to spatial disorientation. It is also important to realize that while motion perception is possible due to sensory integration, it is strongly influenced by the brain's interpretations and assumptions due to often incomplete or conflicting sensory data.

3.1.1. Self-Orientation through the Visual System

The visual system provides the strongest cues for self-orientation. It can overrule very strong vestibular cues, a phenomenon called ”visual dominance” (Gillingham & Previc, 1993). The visual cortex section of the brain is responsible for processing visual information.

Many ways of ”dividing” the visual system exist. Some base it on the difference in function: object recognition (the ”what” system) and spatial orientation (the ”where” system) (Gillingham & Previc, 1993). Others differentiate in terms of form versus motion. In this discussion, the terms ”focal vision” and ”ambient vision” will be presented as they will be used in the following chapters as well.

Focal vision Focal vision supports object recognition and high acuity perception (Wickens, 2008). It consists primarily (but not solely) of foveal vision, which is a very small central part of the visual field in which humans can see sharp and in color. Focal vision allows for the judgment of distance and depth. It also selects certain objects of the pre-attentive array for further elaboration. Pre-attentive processing happens automatically and organizes the visual world into objects and groups of objects. This concept will be explained in more depth in Chapter 5.

Ambient vision Ambient vision is primarily involved with orienting the individual in the environment and is largely independent of the function of focal vision. Ambient vision is stimulated much more effectively by large images or groups of images that appear to be at a distance rather than those appearing to be close. The function of ambient vision can be split up into two processes (Gillingham & Previc, 1993):

- Providing self-motion cues: The detection of moving contrast over a large area of the visual field will result in vection. The visual stimulus causing this is called optical flow. The gradient of optical flow gives the observer a feeling of how fast they are moving whereas the pattern of optical flow gives the observer a feeling of the direction in which they are moving. Vection can either be correct, or

illusory, depending on whether actual or only apparent motion is occurring. A well-known example of a vection illusion is: When a train next to the one a perceiver is sitting in starts moving, the perceiver will feel as if they are moving. Angular vection is the same principle, except when the moving contrast is rotational relative to the subject, making them feel as if they are rotating.

- Providing self-orientation cues: The detection of the motion of the retinal image that results from minor deviations from one's desired posture, results in a sense of self-orientation. The orientation of the horizon can give an indication of one's orientation. The horizon line being at an angle would indicate the observer being at an angle.

In general, the main difference between the two types of vision is that focal vision provides the orientation of a perceived object relative to the individual while ambient vision provides the orientation of the individual relative to the perceived environment (Gillingham & Previc, 1993). This explains why it is difficult to orient oneself when only focal vision is available.

3.1.2. Self-Orientation through the Vestibular System

The vestibular system, shown in Figure 3.1, is located in the inner ear and while its role in spatial orientation is not as large as vision, it is still important. The vestibular system consists of two parts: the semicircular canals and the otolith organs.

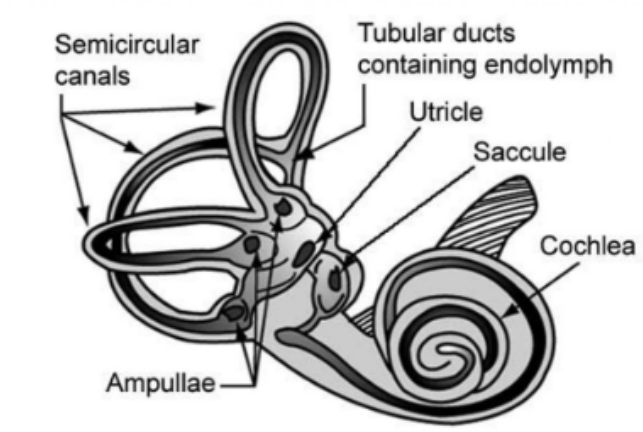

Figure 3.1: Vestibular system (The Human Memory, 2022)

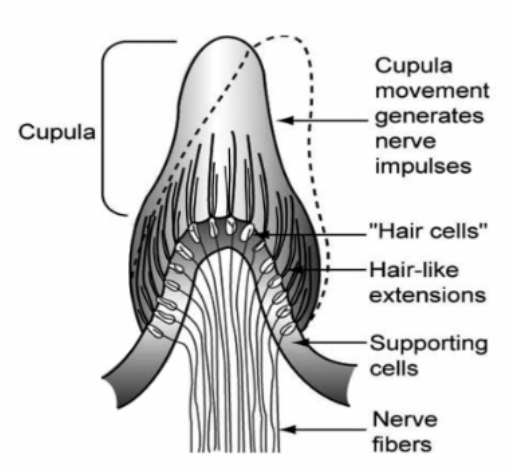

Figure 3.2: Ampulla (The Human Memory, 2022)

Semicircular canals The semicircular canals are three canals in orthogonal planes for sensing rotational acceleration around three axes. They are filled with a fluid (endolymph) and have a gelatinous membrane (cupula) that covers the crista ampullaris which contain hair cells. The anatomy of the crista ampullaris is shown in Figure 3.2.

Otolith organs The otolith organs are the saccule and utricle and both consist of tiny crystals (otoconia) on a gelatinous substance with embedded sensitive hair cells. The saccule is sensitive to specific forces in the vertical direction and the utricle is sensitive to specific forces in the horizontal direction. These "specific forces" are the sum of motion acceleration and gravitational acceleration. In the absence of visual stimuli, this can lead to confusion. For example, acceleration in the horizontal direction can feel like a backward tilt of the body. Figure 3.3 shows what happens in the otolith organs when a person moves their head backward.

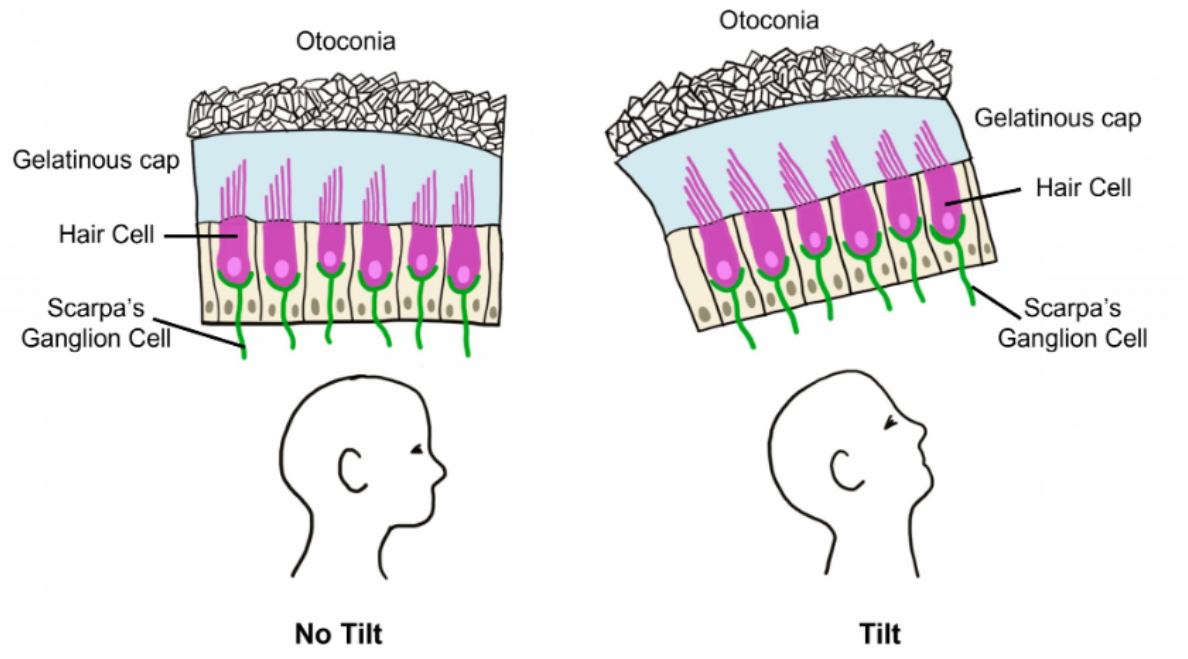

Figure 3.3: Illustration of workings of the otolith organs during movement of the head (Hedges, V., 2022)

Both parts of the vestibular system have their thresholds. It is hard to put a number on these as they can be raised due to a low state of mental arousal, fatigue, or just individual variation (Gillingham & Previc, 1993) and vary across the different degrees of freedom and with frequency. The value of these thresholds is dependent on sensor limits (sensory thresholds) and perception limits (indifference thresholds). However, the threshold is estimated to be around 0.05 m/s^2 for the otolith organs and about 0.5 to 3 deg/s for the semicircular canals (Heerspink et al., 2005).

Pilots can, with time and practice, develop the ability to suppress vestibular responses. By repeatedly experiencing certain stimuli, they can estimate how their vestibular system will respond and what they can do to counteract this. Vestibular oppression does disappear in the absence of vision, indicating that visual dominance has a big influence on it. The opposite of vestibular suppression also exists, namely ”vestibular enhancement” (Gillingham & Previc, 1993). This phenomenon is a result of a lack of available estimates of vestibular responses.

3.1.3. Self-Orientation through the Proprioceptive System

The proprioceptive system involves determining the body's orientation in space. It relies primarily on stretch receptors in the muscle. The muscles and tendons provide a sense of the relative position of neighboring body parts, which is highly important to maintain postural stability. The proprioceptive system also uses somatosensory information, which informs humans about objects in their environment through touch, i.e., physical contact with skin (Gillingham & Previc, 1993).

The exact contribution of the proprioceptive system to self-orientation is unclear. It has been argued that the proprioceptive system contributes to a phenomenon called the ”subjective vertical” which is an internal ”gravity” vector that defines our sense of upright (Bos, 2002). This phenomenon, however, only exists in the brain and does not always match the real orientation but it is important for flying and other orientation-dependent tasks.

3.1.4. Self-Orientation through the Auditory System

On Earth, the ability to determine the location of a sound source can play a role in spatial orientation, e.g., a revolving sound source can create a sense of self-rotation. In flight, binaural sound location is of little use in spatial orientation due to high ambient noise levels and the lack of audible external sound sources. However, experienced pilots can extract some information on orientation. Namely, the sound frequencies and intensities of various airspeeds and angles of attack can, in combination with other orientation information, give a perception of the velocity and pitch attitude of the aircraft. However, pilots have become more insulated from acoustic stimuli, so the usefulness of these auditory orientation cues has severely decreased (Gillingham & Previc, 1993).

3.2. Pilot Spatial Orientation Cycle

The previously discussed orientational senses are all simultaneously used while flying an aircraft. While in commercial aviation a pilot's task is mainly monitoring the aircraft, they still process a stream of visual, auditory, vestibular, and tactile stimuli. Figure 3.4 shows a concept map illustrating the perceptual and cognitive modalities that are involved in a pilot forming an image of their spatial orientation as well as how they relate to the aircraft. For most parts of a commercial flight, "manual control" would have to be swapped out for "autopilot control" as commercial pilots usually do little manual flying.

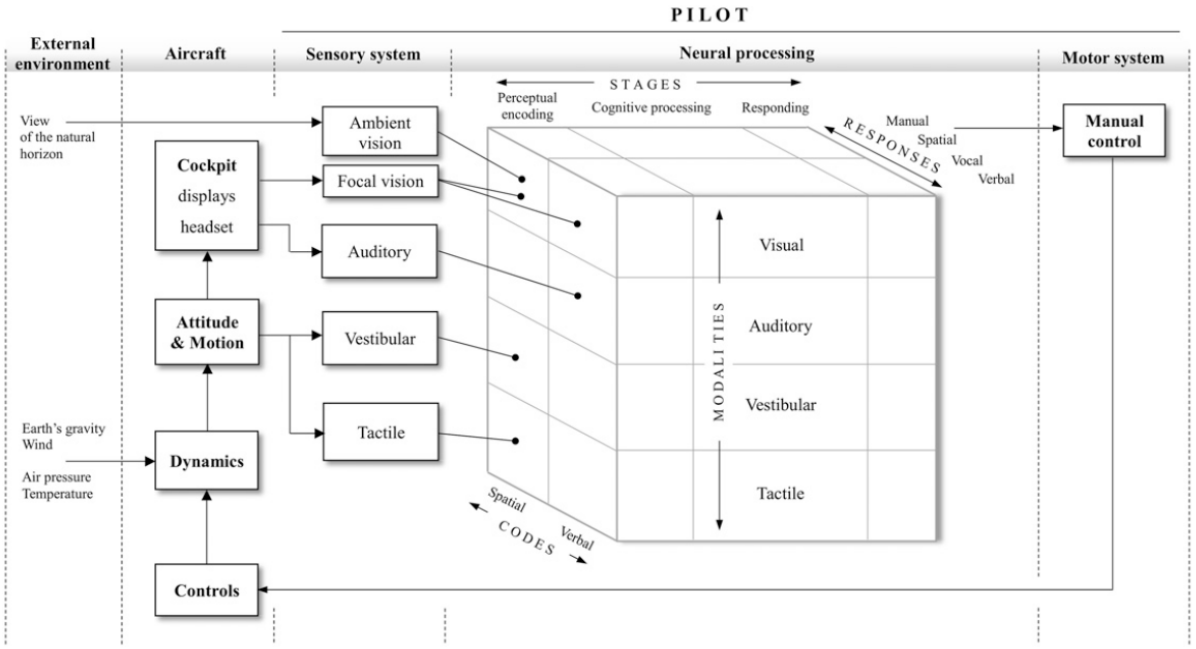

Figure 3.4: Concept map of the closed-loop control of a pilot's spatial orientation in flight (Fudali-Czyż et al., 2022)

Flying an aircraft includes multitasking, however, the human ability to multitask could be limited to what one can perceive and how one can operate in a multitasking environment. The concept map includes the "Multiple Resource Model" (Wickens, 2008), which is visualized by a cube. This cube shows three sets of information processing: stages of processing, codes of processing, and modalities. Their respective subdivisions use different parts of the brain, e.g., spatial activity and verbal activity are processed by the right and left cerebral hemisphere of the brain respectively (Wickens, 2008).

It has been shown that human performance heavily depends on the compatibility of input-output modality mapping (Stephan & Koch, 2010; Wickens, Sandry, & Vidulich, 1983; Göthe, Oberauer, & Kliegl, 2016). Going from one task to the other and even performing two tasks at the same time is "easier" when the input-output modality is compatible. For example, auditory-vocal tasks combined with visual-manual tasks are more compatible than auditory-manual and visual-vocal tasks combined. The more "distinct" tasks are (i.e., the use of different levels along the three sides of the cube) the less effort it requires to perform

them simultaneously. If tasks compete for a similar resource or require a high level of processing, they may interfere with each other, making them harder to perform simultaneously (Fudali-Czyż et al., 2022). Most information in an aircraft cockpit is presented visually, for which focal vision is used. However, visual orientation cues are processed by the ambient vision system. Due to the limitations in a human's processing capacity, directing visual attention to one stimulus comes at the cost of neglecting others.

The theory behind the Multiple Resource Model has been around for several decades and has been adapted over time when new findings arose. However, it does not explain why humans sometimes cannot deal with two tasks that should not compete too much with each other (Wickens, 2008). For example, driving a car while calling: Driving is a visual-manual task, and calling is an auditory-vocal task. These tasks are supposedly relatively compatible, however, many accidents have happened as a result of people not paying attention to the road due to the distraction of making a phone call. More research will thus need to be done on resource allocation.

The addition of the ”External environment”, the ”Aircraft” and ”Motor system” parts of Figure 3.4 is new. As mentioned before, the use of ”manual control”, does not really fit with commercial flying as the autopilot is used for the greater part of a commercial flight. Using the autopilot takes the pilot out of the loop. They are not in control of the dynamics of the aircraft unless they need to take over. It would be interesting to see what impact this has on the loop and resource allocation.

4

Previous Research

The moving horizon attitude indicator is so ingrained in modern, Western, aviation that changing its basic movement relationship would be nearly impossible. However, the fact that pilots continue to make control reversal errors using this display cannot be ignored. The presentation of the aircraft attitude needs to be modified in some way to reduce these. Section 4.1 will focus on the occurrence of control reversal errors, more notably those along the roll axis (roll reversal errors) as these are the most common ones. It has been found that the expectation of a certain bank angle can have an effect on roll reversal errors as will be explained in Section 4.2. How the leans illusion can be simulated for research and training purposes will be discussed in Section 4.3. The design deficiencies of the currently used moving horizon attitude indicator will be presented in Section 4.4. How previous researchers have attempted to overcome these deficiencies by either replacing the standard AI or enhancing it will be elaborated on in Section 4.5. Section 4.6 will identify the research gap and explain the goal of the current research.

4.1. Occurrence of Roll Reversal Errors

Control reversal errors commonly only occur along the roll axis, hence the name ”roll reversal error” (RRE). This is when the pilot gives a roll control input in the opposite direction of the required side. Multiple studies have investigated the occurrence of RREs for both pilots and non-pilots and have tested the effects of various displays. These studies were done using fixed-based or PC-based simulators as well as motion-based simulators and even in real flight (Landman et al., 2020; van den Hoed et al., 2020; Landman et al., 2019; Roscoe & Williges, 1975; Singer & Dekker, 2002; Wickens, Self, Andre, Reynolds, & Small, 2007; Gross & Manzey, 2014; Ding & Proctor, 2017; Müller et al., 2018).

When no physical motion is present, an RRE can be the result of misinterpretation of the AI or by creating an incorrect expectation of the bank angle (Landman et al., 2020) as will be explained in the next section. On one hand, one could say that having no physical motion does not give a very realistic sensation but on the other hand, pilots are trained to only rely on their instruments. When motion was present, a combination of motion cues and misinterpretation of the AI would cause an RRE. In fixed-base simulators, there was an RRE rate of 15-20% for non-pilots (Ince, Williges, & Roscoe, 1975; Müller et al., 2018) and 3.9-8.7% for pilots (Müller et al., 2018; Beringer et al., 1974). In-flight, non-pilots had an RRE rate of 21.9% (Roscoe & Williges, 1975) whereas pilots had a rate of 1.5-3.1% (Beringer et al., 1974; Hasbrook & Rasmussen, 1973). While this last number might seem low, from a safety perspective, it is still very high. It should also be noted that none of these earlier experiments considered the effect an expectation of the bank angle could have on the occurrence of RREs and even prevented participants from building up an expectation.

4.2. Influence of Expectation

When a pilot is disoriented, an incorrect expectation of the bank angle could be present, something that happens in the most frequently reported form of spatial disorientation called ”the leans”, which was briefly explained in Chapter 2. Research at the Delft University of Technology has been performed into the effect of bank angle expectation on RREs (Landman et al., 2019, 2020).

First, two experiments were done with non-pilots, one in a fixed-base simulator and another in-flight. In both experiments, participants were led to believe the AI would be indicating a certain attitude, either due

to vestibular cues in the in-flight experiment or by what the AI showed before the AI and outside visuals went blank in the simulator. Sometimes, the expectation would match the display, other times it would not. The in-flight experiment (Landman et al., 2019) was performed with non-pilots. The presence of leans cues caused the number of RREs to go up by a factor of 2.6 with no difference between leans-opposite (leans cues opposite to shown bank angle) and leans-level (leans cues but level flight), indicating that the participants responded to vestibular cues instead of to information from the AI. In the fixed-base simulator experiment (Landman et al., 2020), also performed with non-pilots, participants made significantly more RREs when the expectation of their bank angle did not match with the subsequently shown bank angle. They made 11.2 times more RREs when the shown bank angle was in the opposite direction of what they expected and 2.5 times when the aircraft was shown as level but was actually in an ongoing turn, indicating that RREs were in many cases caused by expectation-induced misinterpretation of the AI bank angle.

These results cannot be completely extrapolated to experienced pilots as they are taught to ignore vestibular cues and only rely on the AI as well as them knowing how to use and interpret the AI. However, even experienced pilots are not immune to their expectations influencing their judgment of their attitude, as was discussed in Section 4.1.

Another experiment was done with pilots where a new way of simulating the leans illusion (van den Hoed et al., 2020), which will be explained in Section 4.3, was tested but at the same time showed the influence of expectation. Pilots were tasked with leveling the wings of the aircraft. On average they made RREs 19.4% of the time when the motion cues indicated a roll in the opposite direction of what the AI showed and 6.9% of the time when no motion cues were given but the AI simply indicated a bank angle.

4.3. Simulating Spatial Disorientation

Correctly interpreting the AI is vital when in a situation of spatial disorientation. Thus, to truly put an adapted version of the AI to the test, spatially disorienting motion cues should be used. This section will focus on finding ways to simulate the leans illusion as it is one of the most experienced in-flight illusions. Unfortunately, very few ways of simulating the leans illusion, and spatial disorientation in general, currently exist. A total of four specialized spatial disorientation simulators were found: Airfox ASD, GYRO-IPT II, Desdemona, and the Polish Spatial Disorientation Simulator. However, no simulation of the leans procedure, or any disorientating procedure for that matter, could be found for the Polish simulator (Dariusz, 2018). Desdemona can simulate several disorientation effects, but no detailed procedure was found either (Desdemona, 2018).

Airfox ASD The Airfox ASD was developed by AMST and the way it simulates the leans illusion is as follows (Bles, 2008): The participant follows instructions during instrument flight. While the participant slowly rolls into a 30° banked turn, the simulator stays upright due to a special asymmetric parameter setting of the washout filters. As the participant is tasked to roll the aircraft back to wings-level, the simulator platform quickly rolls to the opposite side, where it then stays for a moment due to filter settings, before slowly rolling upright again. In essence, both a super-threshold roll motion as well as a moment of maintaining the roll angle are used to instill the leans sensation onto the participant. This procedure does not fully correspond to the actual sensations felt by pilots during the leans. The tilt angle of the simulator to make the pilot ”lean” to the side, also tilts the specific force, which does not happen in flight. An experiment done with ten air-force pilots (Ledegang & Groen, 2018) using this procedure did not cause a significant change in pilots' roll inputs. That same experiment did show that during the leans illusion, albeit the cloud leans, the number of glances by pilots to the AI increased while the glance duration decreased. This shows the importance of correct interpretation of the AI.

GYRO-IPT II The GYRO-IPT II was developed by the Environmental Tectonics group and uses the Coriolis illusion to create a roll sensation (Bles, 2008). The participant is tasked with flying a maneuver during the night. They thus have no real horizon to base the aircraft's attitude on and follow instructions given to them. While the participant rolls to a 45° banked turn, the simulator platform is tilted at a super-threshold rate to a 10° roll angle and simultaneously pitches subliminally to a 10° nose up angle and accelerates subliminally to a yaw rotation of 12°/s. When the pilot rolls out of the turn-to-level flight, the simulator rolls

back to an upright position and pitches to level in about three seconds while yaw motion slows down to a full stop in four seconds. The leans illusion is instilled onto the participant by a cross-coupled Coriolis effect due to the simulator leveling while yaw rotation is still occurring. This adds to the roll sensation caused by the super-threshold roll motion back to level, initiated by the pilot. After this, the attitude displays freeze for ten seconds to take the pilot out of the loop and the pilot is tasked to maintain level flight. Several studies have been performed with this simulator, however, leading to mixed results in terms of its effect (Lewkowicz, Bałaj, & Francuz, 2020; Stróżak et al., 2018; Lewkowicz, Strozak, Balaj, & Francuz, 2019). The Coriolis effect also adds undesired and confusing pitch and yaw cues, making it less accurate in simulating the leans illusion.

Not only do the previously mentioned procedures induce unrealistic sensations that are not felt during an actual leans illusion, but they also require special hardware. Only procedures that are viable with a conventional hexapod are of interest. Researchers at the Delft University of Technology have set up a procedure that can induce the leans illusion in any hexapod motion simulator, making it very cost-effective (van den Hoed et al., 2020).

Leans in hexapod simulator Participant pilots are tasked to behave as if in real flight and to only take over the autopilot and roll back to wings-level when the ”autopilot disconnect” alarm sounds. The procedure starts with straight and level flight with autopilot engaged. First, throughout the entire procedure, light turbulence was simulated in the vertical axis to mask any motion onsets. Second, pilots performed a distraction task on a tablet attached to the surface of the center pedestal to their right side which required them to slightly lean sideways and turn their head to the side. After approximately 10 seconds of flight, a simulator prepositioning phase starts during which the simulator is subliminally tilted to a roll angle of 3.5°. After this phase, the pilot gets momentarily distracted from the instruments and outside view. For the next 33 seconds, the AI and outside vision turn black while the simulator maintains a steady roll angle of 3.5° to induce vestibular adaptation to the roll angle. This was done for two reasons: Prolonged exposure to a roll angle can cause an aftereffect wherein a subsequent roll angle towards the opposite direction is overestimated in that direction, and to realistically simulate a situation in which the aircraft rolls to a new bank angle below the pilot’s perceptual threshold. At the end of the adaptation phase, the ”autopilot disconnect” alert sounds, indicating that the pilot should prepare themselves to intervene by facing the still-black AI and by holding the control column. Two seconds after the alert, the simulator is rotated back to level in two seconds, i.e. at 1.75°/s, which is above the perceptual threshold of the vestibular system. This presents tactile cues as the motion shifted the pilot into their seat. One second after this super-threshold cue ends, the AI is shown again, and the pilot has to roll back to wings-level.
With this procedure, cues that would not occur in an in-flight leans, such as pitch or yaw cues or a pronounced roll angle, are minimized and the simulator platform is upright when the pilot performs the response task. The latter is important as it ensures that pilots respond to the leans illusion and not to simultaneously occurring motion cues. A study was done with eighteen commercial airline pilots where the previous procedure was used with different scenarios: roll cues matching the AI indicated bank angle but in opposite direction (leans-opposite condition), no roll cues but AI indicating a bank angle (baseline condition), and roll cues but with AI showing wings-level (leans-level condition). On average in four runs, pilots made significantly more errors in the leans-opposite condition (19.4%) compared to the baseline (6.9%) or leans-level condition (0.0%). It also showed a pronounced learning effect as during the first encounter of the leans-opposite condition, 38.9% of pilots made an RRE which linearly decreased to 0.0% in the fourth, and last, encounter.

This procedure can be done in a regular hexapod and gives the most accurate sensation of the leans illusion. One run of this procedure takes quite a long time and due to the steep learning curve, it might be better to limit the amount of experiment runs done with this procedure. Perhaps the option of keeping it simpler and just focusing on surprising the pilot by letting the simulator perform a simple roll motion and then either showing a matching bank angle or a bank angle in the opposite direction, should be explored. While this would not give a very accurate representation of the leans illusion, it would still be disorienting. A two-part experiment could be done with first the longer, more accurate leans illusion and then the simpler, shorter runs afterward.

4.4. Design Deficiencies Moving Horizon Attitude Indicator

The moving horizon (MH) attitude indicator used in the West has been linked to spatial disorientation and roll reversal errors and has been called ”less intuitive” than the moving aircraft (MA) display used in Russian planes. However, the switch to moving aircraft will most likely never be made in the West due to, amongst other things, enormous effort in terms of investments and new certifications. Yet, it may be possible to make the display more intuitive to use, so it is important to look at why the MA display has been deemed more intuitive and what the design deficiencies are of the MH display to improve it. It is necessary for pilots to think ”The aircraft is moving”. If they think the outside is moving, they get disoriented and become subject to vertigo (Johnson & Roscoe, 1972). The main issues with the MH display relate to display control compatibility and figure-ground reversal.

Display-control motion compatibility The operator may consider the movement of a display symbol from a fixed reference as something they must follow to correct their error or as something they have control over and must ”bring back” to the fixed reference. It is important for pilots to realize which of the two it is as the outcomes of both options are very different. In the case of the MH display, the movement of the horizon is something they must bring back to the fixed reference. However, two main issues make this realization much more difficult (Müller et al., 2018):

- Response-effect compatibility: The relationship between the direction of movement of the controls and the anticipated effect in terms of a change indicated in the display is compatible when the direction of movement within the display directly responds to the direction of movement of the control input device that causes that movement. For the MH display, a leftward (or counterclockwise) movement of the side stick or control column results in a clockwise movement of the moving element (the horizon). This violates the response-effect compatibility principle.
- Stimulus-response mapping: The relationship between the observed changes in the display and the control response required to compensate for these changes must fit the mental representation of the task. For example, to compensate for a movement in the left direction, a control response to the right would make sense. However, in the case of the MH display, a control response to the left would be needed. This violates the stimulus-response mapping principle.

The display-control compatibility of the MH display cannot be changed as that would mean completely changing the dynamics of the display and, as mentioned before, that will not happen. Several researchers have proposed displays that have different dynamics, as will be discussed in Section 4.5, however, none of them have been implemented.

Figure-ground reversal Figure-ground organization is a process of how the brain distinguishes between a figure and the (back)ground. This concept will be explained in more detail in Chapter 5. Psychologically, the part of the field of view that moves is the ”figure”, and the stationary part is the ”ground” (Johnson & Roscoe, 1972). Yet, if most of the visual field moves uniformly, it can be perceived as a stationary background while the observer is moving. This is what happens when pilots look out of the cockpit windscreen. When flying a turn, they see the natural horizon moving but they interpret it as a movement of the aircraft. However, this is different from looking at the movement of the artificial horizon line of the MH display as the horizon does not satisfy the typical characteristics of a background (Müller et al., 2018): It is not represented far behind the aircraft symbol and is a comparatively small moving element included in a much larger and stable (relative to the pilot) instrument panel. When the outside world horizon disappears, e.g., in bad visibility or when flying through clouds, the pilot seems to mentally shift to the cockpit of their aircraft as being the stable reference (or ground), against which other elements, such as the AI horizon, move, which will then be considered as figures/Prelim. This leads to a reversed interpretation of figure and ground (Grether, 1947). In essence, due to the horizon not satisfying the characteristics of a background, the pilot identifies with the moving part, the horizon, and tries to move the horizon bar instead of the fixed aircraft symbol, also known as horizon-control reversal (Roscoe, 2004).

The neuropsychological explanation for figure-ground reversal is based on the assumption that objects close to the pilot, like the cockpit instruments, are perceived and processed differently than information that is further away, like the natural horizon. More specifically, four major brain systems are involved when interacting with the external three-dimensional world (Müller et al., 2018). The closest system is the

peripersonal system which is involved in manipulating and interacting with objects near our bodies. The movement of objects in this space is usually recognized as what they are and are not consequences of self-motion. The opposite of this system is the ambient extrapersonal system which processes information in faraway distances of the field of view and is mainly concerned with monitoring, controlling, and stabilizing a person's position in reference to Earth. Large-scale movement in this domain is usually understood as a consequence of self-motion. Based on this, the main issue with the MH display and the basis for figure-ground reversal seems to be that movements of the natural horizon, which are usually seen as large-scale changes in the far domain and are processed by the ambient extrapersonal system, are shown by a small instrument that is placed in the peripersonal space. It can thus be expected that the artificial horizon of the MH display is intuitively perceived as the controllable element instead of a consequence of self-motion.

Gillingham and Previc (1993) has a very similar theory, however, his theory is not limited to the MH attitude indicator but also applies to the MA display. According to them, the visual-spatial orientation information is presented to the wrong sensory system, namely the focal visual system. As mentioned in Chapter 3, focal vision is not naturally equipped to provide spatial orientation cues. Focal vision must now serve a dual purpose: It has to process the numeric data from several instruments but also has to take on the task of spatially orienting the pilot. This leaves the ambient system, which *is* naturally equipped for spatial orientation, unutilized, or worse, harassed with misleading orientational stimuli.

4.5. Mitigation Efforts

Several attempts at improving the AI to decrease the number of roll-reversal errors have been made, most of which have not been implemented. These attempts can be categorized into two groups: concepts that are very different from the currently used AI (including different dynamics) or enhancements to the moving horizon AI.

4.5.1. AI Replacements

The following AI concepts differ greatly from the currently used MH AI, either due to their different dynamics, use of ambient vision system, or because they look very different. It is highly unlikely these concepts will ever replace the commercial MH AI, but inspiration can be drawn from them.

Frequency-separated display As explained in Chapter 3 the vestibular system only senses accelerations and no information on rates or positions. Keeping this in mind Fogel (1959) concluded that to achieve visual and vestibular compatibility, only the initial motion of the display should be in the same direction as the angular acceleration and thereafter the direction of motion of the display may be reversed without conflicting with vestibular and kinesthetic cues. In essence, it appears that it is critical that elements of the display that respond immediately to pilot inputs move in the expected direction whereas the direction of movement of the more slowly responding display indications are far less critical. Fogel thus introduced the Kinalog display, the best-known example of a frequency-separated display, where the initial response of the attitude presentation follows the principle of the moving part and once the aircraft is in an established turn, the horizon line and aircraft symbol slowly rotates such that the steady turn is indicated by a tilted horizon. What a 45° roll would like on a Kinalog display is shown in Figure 4.1. It has, however, been found that this display type can also lead to confusion and can even be nauseating for some pilots (Roscoe & Williges, 1975). It is unclear whether this display might still be confusing in a sustained roll when there are no visual inputs. During a long turn, pilots no longer feel that the aircraft is banked so when they look back at the AI showing the tilted horizon, they could still be subject to figure-ground reversal.

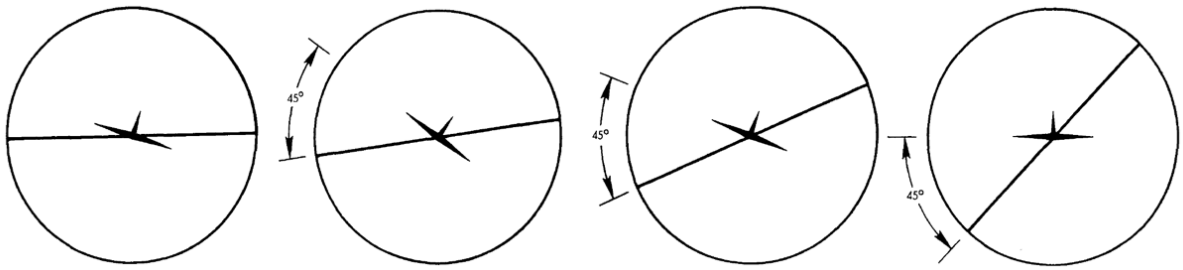

Figure 4.1: A 45° roll shown on a Kinalog display (Fogel, 1959)

"Mixed" display The "mixed" display was researched by Gross and Manzey (2014). In the display, both the aircraft and the horizon symbol move in a certain ratio to each other. Neither the aircraft nor the horizon shows the actual bank angle, however, the angle between the aircraft and horizon line does depict the actual angle of the aircraft, i.e., similar to the second and third display portrayed in Figure 4.1. This causes extreme deviations from a horizontal attitude to be depicted as moderate angles on the display, making it easier to identify the necessary steering direction. However, this display type is very artificial as it does not depict reality and it might be the most confusing for pilots trained in instrument flying. While the research showed that significantly more errors were made using the MA and MH display, it was done in a fixed-base simulator so the results can be disputed.

Malcolm horizon The Malcolm horizon is based on the fact that humans use their ambient visual system for spatial orientation. A long thin line representing the true horizon is projected across the instrument panel and moves in the same way as the true horizon. Its size and utilization of ambient vision, meaning it does not have to be consciously monitored, reduces the likelihood of deviations not being noticed and corrections can be made before unusual attitudes have the chance to occur. It also still provides orientational cues when focal vision is worsened by turbulence. There have been conflicting findings regarding its effectiveness. Due to its limited pitch display range problems with installations, not being fully compatible with many instrument panels, and lack of evidence on its effectiveness, it was not widely implemented in commercial aviation. Current technology would permit other methods of presenting the extended horizon line, however, the effectiveness would still need to be researched further (Gillingham & Previc, 1993; Comstock., Jones, & Pope, 2003). Completely changing the current AI to one that would only use ambient vision does not seem like a good idea according to Taylor (1988): Ambient processing would work in theory but not in practice. It is unlikely to allow for accurate pitch and bank angle control that is necessary for precision maneuvers nor is it likely to assist in unusual attitude recovery that involves focal attention and the conscious application of rules and heuristics such as "roll and pull to the nearest horizon". A combination of focal and ambient processing would be needed.

Background attitude indicator The background attitude indicator (BAI) seems to be more geared towards military aviation. Pilots can look at tactical information in the center of the screen while the attitude information is displayed behind it, making use of parafoveal vision. The original BAI was created by Dawson and Spangler at General Dynamics and was good at portraying roll but not so much at portraying pitch, thus changes were made to include a "ghost horizon" that moves in the same way as the actual horizon but would still be present when the true horizon left the field of view. It was found by Liggett, Rebing, and Hartsock (1992) that by adding a combination of color shading and color patterns, as can be seen in Figure 4.2, the initial input time to recover from an unusual attitude decreased. The shading, a lighter color near the horizon, would indicate whether the nose was up or down and the color pattern, a truncated arrowhead, directs the pilot back to the horizon. Adding pitch lines with numbers increased the initial input time, most likely because it broke up the optical flow and the numbers had to be read. However, pilots still preferred it. Other adaptions to the BAI have also been made, such as the number of displays encapsulated by the BAI, however, for the current research, this is less relevant.

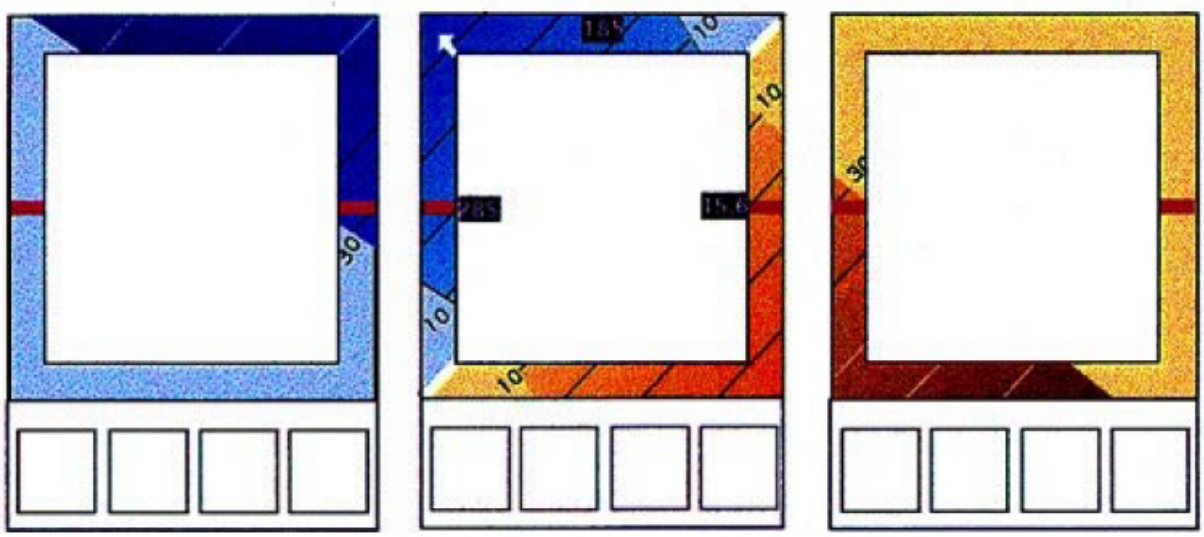

Figure 4.2: Use of color shading and color patterns in the background attitude indicator (Reising et al., 1995)

Arc-segmented attitude reference display While the previously mentioned displays still had some similarities with the regular AI, the arc-segmented attitude reference (ASAR) display looks, as can be seen in Figure 4.3, and works completely differently. Level attitude is indicated by a semi-circle. Pitch deviations are shown by the amount of arc displayed and deviations in bank are indicated by how much the center of the arc is rolled left or right. The ASAR display is mainly looked at to use as a Head-Up-Display (HUD), but it is not advised to be used for a standard forward-looking HUD, as it presents the attitude in a different reference frame from that of the visual world. Research comparing ASAR to an MH and MA HUD in unusual attitude recoveries did not have generalizable results (Wickens et al., 2007).

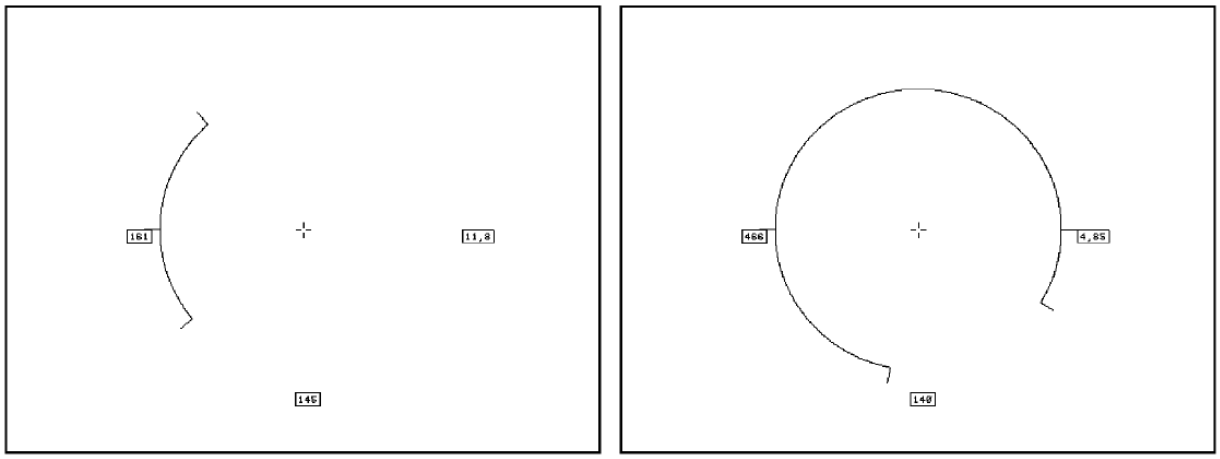

Figure 4.3: Arc-segmented attitude reference display (Self et al., 2002)

Spatial Disorientation Icon Wickens et al. (2007) proposed to add a command icon, as can be seen in Figure 4.4, that points to the appropriate airplane rotation in pitch and roll to recover to wings-level. A computer-based experiment where both novice and experienced pilots had to recover from unusual attitudes showed that the spatial disorientation icon decreased initial correction time and reduced the number of RREs. Out of the 22 subjects, nineteen also felt that the addition of the icon helped them perform better.

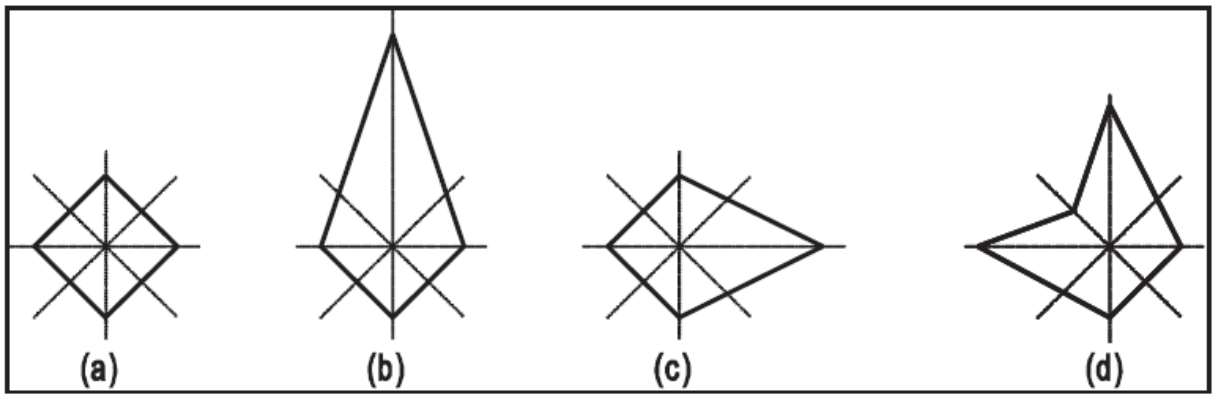

Figure 4.4: Spatial Disorientation Command Icon for an aircraft whose state is: (a) 0° pitch, 0° roll; (b) -90° (down) pitch, 0° roll; (c) 0° pitch, -45° (left) roll; (d) -45° pitch, +45° roll (Wickens et al., 2007)

4.5.2. AI Enhancement

In this subsection, an overview of several design elements that have been previously added to or changed about the AI in an attempt to decrease the number of roll reversal errors will be given.

Three-dimensional displays Some research has been done on three-dimensional displays, however, the research either did not compare it to two-dimensional displays showing equivalent information and the very few that did, have limitations on their generalizability (Haskell & Wickens, 1993). Three-dimensional displays are subject to clutter, making it harder to find information, and the created depth perception is less accurate. Some also integrate changes of all variables into one object, causing the loss of variation in different variables. Research has also been done on using a multi-layer display (Arrundell et al., 2021) to create real physical depth, however, the results of this research were not in favor of it.
The main advantage attributed to three-dimensional displays is the realism. However, users often naively predict superior performance and strongly prefer realistic displays over non-realistic ones even though performance with realistic displays has been demonstrably worse. This is called ”naive realism”, the misplaced faith in people’s ability to extract accurate information from realistic displays (Smallman & John, 2005).

Roll index The roll index, also known as the sky pointer, is designed to indicate the bank angle of the aircraft, however, it can also be used to identify in which direction the aircraft is banking. A spatially compatible roll index should move in the same direction as the airplane roll in relation to Earth, this is however not always the case (Ding & Proctor, 2017). Commercial, general, and military aviation all use a different type of roll index (Singer & Dekker, 2002) as can be seen in Figure 4.5.

- Commercial aviation: The roll index is positioned on the top and slaved to the horizon. When flying back to wings-level, the roll index will move in the opposite direction of the control movement, meaning the roll index is incompatible.
- General aviation: The roll index is on top and slaved to the aircraft symbol. The roll index and the control movement always move in the same direction. For example, when recovering from a right bank, the pilot performs a control input to the left, and the roll index also moves to the left.
- Military aviation: The roll index is positioned at the bottom and slaved to the horizon, this is also called an ”Earth pointer”. The pilot needs to make sure that the index points straight down instead of up. As it is slaved to the horizon, the roll index will move in the same direction as the control movement, it can be seen as spatially compatible.

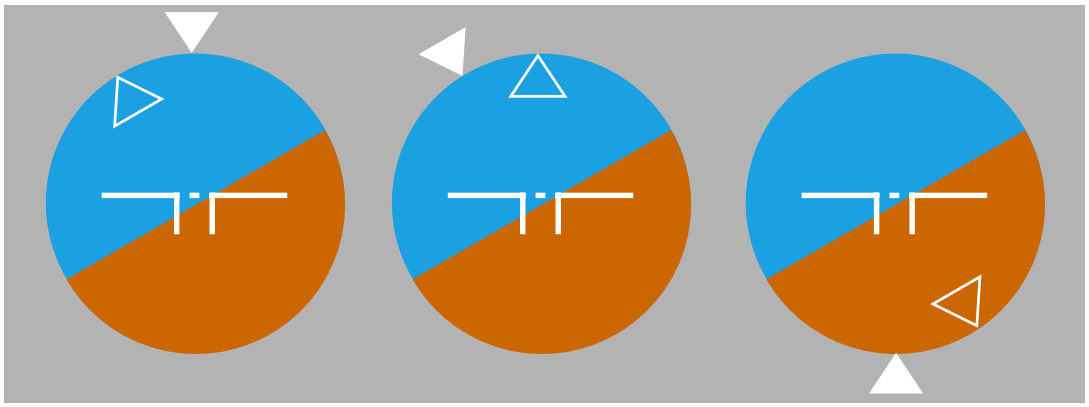

Figure 4.5: The three roll index configurations: commercial (left), general aviation (center), and military (right)

Research in which commercial pilots had to perform roll recovery tests using all three types has shown that the number of roll reversal errors is five times as high using the commercial roll index compared to the other two (Singer & Dekker, 2002). While this experiment was done using a PC setup, meaning there was no vestibular input that could have given cues to the pilots, the large differences do indicate that compatibility of the roll index does make a difference.

Color gradient and isosceles triangles This idea by Maertens (2009) is based on the findings of Liggett et al. (1992) where the original BAI was adapted using color gradients and color shapes. It seems that up until today, this idea has unfortunately not been tested but it will be discussed as some inspiration could be drawn from it. Three adaptations to the AI were proposed:

- Horizon indicator: To ensure the pilot will always find their way back to the horizon, even in extreme attitudes, isosceles triangles will be drawn on the ground and sky of the AI with their apices meeting at the horizon, forming an hourglass shape. The triangles will be colored with a gradient that is dark near 90° pitch and lighter towards the horizon. The color gradient gives an indication of whether the horizon is up or down and the shape points in the left or right direction. Figure 4.6 shows what exactly this would look like
- Roll and pitch indicator: These indicators, as can be seen in Figure 4.7 would be right outside of the AI and would become green in the direction of the correction necessary to recover to straight and level flight but only in cases that could become dangerous to avoid human misuse of the automation. They would also raise awareness of hazardous situations as they develop and would blink if a pilot fails to recognize the warnings. The turn-off threshold should be lower than the turn-on to prevent issues where the pilot is flying on the cusp of the illumination settings and the indicator would turn on and off with slight changes in bank.
- Throttle guidance indicator: A horizontal line will be placed above the horizon if the throttle input needs to be decreased and below the horizon if it needs to be decreased.

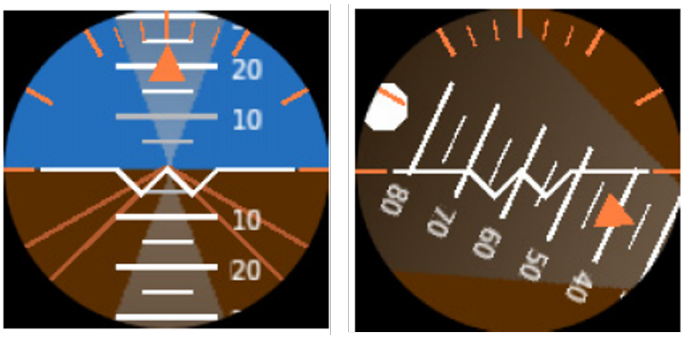

Figure 4.6: Horizon indicator with isosceles triangles with color gradient (Maertens, 2009)

Figure 4.7: Roll and pitch indicators commanding a right bank and pull up (Maertens, 2009)

Increasing display size Although display sizes have increased in current glass cockpits, the AI is still quite small compared to the natural horizon, which places an unnatural demand on focal vision so the question is whether a larger display could help with this problem. Results from research into the display size on attitude tracking and upset recovery tasks have been inconsistent. Some studies show no significant difference (Hiremath, Proctor, Fanjoy, Feyen, & Young, 2009; Kelley, de Groot, & Bowen, 1961), others say bigger is better (Comstock. et al., 2003) and some show deterioration in performance with increased display size claiming it is difficult to integrate attitude information over large areas (Taylor, 1988).

Extended horizon In most aircraft, the altitude, and speed tapes are positioned to the side of the AI, completely separating it. Early research into AI enhancements has shown that extending the horizon such that the speed and altitude tape overlap it, improved spatial awareness. It supports the interpretation of the artificial horizon as (back)ground and thus reduces the figure-ground reversal issue. The B787 has one of these extended horizons, a comparison between the extended horizon and a classic horizon can be seen in Figure 4.8. Experiments (Comstock. et al., 2003), albeit on a PC, where pilots had to recover from unusual attitudes showed that the extended horizon decreased the differences between MA and MH display for experienced pilots. For novices, the extended horizon did not make much of a difference, but this is most likely because the familiarization phase might not have been sufficient for novices to get a proper understanding of the basic logic behind the MH format and its relationship with the natural horizon. Any design choice that was made to make the figure-ground relationship more intuitive might have been affected by this lack of understanding. Experienced pilots do have this understanding and have much more experience with both visual and instrument flying and could thus benefit more from a better figure-ground separation (Comstock. et al., 2003). The extended horizon seemed to reduce or even eliminate the differences between MH and MA.

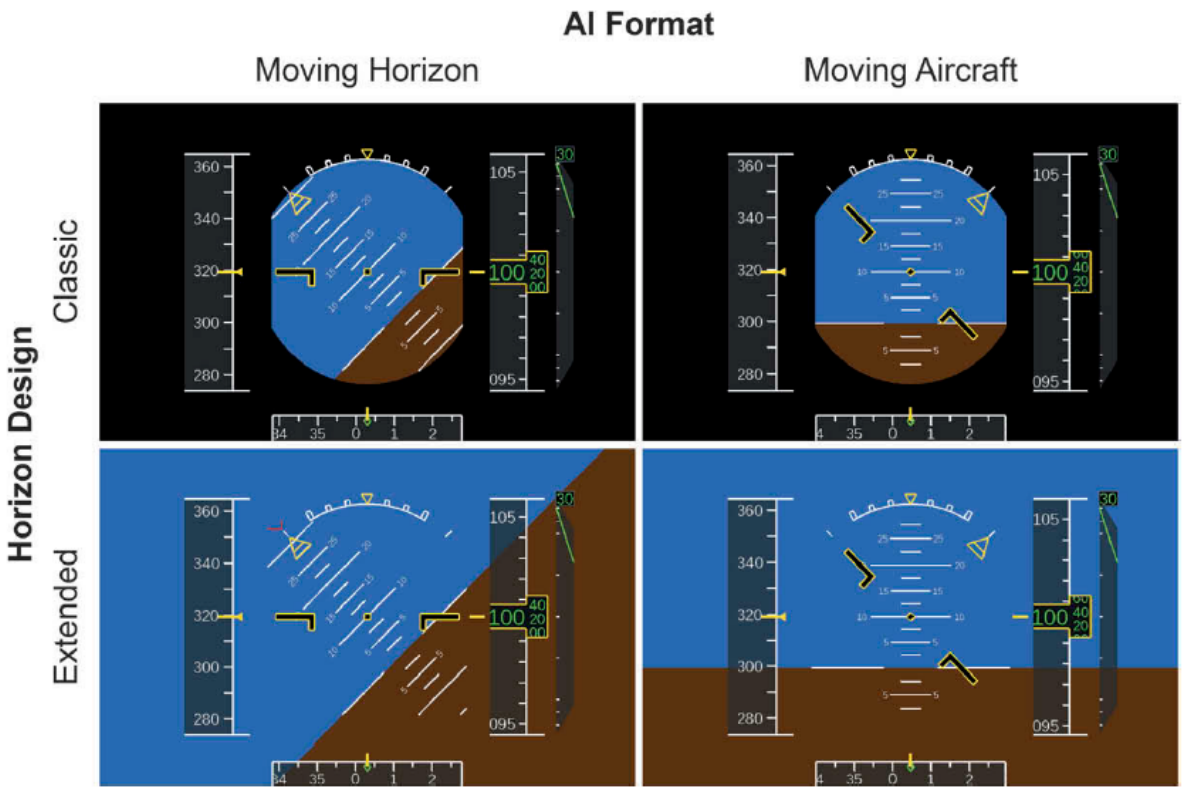

Figure 4.8: Attitude indicator formats showing the effect of the extended horizon for both moving horizon and moving aircraft displays (Müller et al., 2018)

Synthetic Vision Systems Synthetic vision systems (SVS) aim to show more realistic images of the real world and make use of static depth cues such as texture gradients and the extended background. Some also use motion-based depth cues, such as motion parallax. Motion parallax is used in AIs that indicate the path that a pilot has to fly through a tunnel, which is known as the tunnel-in-the-sky (TIS) display. The primary flight information overlaps the background, further increasing the figure-ground. Figure 4.9 shows a display using both SVS and TIS. As mentioned before with three-dimensional displays, one has to be careful with drawing conclusions about the benefits of providing realism with these displays.

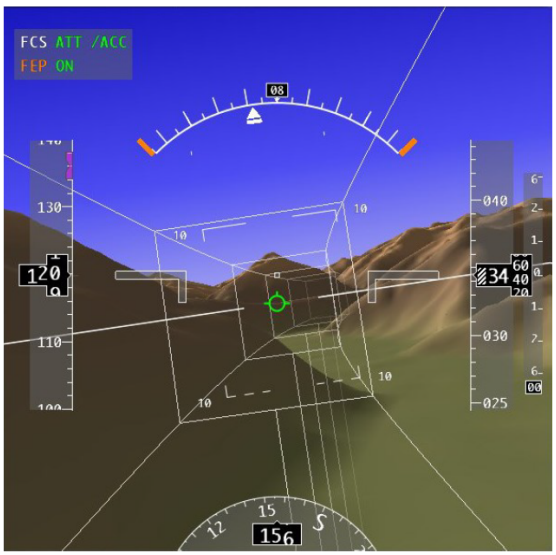

Figure 4.9: Synthetic vision system with tunnel-in-the sky effect (Borst, C., 2021)

4.6. Research Proposal

The AI display shows the attitude of the aircraft, which is a crucial variable to safely fly. However, the currently used AI display is not optimal when looking at it from a figure-ground perspective: First, humans tend to view the moving part of a display as the ”figure” compared to a static background, which is the opposite of what happens in the moving horizon AI. Second, AI displays do not satisfy the characteristics of a background. Most AI displays do not have any depth, they are abstract blue-brown colored rectangles, which inhibits humans from seeing the horizon as something ”behind” the aircraft symbol and the display is small compared to a much larger and stable instrument panel. These issues could have disastrous consequences in situations where pilots are disoriented and/or end up in situations where they have to quickly, and preferably without thinking, correct the aircraft's attitude.

Research Gap Researchers have attempted to solve both issues mentioned before. However, to resolve the moving part issue (e.g., by using the Kinalog display), the dynamics of all AIs in Western aircraft would need to be changed and pilots would need to be retrained, which in itself could lead to dangerous situations if pilots revert to their old habits. This is not realistic, leaving the figure-ground issue to be resolved. The extended horizon and multi-layer displays have attempted to solve this issue with some success for the extended horizon (Comstock. et al., 2003), but multi-layer displays did not have the wanted effect (Arrundell et al., 2021). Increasing the display size also had mixed results (Hiremath et al., 2009; Kelley et al., 1961; Comstock. et al., 2003; Taylor, 1988). Most experiments did not attempt to recreate a situation of spatial disorientation and did not investigate the effect of their displays in situations like these. Also, most experiments were done in fixed-base simulators or using regular PCs, thus not considering the influence of vestibular cues.

Research Proposal Creating the illusion that the horizon is behind the aircraft symbol can also be done by adding static monocular depth cues and applying principles of grouping, which will be explained in Chapter 5. Static monocular depth cues have been added in SVS displays but their specific impact is unclear as the extended horizon was also used and motion-based depth cues were added to the SVS displays that use TIS. Enhancing the figure-ground relationship using purely static monocular depth cues and seeing the effect of this has thus not yet been explored. The research question for the thesis project will thus be:

”What is the effect of the addition of static monocular depth cues to the moving horizon attitude indicator display on the interpretation of the attitude indicator bank angle measured by roll reversal errors made?”

An experiment will be performed where the adapted AI display will be compared to the regular moving horizon AI display. The interpretation of the attitude indicator will be tested in terms of the following dependent measures, which also have been used in previous experiments (Liggett et al., 1992; Haskell & Wickens, 1993; Singer & Dekker, 2002; Wickens et al., 2007; Gross & Manzey, 2014; Ding & Proctor, 2017; Müller et al., 2018; van den Hoed et al., 2020) :

- *Error Rate*: A roll reversal error is recorded when a control input is received in the opposite direction of the control input necessary to fly back to wings-level and exceeds 1.5 degrees (Landman et al., 2020). The error rate is the percentage of the total number of runs in which an error is recorded.
- *Error Duration*: This is the time between when the error was recorded and the participant gives a correction to the correct side. It is the time it takes for the participant to correct their error.
- *Error Severity*: This is the measured bank angle deviation from level flight when an error was made.
- *Reaction Time*: This is the time between the AI being shown again and the first control input the pilot gives.
- *Subjective Workload*: Pilots will be asked to give a subjective rating of the workload experienced.

The experiment will be performed in a motion-based simulator and will recreate situations of spatial disorientation. This would make the experiment more realistic and would also increase the likelihood of creating RREs, which would give more data to work with when comparing different displays.

5
Human Visual Perception

Understanding human visual perception can significantly improve the quality of the information being shown on displays with which they need to interact. To improve the attitude indicator to decrease roll reversal errors, it is thus vital to look into how humans perceive their surroundings. It should be noted that humans make a ”complete picture” of their surroundings based on the stimulus world which they process through their senses. This is known as ”bottom-up” processing. They also make this picture based on their knowledge, experiences, and desires, which is the ”top-down” approach. The latter approach is an active voluntary process whereas the former is passive (Theeuwes, 2010; Connor, Egeth, & Yantis, 2004). Section 5.1 will display depth perception and the different static monocular depth cues that can be used to improve the AI display. Section 5.2 will describe pre-attentive processing. Lastly, Section 5.3 will explain the concept of perceptual organization. All these aspects are bottom-up approaches, although experimental research has argued that depth perception is influenced by the top-down principle and attributes this to the fact that humans have expectations of three-dimensional objects that override the true depth information (Bülthoff, Bülthoff, & Sinha, 1998).

5.1. Depth Perception

Depth perception is the ability to perceive the world in three dimensions and have a sense of the distance of an object. For depth perception to be possible, depth information cues need to be present. Figure 5.1 gives an overview of the various depth cues and their classification.

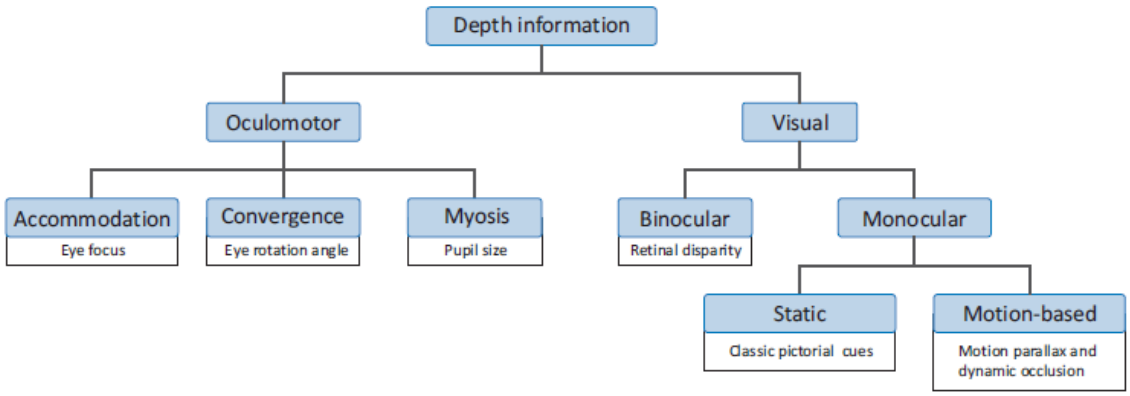

Figure 5.1: Overview and classification of depth information cues (Tovée, 2008)

The first layer of categorization divides the dept cues into oculomotor and visual cues. The oculomotor cues refer to the oculomotor muscles which can move the eyes. These muscles tighten when the eyes move inwards, i.e., when looking at an object nearby, and relax when the eyes move outwards. The brain senses this tensing and relaxing and gives an estimate of how far away an object is. The visual cues are the ones that ’trick’ the brain into thinking depth is present. Visual cues can be further divided into binocular cues and monocular cues which make use of both or either one eye respectively. Monocular cues come in two categories: the static ones and the motion-based ones. The latter one includes motion parallax, also known as optical flow, where objects closer-by have a greater displacement than objects further away when moving linearly through the environment (Tovée, 2008). The static monocular depth

cues are often referred to as ”pictorial depth cues”, such as (Gibson, 1950; Gillingham & Previc, 1993; Haber, 1980):

- Size constancy: The size of objects that are known and object sizes compared to each other. The smaller an object, the further away it will be perceived.
- Shape constancy: The shape of an object compared to the known shape of that object (e.g., a circle becoming more ellipsoid the further away it is).
- Interposition: An object overlapping another object is perceived as being closer by.
- Texture gradient: The apparent loss of detail with increased distance.
- Linear perspective: The distance between parallel lines decreases the further away the lines are.
- Light and shadow relation: This comes from the tendency to perceive the light source to be above an object and the association that more deeply shaded parts of an object are further away from the light source.
- Height in plane: The more upward an object is placed in a frame, the further away it is perceived (often combined with size constancy).
- Aerial perspective: Surfaces in the foreground appear brighter and have more saturated colors whereas distant objects appear less bright and less saturated. This is caused by the scattering of light air molecules and by particles in the air, also known as atmospheric haze.

These cues are often combined to strengthen the idea of depth.

5.2. Pre-attentive Processing

As mentioned before, detailed vision for shape and color is only possible in a small portion of the visual field. To see detailed information from more than one region, the eyes move rapidly. This is known as saccadic eye movements where the eyes alternate between short stationary periods (fixations) and brief periods of blindness (saccades). The short periods happen when detailed information is acquired, and the brief periods of blindness happen when the eyes quickly flick to a new location. This cycle repeats 3 to 4 times per second without humans being aware of it (Healey & Enns, 2011). Once the brain has guided the attention to a visual stimulus, the visual processing of a multi-element world consists of two main phases:

1. The pre-attentive phase which is carried out automatically and organizes the visual world into (groups of) objects.
2. Focal attention selects certain objects of the pre-attentive array for further elaboration.

Thus, the brain does not process each stimulus the same way and makes a decision on which stimuli are ”interesting” and which ones are not as much. The interesting stimuli have so-called ”pre-attentive properties” which make them stand out and cause them to be processed before others. Typically, a task that can be performed in less than 200-250 milliseconds is considered pre-attentive (Healey & Enns, 2011). Common properties are divided into three main groups: form, position, and color. Their respective subdivisions are shown in Figure 5.2. It should be noted that the conjunction of two properties is not always pre-attentive, as is the case with color and shape, which can be seen in Figure 5.3. However, it has been found that a combination of a depth cue and color can be pre-attentively processed in parallel (Cave & Wolfe, 1990).

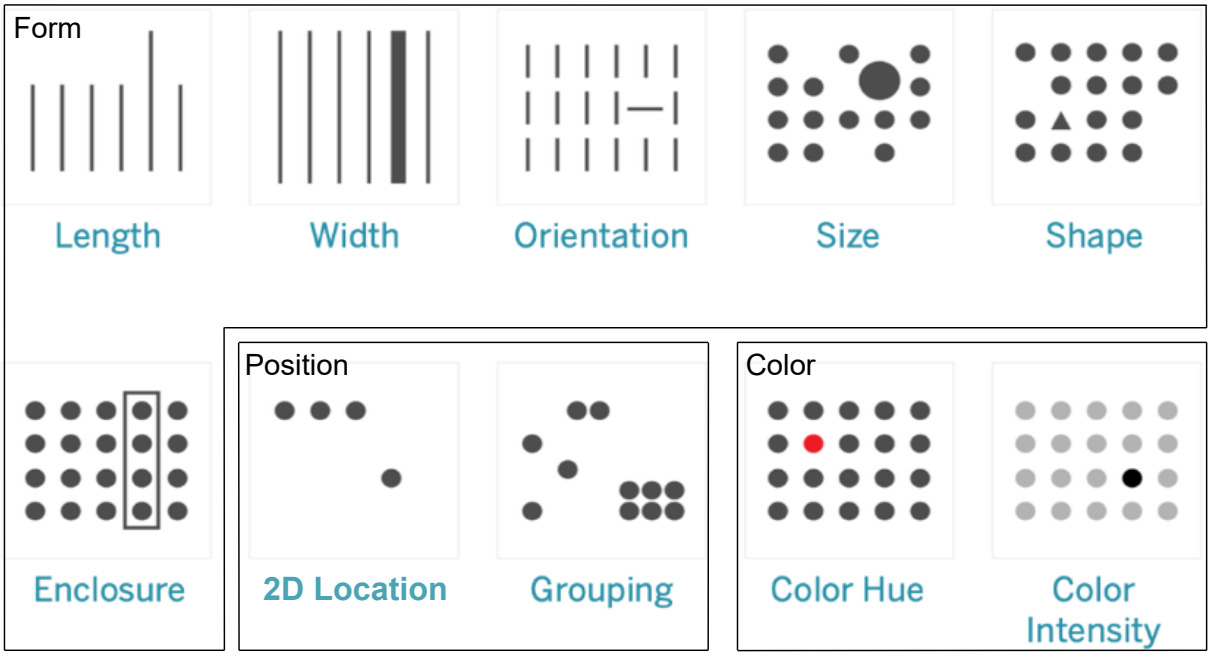

Figure 5.2: Common pre-attentive properties (Tableau, 2023)

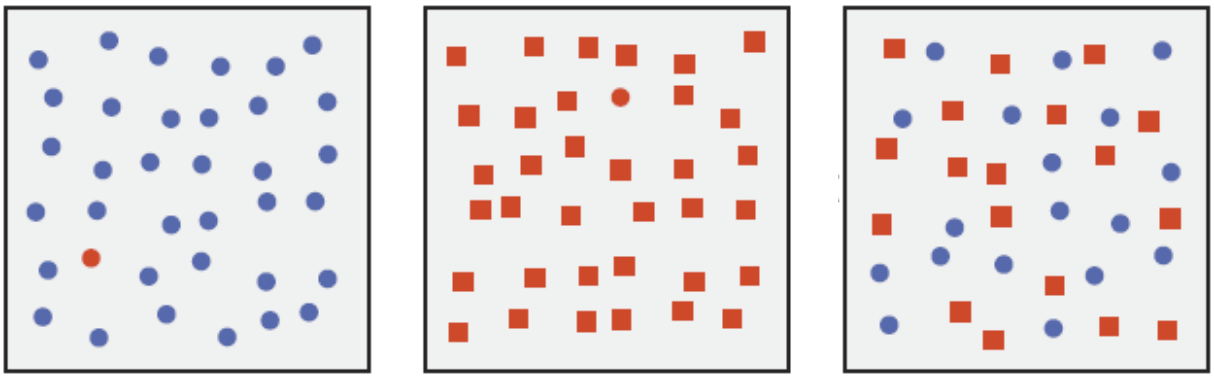

Figure 5.3: Example showing that conjunction of color and shape is not pre-attentive (Healey & Enns, 2011)

5.3. Perceptual Organization: Gestalt Theory

Once the brain is done with the pre-attentive processing of stimuli, it has to decide on how to group these stimuli and form a pattern. Gestalt psychology is often summarized as ”the whole is different than the sum of its parts” which also explains why the conjunction of two pre-attentive properties is not always pre-attentive. In the early days of Gestalt psychology, three key observations stood at the base of the ideology (Wagemans, 2018):

- The perceptual experience is organized in a particular way, it consists of objects and background.
- Organization depends on a particular grouping, seemingly going hand in hand with segregation from the rest.
- Perceptual organization appears definite and lawful, not arbitrary and the lawfulness does not result from an act of will.

The early founders of Gestalt psychology investigated the underlying principles of grouping and segmentation, which have now become known as Gestalt principles. These principles are (Wagemans, 2018):

- Proximity: Elements closer to each other are grouped, and elements further apart are segregated.
- Similarity: Elements similar (can be in terms of shape, color, size, luminance, motion, etc.) to each other are grouped, and dissimilar items are segregated.
- Common fate: Elements that undergo a particular change together (e.g., moving in the same direction) are grouped together.
- Good continuation: Grouping depends on the relative configuration or arrangement of elements, specifically elements forming continuous lines or curves.
- Closed form: Elements that form closed units tend to be grouped together.
- Past experience: The perceiver's life experience plays a role in grouping, albeit limited.

Some adaptations to these principles have been made over the years as traditional Gestalt psychology received criticism for proposing a new law for every factor shown to have influence. Some could be considered extensions of the old principles whereas others are completely new. The ones that have deep implications on the nature of perceptual grouping and its role in perceptual organization are the following (Wagemans, 2018):

- The principle of grouping by synchrony: The tendency for elements that change simultaneously to be grouped together, independent of the common direction of change or motion of change. This principle can be seen as a more general form of the principle of common fate.
- The principle of common region: The tendency for distinct elements to be grouped together when they lie within the same bounded region. This principle seems to overrule grouping by similarity. See Figure 5.4.
- The principle of element connectedness: The tendency for distinct elements to be grouped together when they are connected in some way. See Figure 5.5.
- The principle of uniform connectedness: The principle by which the visual system initially subdivides an image into a set of mutually exclusive connected regions that have uniform (or smoothly changing) properties such as luminance, color, texture, motion, and depth.
- The principle of induced grouping: The tendency for ungrouped elements to become grouped when there are similar arrangements in the surroundings that are grouped by any of the more standard principles of grouping, such as proximity or element connectedness. See Figure 5.6.

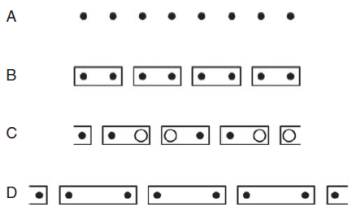

Figure 5.4: Principle of common regions (Wagemans, 2018)

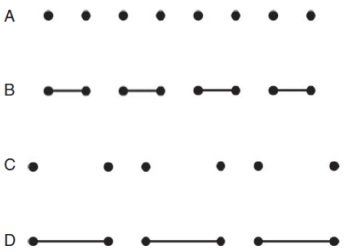

Figure 5.5: Principle of element connectedness (Wagemans, 2018)

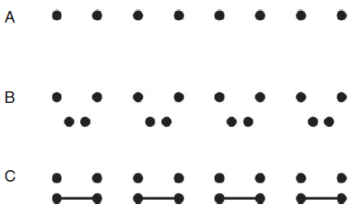

Figure 5.6: Principle of induced grouping (Wagemans, 2018)

Figure-ground organization is another major process in perceptual organization and is closely linked to perceptual grouping. Figure-ground is often also seen as one of the principles of Gestalt but here it will be discussed separately.

Figure-ground organization is the process of how the brain distinguishes between a figure and a background, or ground for short. Which feature is the figure, and which is the ground can sometimes switch, but it can never be both at the same time. The mind insists on one or the other as can be seen in Figure 5.7, which shows the well-known image where either a vase or two faces are seen. Two main mechanisms work in the segregation of figure and ground: boundary detection, which is the enhancement of the borders of the figure, and region growing, which groups regions of the image with similar features together.

Figure 5.7: Example of figure-ground relation: the Rubin face (Schooler, 2015)

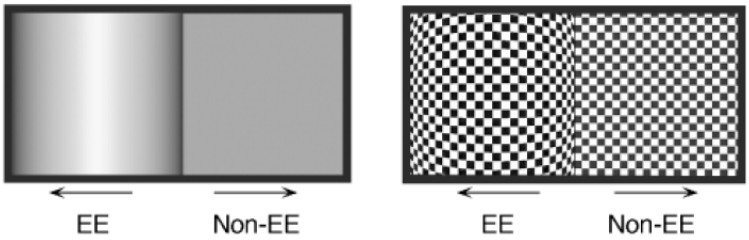

Figure 5.8: Example of an extremal edge with the use of shading on the left and the use of texture on the right (Palmer & Ghose, 2008)

The old principles of figure-ground were: small area, convexity, symmetry, parallelism, and enclosure. However, over the past decades, new principles of figure-ground organization have been discovered. The new principles are relevant to this research as they come into play in displays that contain motion (Wagemans, 2018).

- Lower region: When a rectangular display is divided in half by a clear horizontal border, the region below is more likely to be perceived as the figural region than the one above the border.
- Top-bottom polarity: Regions that are wider at the bottom and narrower at the top, are more likely to be perceived as the figure than regions that are wider at the top and more narrow at the bottom. This principle can be seen as a perceptual consequence of gravity.
- Extremal edges and gradient cuts: An extremal edge is a projection of a viewpoint-specific borderline of self-occlusion on a smooth convex surface, e.g. the straight side of a cylinder. The side with an extremal-edge gradient is almost always perceived as being closer to the observer than the opposite side of the edge, even when placed in conflict with other factors. An example of an extremal edge is shown in Figure 5.8.
- Edge-region grouping: When viewing two surfaces at different distances, two adjacent regions with an edge, form in the optical image. Determining to which region this edge belongs, determines which surface is in front of the other, with the edge belonging to the closer surface. This edge-region grouping works, albeit in widely varying degrees, for the following similarity-based factors: common fate, blur similarity, color similarity, orientation similarity, proximity, and flicker synchrony (Palmer & Brooks, 2009).
- Articulating motion: When a contour segment that is concave on one side and convex on the other deforms dynamically, observers tend to assign the figure to the convex side.
- Advancing region motion: When a border in a limited space moves such that one bounded area becomes larger while the other gets smaller it is perceived as the figure advancing onto a shrinking area.
- Contour entropy: When one area is in front of another, lines of the further away area are terminated by the one in front. When the irregularity (entropy) of the terminated lines is higher, the more often this area of the visual field is perceived as ground.

6

Proposed AI Adaptation

The goal of this research is to see whether adding static monocular depth cues can strengthen the figure-ground relationship of the moving horizon attitude indicator to reduce the number of roll reversal errors. Based on the previous chapters, and in particular human visual perception, some adaptations will be proposed. Various static monocular depth cues will be combined as they can strengthen each other. The additions to the display should not lead to display clutter as this can have a negative effect on pilot performance (Moacdieh & Sarter, 2015). The benefit of slightly adapting the currently used AI is that it would be easy for experienced pilots to transition into. It should be noted that the figures shown in this chapter might not be what the eventual attitude indicator display will look like when actually testing it in an experiment.

First, a shadow below the aircraft symbol will be added. This creates the illusion that the aircraft symbol is closer-by, making the display less ”flat” and causing the symbol to be pre-attentively processed. This effect is shown in Figure 6.1.

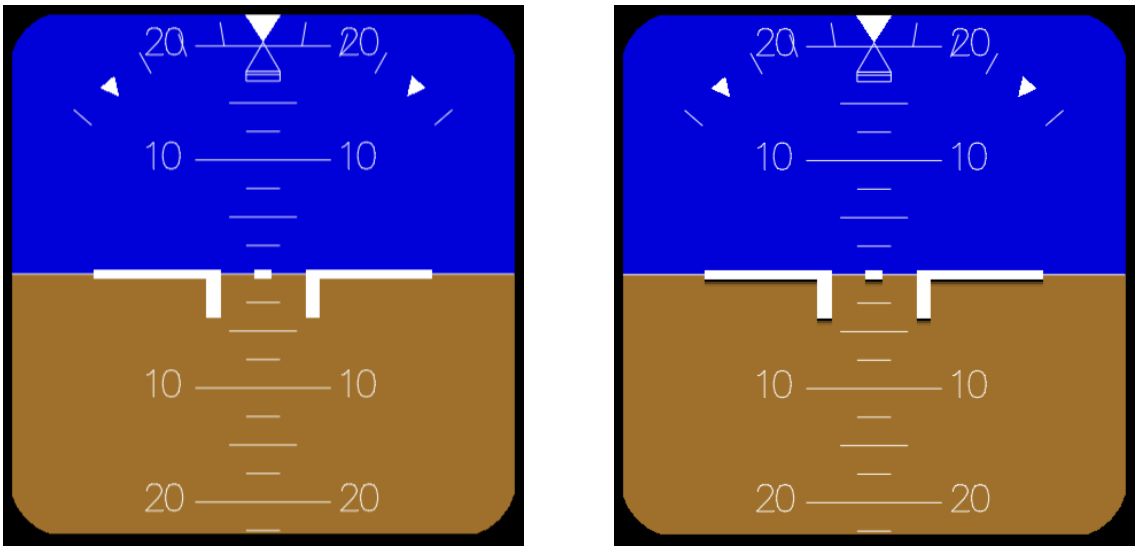

(a) Normal attitude indicator

(b) Attitude indicator with shadows added to the aircraft symbol

Figure 6.1: The effect of adding shading to the aircraft symbol

Another depth cue that can be added is a change in saturation of the background. This is based on aerial perspective where objects in the distance appear less bright and less saturated. The effect of this can be seen in Figure 6.2.

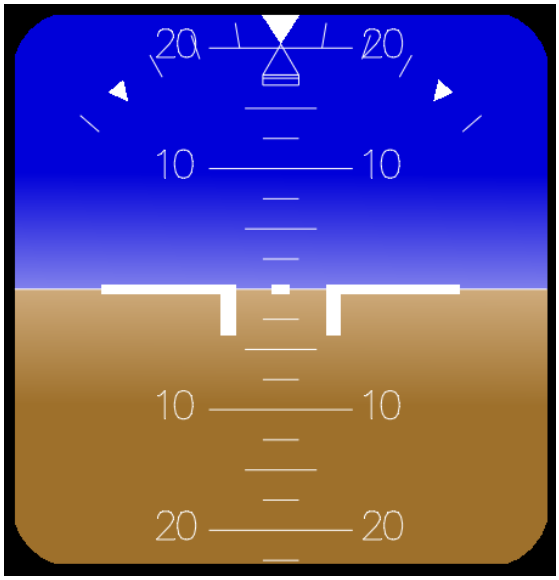

Figure 6.2: The effect of color saturation

Now there are two different options for creating more depth: Adding a texture gradient or creating linear perspective with straight lines coming together into a point in the distance. The effect of the latter is shown in Figure 6.3. Initially, the idea was to create texture using horizontal lines that would become smaller (both in width and height) and get closer to each other (vertically and horizontally) as they get more distant, as shown in Figure 6.4. However, there are a few issues with this: First, the pitch ladder and the texture almost merge into each other, making the pitch ladder harder to interpret. Second, when the display is moving, the dashed lines used to create the texture move across the Earth part of the display. This is a known artifact in OpenGL (the application used to code the AI) and is undesirable. A new way to add texture to the AI will thus have to be found.

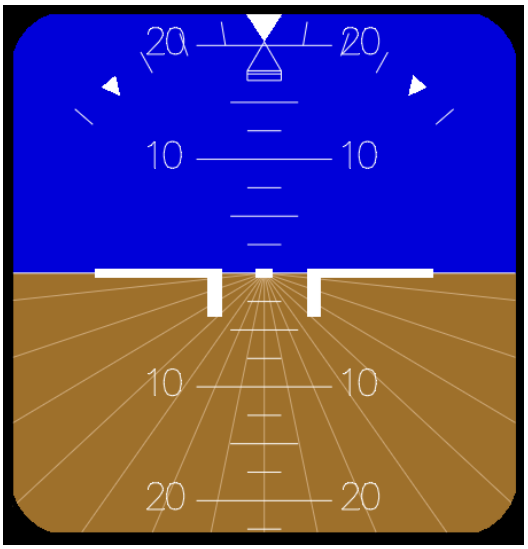

Figure 6.3: AI with perspective lines

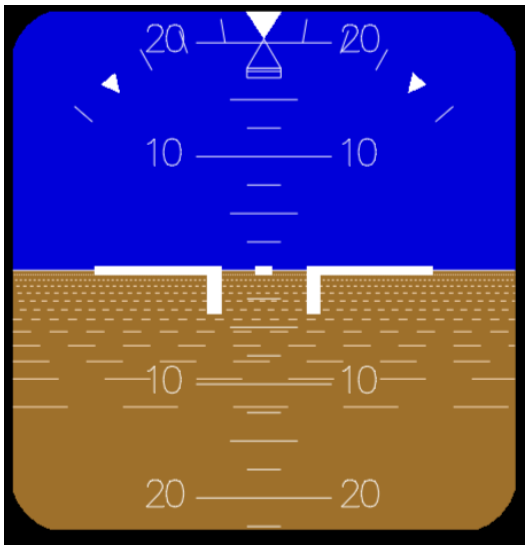

Figure 6.4: AI with texture

The three previously mentioned depth cues strengthen each other when combined, as can be seen in Figure 6.5. The color gradient, texture gradient, and linear perspective lines all adhere to the Gestalt principle of ”good continuation” as both the color gradient and texture gradient or linear perspective lines go on behind the aircraft symbol. The color gradient also adheres to the Gestalt principle of ”common fate” as it presents a continuous change of luminance. Due to the color of the sky and Earth part smoothly

changing whereas the aircraft symbol remains the same color, the display also complies with ”the principle of uniform connectedness”. These grouping principles strengthen the figure-ground relationship as they group the background, separating it from the figure (the aircraft symbol). It should be noted that no optical flow cues, e.g., optical splay, will be added so the focus remains on *static* monocular depth cues.

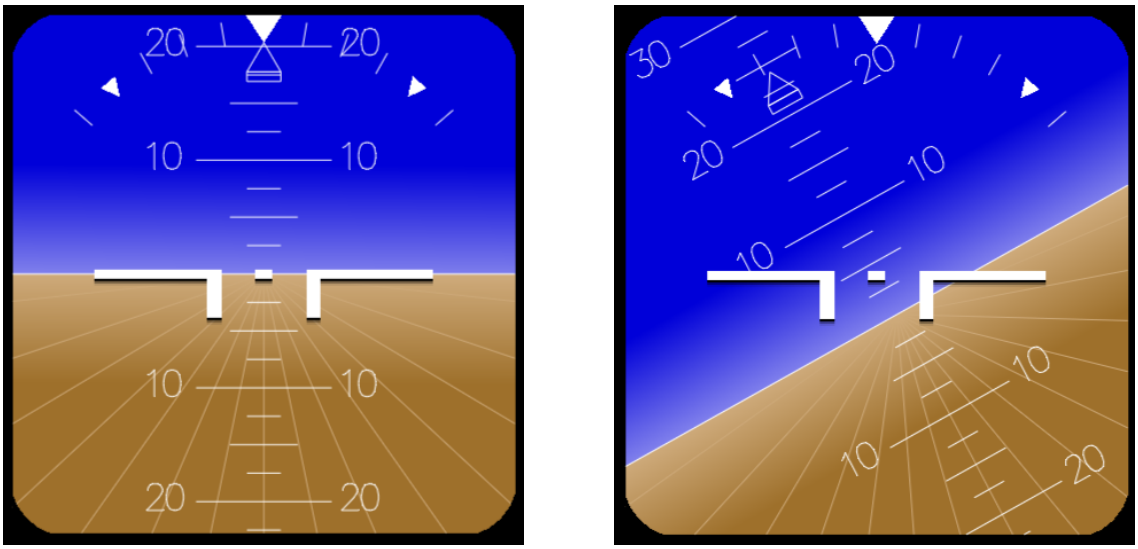

Figure 6.5: The effect of combining the aircraft symbol shadow, color gradient, and linear perspective lines

The color of the texture or linear perspective lines should be the same as the least saturated color in the ground, as this creates a loss of detail, which further enhances the perception of depth. Figure 6.6 shows that this loss of detail does not happen if the colors are not the same.

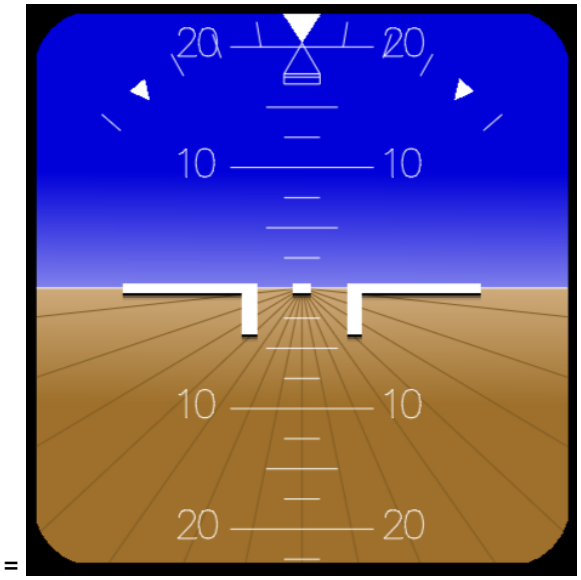

Figure 6.6: The effect of mismatching line and gradient color

A decision will need to be made on which of these two options (texture gradient or linear perspective lines) will be further researched. This decision will be made based on two aspects: What the adaptations look like when programmed into a moving display and pilot opinion. Once a display is chosen, it will be compared to the original AI in an experiment, of which a preliminary plan will be explained in Chapter 7.

7 Experiment Plan

To test the influence of the display adaptions, an experiment will have to be performed. This chapter will discuss the setup of this experiment, however, changes can be made at a later stage if deemed necessary.

7.1. Participants

For this experiment, twenty commercial pilots will be invited who would not experience ambiguity when using the AI, based on their training and experience. By using pilots who are used to the moving horizon AI, there is no need for the pilots to familiarize themselves with the dynamics of it. Pilots also have been taught to rely solely on the AI and ignore vestibular inputs, and while they cannot fully ignore it, the impact of the AI will still be more prevalent compared to non-pilots who would rely on vestibular input more.

7.2. Briefing

The participants will be told that the goal of the experiment is to evaluate the adapted AI display by measuring their reaction time and that a direct response is required. This is to elicit a natural and intuitive response, which will indicate whether the adapted AI display is easier to understand and less prone to horizon-control reversals. The participants will be told that their reaction time will be tested for both the regular AI and the adapted AI.

The participants will be informed that the experiment will consist of two main parts with a break in between. For both parts, their task is to roll the aircraft back to level as soon as possible. They do not need to worry about thrust as the throttle will be controlled by the autothrottle. The main differences between the two tasks will be explained, i.e., that the first runs will take longer and will require the participants to perform a secondary task, which consists of finding the next number in a series of numbers (LLC, 2012), and that they should prepare themselves to take over the simulator when the ”autopilot disengaged” sound appears. Participants will have to keep their hands on the joystick or control column at all times. There will be short breaks after several runs to not make the experiment too tiring. However, the participants will not be told that they will be subjected to spatially disorientating motion cues.

Participants will have to read the experiment briefing document before the experiment. This document also states that participation is voluntary and that participants can thus take breaks or quit the experiment at any time. They are also ensured that the collected data will remain confidential and anonymous, meaning that published results cannot be traced back to a particular person. They are also asked to not discuss the experiment with anyone until it is finished to prevent other participants from becoming biased. When they have finished reading the briefing document, they will be asked to sign the informed consent form, which summarizes the briefing document.

7.3. Apparatus

The experiment will be conducted in the SIMONA Research Simulator, of which the outside is shown in Figure 7.1. The AI of the primary flight display will be changed to the adapted AI for half of the experiment runs. The pilots will be seated in the left seat of the cockpit and use either a control column or side stick depending on what that participant is used to. For the dynamics, an aircraft model of an A320 will be used as these dynamics closely match what the participants are accustomed to.

The participants will only be able to control the roll when an input is desired, the throttle will be controlled by the autothrottle during the entire flight. Noise-canceling headphones will also be used to provide general aircraft noise to reduce the possibility that participants hear the hydraulic actuators of the simulator, which is especially important for the task where the leans illusion will be simulated.

Figure 7.1: The SIMONA Research Simulator (SIMONA, 2023)

7.4. Experiment Procedure

After reading the briefing and signing the informed consent form, the participants will be presented with the two displays. They then get two minutes of free flight per display to familiarize themselves with the display and the simulator. As mentioned before, the experiment will consist of two parts, participants will thus need to practice these runs. For both parts, they will get two practice runs per display. After these practice runs, the participants can take a short break. Both parts of the experiment use ”matching” and ”opposite” conditions. ”Matching” means that the motion of the simulator matches the bank angle shown by the AI whereas ”opposite” means that the motion of the simulator goes in the opposite direction of the bank angle shown by the AI, e.g., the simulator rolls to the left, but AI shows a bank angle to the right. However, for the practice runs, only the ”matching” conditions will be used as the participants cannot know about the disorienting cues to keep them surprised.

First, the participants will experience the leans illusion as designed by van den Hoed et al. (2020), which was explained in Section 4.3. Three runs will be done of which two are matching and one is leans-opposite as can be seen in Figure 7.2. These three runs will be done with both displays but in different orders. In van den Hoed et al. (2020), it was apparent that there was quite a steep learning curve between subsequent leans encounters. Thus, if all participants do the first three runs with one display, the error rate for the second display will be lower, making it seem as if it is better at preventing errors. To avoid this, half of the participants will first use the regular AI and half will first use the adapted AI. In between the two displays, participants will get a short break. They will also get a five-minute break before moving on to the next part of the experiment.

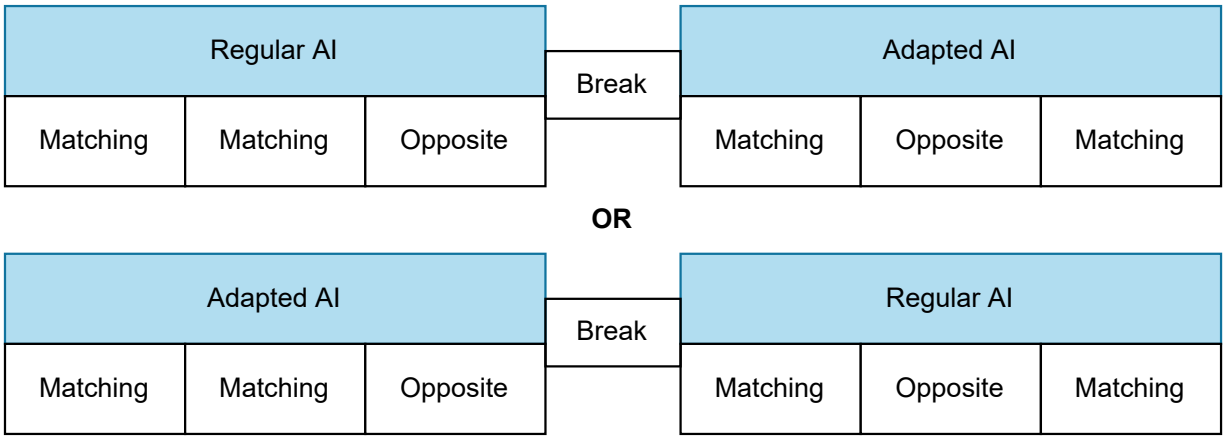

Figure 7.2: Scenario sequence for long runs

Few mistakes are made so as many runs as possible (within a reasonable amount of time) will need to be performed to get statistically relevant data. Thus, the decision was made to make shorter runs, which are less accurate but still disorienting. For half of the runs, the simulator's motion will match the bank angle shown by the AI and for the other half, it will be in the opposite direction, the same holds for each display type. There will be a cycle of six runs for one display, a short 45-second break, six runs for the other display, a 45-second break, etc. until each display has had 48 runs. Just like with the long runs, half of the participants will start with the regular AI and the other half will start with the adapted AI. The order of the scenarios (matching and opposite) is randomly generated and will be turned into a Latin Square so all participants have a different scenario order.

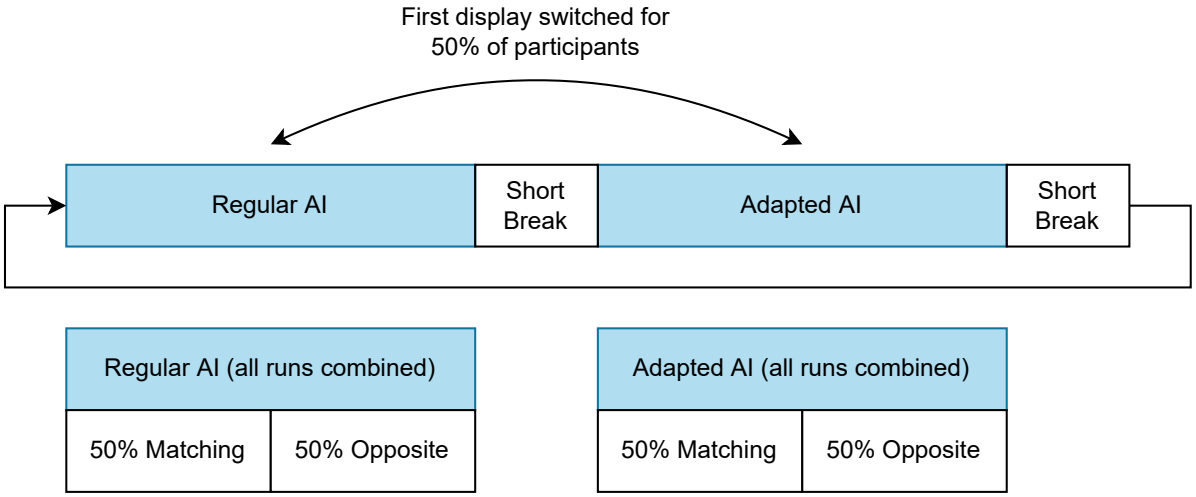

Figure 7.3: Scenario sequence for short runs

The experiment will take about 70 minutes, including breaks but excluding the pre-experiment briefing and the post-experiment questionnaire. The total time of the experiment is estimated to be around two hours.

7.5. Dependent Measures

Based on previous research the following dependent measures will be taken during the experiment (Liggett et al., 1992; Haskell & Wickens, 1993; Singer & Dekker, 2002; Wickens et al., 2007; Gross & Manzey, 2014; Ding & Proctor, 2017; Müller et al., 2018; van den Hoed et al., 2020) :

- *Error Rate*: A roll reversal error is recorded when a control input is received in the opposite direction of the control input necessary to fly back to wings-level and exceeds 1.5 degrees (Landman et al., 2020). The error rate is the percentage of the total number of runs in which an error is recorded.

- *Error Severity*: This is the measured bank angle deviation from level flight when an error was made.
- *Error Duration*: This is the time between when the error was recorded and the participant gives a correction to the correct side. It is the time it takes for the participant to correct their error.
- *Reaction Time*: This is the time between the AI being shown again and the first control input the pilot gives.
- *Subjective Workload*: Pilots will be asked to give a subjective rating of the workload experienced.

The error rate is a direct indicator of whether the adapted AI leads to fewer roll reversal errors. The other dependent measures give an insight into how easy to understand and intuitive the adapted AI is compared to the conventional AI. As mentioned before, pilots will be asked to respond quickly to the bank angle shown on the AI so the reaction times will be low. However, a longer reaction time could indicate that the AI display is confusing to interpret at first glance.

Participants will also be asked for their opinions in a post-experiment questionnaire. This questionnaire will include questions regarding the difference in perceived workload between the two displays as well as whether the adapted AI was easy to understand and did in fact give a sense of depth. Participants will be asked to explain their answers and to leave any other comments to fully understand the results of the experiment.

7.6. Hypotheses

The research question that is to be answered investigates the effect of the addition of static monocular depth cues to the moving horizon attitude indicator display on the interpretation of the attitude indicator bank angle. Based on the previous chapters, and the dependent measures, the following is hypothesized:

1. Participants will show a *decrease in error rate* with the adapted AI display compared to the conventional AI display.
2. Participants will make *less severe errors* with the adapted AI compared to the conventional AI display.
3. Participants will have a *lower reaction time* with the adapted AI compared to the conventional AI display.
4. Participants' *error duration* will be *lower* with the adapted AI compared to the conventional AI display.
5. Participants will experience a *lower subjective workload* with the adapted AI compared to the conventional AI display.

These hypotheses are rooted in the idea that the adaptations of the AI should cause a strengthened figure-ground relationship which in turn would make it easier to interpret and more intuitive to understand. Even when errors are made, participants will realize it quicker, and thus the error will not be as severe.

Two different means of creating spatial disorientation will be used. One of which is an accurate sensation of the leans illusion whereas the other one is less accurate but should still be confusing. However, as there will be few runs with the accurate illusion and a much higher number of runs of the less accurate one, no hypothesis will be formulated that compares these two. To still get some insight, participants will instead be asked if they found one of the two procedures to be more disorienting than the other.

8

Conclusion

The aviation industry has identified the need to decrease the number of accidents caused by Loss of Control In-flight (LOC-I) as it is the number one fatal accident category. The main cause of LOC-I accidents is spatial disorientation. Spatial disorientation can lead to misinterpretation of the attitude indicator (AI), causing pilots to give an incorrect response when trying to level the aircraft. This is a phenomenon known as a control reversal error, of which the most common is a roll reversal error (RRE).

Correct interpretation of the AI is crucial for safe flying and the currently used moving horizon AI display is not optimal. The two main issues with the moving horizon AI that lead to these errors have been identified, both of which have to do with the lack of figure-ground separation of the AI display: First, people tend to assign the ”figure” to the element of the display that is moving. Second, the display does not satisfy the characteristics of a background; the displays lack depth and are small compared to the much larger and stable instrument panel. A great deal of research has gone into solving the former issue, however, it cannot be solved without changing the dynamics of the AI. If this route is taken, the AI of all Western aircraft would need to be changed and pilots would have to be retrained, which poses a risk in itself. Thus, the second issue needs to be addressed. Extending the horizon behind the altitude and speed tapes and a multi-layer display have been investigated, with the former having some success but the latter did not lead to the desired effect. Increasing the display size also had mixed results. Little research has been done into adding static monocular depth cues and their effect on the interpretation of the AI. The thesis that will follow from this literature study will attempt to answer the following research question:

”What is the effect of the addition of static monocular depth cues to the moving horizon attitude indicator display on the interpretation of the attitude indicator bank angle measured by roll reversal errors made?”

An adaptation of the AI display will be tested in the experiment described in this report, the results of which will be presented in the final thesis paper. The effect of the addition of static monocular depth cues will be mainly measured by the number of RREs made in comparison with the conventional AI display. The hypotheses that will be tested in the experiment are as follows:

1. Participants will show a *decrease in error rate* with the adapted AI display compared to the conventional AI display.
2. Participants will make *less severe errors* with the adapted AI compared to the conventional AI display.
3. Participants will have a *lower reaction time* with the adapted AI compared to the conventional AI display.
4. Participants’ *error duration* will be *lower* with the adapted AI compared to the conventional AI display.
5. Participants will experience a *lower subjective workload* with the adapted AI compared to the conventional AI display.

As few RREs are made in normal flight situations, it is important to elicit spatial disorientation during the experiment to get statistically significant data. Motion cues will thus be added to the experiment to create an expectation of the bank angle after which the AI display will show a bank angle in the opposite direction half of the time to confuse the participants. This approach has not yet been taken in other experiments where two AI displays were compared.

References

Arrundell, D., Mulder, M., Stroosma, O., van Paassen, M. M., Landman, A., & Groen, E. L. (2021, April). *Using Depth Information to Improve Display Interpretation: Evaluating the Effect of Increasing Figure-ground Separation with a Multi Layer Display on Attitude Indicator Misinterpretation.*

Bednarek, H., Janewicz, M., & Przedniczek, M. (2019, October). The influence of sloping cloud in the visual field on the cognitive determinants of military pilot's behavior. *International Journal of Occupational Medicine and Environmental Health*, *32*(5), 653–662. doi: 10.13075/ijomeh.1896.01430

Belcastro, C. M., Foster, J. V., Shah, G. H., Gregory, I. M., Cox, D. E., Crider, D. A., … Klyde, D. H. (2017, April). Aircraft Loss of Control Problem Analysis and Research Toward a Holistic Solution. *Journal of Guidance, Control, and Dynamics*, *40*(4). doi: 10.2514/1.G002815

Beringer, D. B., Williges, R. C., & Roscoe, S. N. (1974, October). The Transition of Experienced Pilots to a Frequency-Separated Aircraft Attitude Display: A Flight Experiment. *Proceedings of the Human Factors Society Annual Meeting*, *18*(1), 62–70. doi: 10.1177/154193127401800116

Bles, W. (2008, October). *Spatial Disorientation Training – Demonstration and Avoidance (Entraînement à la Désorientation Spatiale – Démonstration et Réponse)* (Tech. Rep.). Neuilly-Sur-Seine, France: NATO Research and Technology Organization.

Borst, C. (2021). *Display Design Principles.* Delft University of Technology, Delft, NL. (Lecture slides)

Bos, J. (2002, February). Somato-Vestibular Interactions Regarding Spatial (Dis)orientation.

Browne, R. C. (1594, December). Figure and Ground in a Two Dimensional Display. *The Journal of Applied Psychology*, *38*(6), 462–467. doi: 10.1037/h0057045

Bülthoff, I., Bülthoff, H., & Sinha, P. (1998, July). Top-down influences on stereoscopic depth-perception. *Nature Neuroscience*, *1*(3), 254–257. doi: 10.1038/699

Cameroon Civil Aviation Authority. (2010). *Technical Investigation into the Accident of the B737-800 Registration 5Y-KYA Operated by Kenya Airways that Occured on the 5th of May 2007 in Douala.* `https://reports.aviation-safety.net/2007/20070505-0_B738_5Y-KYA.pdf`. ((Accessed on 22/04/2023))

Cave, K. R., & Wolfe, J. M. (1990, April). Modeling the Role of Parallel Processing in Visual Search. *Cognitive Psychology*, *22*(2), 225–271. doi: 10.1016/0010-0285(90)90017-X

Comstock., J. R., Jones, L. C., & Pope, A. T. (2003, October). The Effectiveness of Various Attitude Indicator Display Sizes and Extended Horizon Lines on Attitude Maintenance in a Part-Task Simulation. In *Proceedings of the Human Factors and Ergonomics Society Annual Meeting* (Vol. 47, pp. 144–148). doi: 10.1177/154193120304700130

Connor, C. E., Egeth, H. E., & Yantis, S. (2004, October). Visual Attention: Bottom-Up Versus Top-Down. *Current Biology*, *14*(19), R850–R852. doi: 10.1016/j.cub.2004.09.041

Dariusz, B. (2018, 10). Spatial disorientation simulator. *Safety & Defense*, *4*, 10–16. doi: 10.37105/sd.3

Desdemona. (2018). *Spatial Disorientation Training.* `https://desdemona.eu/2018/01/16/spatial-disorientation-training/`. ((Accessed on 16/06/2023))

Ding, D., & Proctor, R. W. (2017, September). Interactions between the Design Factors of Airplane Artificial Horizon Displays. *Proceedings of the Human Factors and Ergonomics Society Annual Meeting*, *61*(1), 84–88. doi: 10.1177/1541931213601487

Fogel, L. J. (1959, April). A New Concept: The Kinalog Display System. *Human Factors*, *1*(2), 30–37. doi: 10.1177/001872085900100204

Fudali-Czyż, A., Lewkowicz, R., Francuz, P., Stróżak, P., Augustynowicz, P., Truszczyński, O., & Bałaj, B. (2022, May). An Attentive Blank Stare Under Simulator-induced Spatial Disorientation Events. *Human Factors*, *0*(0), 1–19. doi: 10.1177/00187208221093827

Gardner, J. F., Lacey, R. J., & Seeger, C. M. (1954, December). *Speed and Accuracy of Response to Five Different Attitude Indicators)* (Tech. Rep. No. 54-236). Wright-Patterson Air Force Base, OH: Wright Air Development Center.

Gibson, J. J. (1950). *The Perception of the Visual World*. Boston: Houghton Mifflin.

Gillingham, K. K., & Previc, F. H. (1993, November). *Spatial Orientation in Flight* (Tech. Rep.). Brooks

Airforce Base, TX: Armstrong Laboratory.
Grether, W. (1947). *A Discussion of Pictorial versus Symbolic Aircraft Instrument Displays (Memo. Rep. No. TSEAA-694-8B)*. Wright-Patterson Air Force Base, OH: Air Material Command.
Gross, A., & Manzey, D. (2014, October). Enhancing Spatial Orientation in Novice Pilots: Comparing Different Attitude Indicators Using Synthetic Vision Systems. *Proceedings of the Human Factors and Ergonomics Society Annual Meeting*, *58*(1), 1033–1037. doi: 10.1177/1541931214581216
Göthe, K., Oberauer, K., & Kliegl, R. (2016, May). Eliminating Dual-Task Costs by Minimizing Crosstalk between Tasks: The role of Modality and Feature Pairings. *Cognition*, *150*, 92–108. doi: 10.1016/j.cognition.2016.02.003
Haber, R. N. (1980, July). How We Perceive Depth from Flat Pictures. *American Scientist*, *68*(4), 370–380.
Hasbrook, A. H., & Rasmussen, P. G. (1973). *In-flight Performance of Civilian Pilots using Moving-Aircraft and Moving-Horizon Attitude Indicators*. Oklahoma City, OK: Federal Aviation Administration.
Haskell, I. D., & Wickens, C. D. (1993, November). Two- and Three-Dimensional Displays for Aviation: A Theoretical and Empirical Comparison. *The International Journal of Aviation Psychology*, *3*(2), 87–109. doi: 10.1207/s15327108ijap0302_1
Healey, C., & Enns, J. (2011, July). Attention and Visual Memory in Visualization and Computer Graphics. *IEEE Transactions on Visualization and Computer Graphics*, *18*, 1170–1188. doi: 10.1109/TVCG.2011.127
Hedges, V. (2022, December). *Introduction to Neuroscience: Vestibular System.* `https://openbooks.lib.msu.edu/introneuroscience1/chapter/vestibular-system/`. Michigan State University, East Linsing, MI. ((Accessed on 05/06/2023))
Heerspink, H., Berkouwer, W., Stroosma, O., Van Paassen, M. M., Mulder, M., & Mulder, B. (2005, August). Evaluation of Vestibular Thresholds for Motion Detection in the SIMONA Research Simulator. In *AIAA Modelling and Simulation Technologies Conference and Exhibit* (p. 6502). doi: 10.2514/6.2005-6502
Hiremath, V., Proctor, R. W., Fanjoy, R. O., Feyen, R. G., & Young, J. P. (2009, July). Comparison of Pilot Recovery and Response Times in Two Types of Cockpits. In G. Salvendy & M. J. Smith (Eds.), *Human Interface and the Management of Information. Information and Interaction* (pp. 766–775). Heidelberg: Springer Berlin Heidelberg.
Horstmann, G. (2006, February). Latency and Duration of the Action Interruption in Surprise. *Cognition & Emotion*, *20*(2), 242–273. doi: 10.1080/02699930500262878
Ince, F., Williges, R. C., & Roscoe, S. N. (1975, August). Aircraft Simulator Motion and the Order of Merit of Flight Attitude and Steering Guidance Displays. *Human Factors*, *17*(4), 388–400. doi: 10.1177/001872087501700410
International Air Transport Association. (2019). *Loss of Control In-Flight Accident Analysis Report 2019 Edition.* `https://www.iata.org/contentassets/b6eb2adc248c484192101edd1ed36015/loc-i_2019.pdf`. (Accessed on 22/04/2023)
Johnson, S. L., & Roscoe, S. N. (1972, April). What Moves, the Airplane or the World? *Human Factors*, *14*(2), 107–129. doi: 10.1177/001872087201400201
Kelley, C. R., de Groot, S., & Bowen, H. M. (1961, May). Relative Motion III. Some Relative Motion Problems in Aviation. Port Washington, NY. doi: 10.21236/ad0256346
Landman, A., Davies, S., Groen, E. L., van Paassen, M. M. R., Lawson, N. J., Bronkhorst, A. W., & Mulder, M. (2019, November). In-flight Spatial Disorientation Induces Roll Reversal Errors when Using the Attitude Indicator. *Applied Ergonomics*, *81*, 102905. doi: 10.1016/j.apergo.2019.102905
Landman, A., Groen, E. L., van Paassen, M. M. R., Bronkhorst, A. W., & Mulder, M. (2017, August). Dealing With Unexpected Events on the Flight Deck: A Conceptual Model of Startle and Surprise. *Human Factors*, *59*(8), 1161-1172. doi: 10.1177/0018720817723428
Landman, A., Groen, E. L., van Paassen, M. M. R., Bronkhorst, A. W., & Mulder, M. (2020, January). Expectation Causes Misperception of the Attitude Indicator in Nonpilots: A Fixed-Base Simulator Experiment. *Perception*, *49*(2), 155-168. doi: 10.1177/0301006619901053
Ledegang, W., & Groen, E. L. (2018, July). Spatial Disorientation Influences on Pilots' Visual Scanning and Flight Performance. *Aerospace Medicine and Human Performance*, *89*(10), 873–882.
Lewkowicz, R., Bałaj, B., & Francuz, P. (2020, January). Susceptibility to Flight Simulator-Induced Spatial Disorientation in Pilots and Non-Pilots. *The International Journal of Aerospace Psychology*, *30*(1-2), 25–37.

Lewkowicz, R., Strozak, P., Balaj, B., & Francuz, P. (2019, June). Auditory Verbal Working Memory Load Effects on a Simulator-Induced Spatial Disorientation Event. *Aerospace Medicine and Human Performance*, *90*(6), 531–539. doi: 10.3357/AMHP.5277.2019

Liggett, K. K., Rebing, J. M., & Hartsock, D. C. (1992, October). The Use of a Background Attitude Indicator to Recover from Unusual Attitudes. *Proceedings of the Human Factors Society Annual Meeting*, *36*(1), 43–47. doi: 10.1177/154193129203600112

LLC, M. S. (2012, November). *Number Series Task.* Retrieved 2023-05-12, from `https://www.millisecond.com/download/library/numberseries`

Maertens, N. B. (2009, April). Proposing Attitude Indicator Modifications to Aid in Unusual Attitude Recovery. In *International Symposium on Aviation Psychology 2009* (pp. 349–354). Dayton, OH.

Moacdieh, N., & Sarter, N. (2015, February). Display Clutter: A Review of Definitions and Measurement Techniques. *Human Factors*, *57*(1), 61–100. doi: 10.1177/0018720814541145

Müller, S., Sadovitch, V., & Manzey, D. (2018, July). Attitude Indicator Design in Primary Flight Display: Revisiting an Old Issue With Current Technology. *The International Journal of Aerospace Psychology*, *28*, 1–16. doi: 10.1080/24721840.2018.1486714

Palmer, S. E., & Brooks, J. (2009, January). Edge-Region Grouping in Figure-Ground Organization and Depth Perception. *Journal of Experimental Psychology, Human perception & Performance*, *34*, 1353–1371. doi: 10.1037/a0012729

Palmer, S. E., & Ghose, T. (2008, January). Extremal Edge: A Powerful Cue to Depth Perception and Figure-Ground Organization. *Psychological Science*, *19*(1), 77–83. doi: 10.1111/j.1467-9280.2008.02049.x

Pennings, H., Oprins, E., Wittenberg, H., Houben, M., & Groen, E. (2020, January). Spatial Disorientation Survey Among Military Pilots. *Aerospace Medicine and Human Performance*, *91*, 4–10. doi: 10.3357/AMHP.5446.2020

Reising, J. M., Liggett, K. K., & Hartsock, D. C. (1995). New Flight Display Formats. In *Proceedings of the 8^{th} International Symposium on Aviation Psychology* (pp. 86–91). Columbus, OH.

Rivera, J., Talone, A. B., Boesser, C. T., Jentsch, F., & Yeh, M. (2014, October). Startle and Surprise on the Flight Deck: Similarities, Differences, and Prevalence. *Proceedings of the Human Factors and Ergonomics Society Annual Meeting*, *58*(1), 1047-1051. doi: 10.1177/1541931214581219

Roscoe, S. N. (1968, August). Airborne Displays for Flight and Navigation. *Human Factors*, *10*(4), 321–332. doi: 10.1177/001872086801000402

Roscoe, S. N. (2004, October). Moving Horizons, Control Reversals, and Graveyard Spirals. *Ergonomics in Design*, *12*(4), 15–19. doi: 10.1177/106480460401200405

Roscoe, S. N., & Williges, R. C. (1975, August). Motion Relationships in Aircraft Attitude and Guidance Displays: A Flight Experiment. *Human Factors*, *17*(4), 374–387. doi: 10.1177/001872087501700409

Schooler, J. (2015, January). Bridging the Objective/Subjective Divide Towards a Meta-Perspective of Science and Experience. In T. Metzinger & J. M. Windt (Eds.), (Vol. 34, pp. 1–40). Frankfurt am Main. doi: 10.15502/9783958570405

Self, B. P., Breun, M., Perry, C., & Ercoline, W. R. (2002, April). Assessment of Pilot Performance Using a Moving Horizon (Inside-Out), a Moving Aircraft (Outside-In), and an Arc-Segmented Attitude Reference Display. In *RTO HFM Symposium on "Spatial Disorientation in Military Vehicles: Causes, Consequences and Cures* (pp. 30-1 – 30-7). La Coruña, Spain.

SIMONA. (2023). *Visual Display System.* `https://cs.lr.tudelft.nl/simona/facility/visual-display-system/`. Delft University of Technology, Delft, NL. ((Accessed on 05/06/2023))

Singer, G., & Dekker, S. (2002, January). The Effect of the Roll Index (Sky Pointer) on Roll Reversal Errors. *Journal of Human Factors and Aerospace Safety*, *2*, 33–43.

Smallman, H. S., & John, M. S. (2005, July). Naive Realism: Misplaced Faith in Realistic Displays. *Ergonomics in Design*, *13*(3), 6–13. doi: 10.1177/106480460501300303

Stephan, D., & Koch, I. (2010, July). Central Cross-Talk in Task Switching: Evidence From Manipulating Input-Output Modality Compatibility. *Journal of experimental psychology: Learning, memory, and cognition*, *36*, 1075–1081. doi: 10.1037/a0019695

Stróżak, P., Francuz, P., Lewkowicz, R., Augustynowicz, P., Fudali-Czyż, A., Bałaj, B., & Truszczyński, O. (2018, July). Selective Attention and Working Memory Under Spatial Disorientation in a Flight Simulator. *The International Journal of Aerospace Psychology*, *28*(1-2), 31–45. doi: 10.1080/24721840.2018.1486195

Tableau. (2023). *Why Visual Analytics?* Retrieved 2023-04-29, from `https://help.tableau.com/`

current/blueprint/en-us/bp_why_visual_analytics.htm

Taylor, R. M. (1988, April). Aircraft Attitude Awareness from Visual Displays. *Displays*, *8*(2), 65-75. doi: 10.1016/0141-9382(88)90037-6

The Human Memory. (2022, May). *Vestibular System.* https://human-memory.net/vestibular-system/. ((Accessed on 05/06/2023))

Theeuwes, J. (2010, October). Top–Down and Bottom–Up Control of Visual Selection. *Acta Psychologica*, *135*(2), 77–99. doi: 10.1016/j.actpsy.2010.02.006

Tovée, M. J. (2008). *An Introduction to the Visual System* (2nd ed.). Cambridge: Cambridge University Press. doi: 10.1017/CBO9780511801556

van den Hoed, A., Landman, A., Baelen, D. V., Stroosma, O., van Paassen, M. M. R., Groen, E. L., & Mulder, M. (2020, December). Leans Illusion in Hexapod Simulator Facilitates Erroneous Responses to Artificial Horizon in Airline Pilots. *Human Factors*, *64*(6), 962–972. doi: 10.1177/0018720820975248

Wagemans, J. (2018, February). Perceptual Organization. In *Stevens' Handbook of Experimental Psychology and Cognitive Neuroscience* (pp. 1–70). John Wiley & Sons. doi: 10.1002/9781119170174.epcn218

Wickens, C. D. (2008, June). Multiple Resources and Mental Workload. *Human Factors*, *50*(3), 449–455. doi: 10.1518/001872008X288394

Wickens, C. D., Sandry, D. L., & Vidulich, M. (1983, April). Compatibility and Resource Competition between Modalities of Input, Central Processing, and Output. *Human Factors*, *25*(2), 227–248. doi: 10.1177/001872088302500209

Wickens, C. D., Self, B. P., Andre, T. S., Reynolds, T. J., & Small, R. L. (2007, December). Unusual Attitude Recoveries With a Spatial Disorientation Icon. *The International Journal of Aviation Psychology*, *17*(2), 153–165. doi: 10.1080/10508410701328821

Part III

Book of Appendices

*This part corresponds to the Thesis paper and is still to be graded.

A

Experiment Briefing

This document provides all the necessary information for participation in the experiment in which adaptations to the attitude indicator (AI) will be evaluated. The experiment will be conducted in the SIMONA Research Simulator operated by the Control & Simulation department of the Faculty of Aerospace Engineering of Delft University of Technology. This document outlines the goal of the experiment, along with general information to the participant regarding the setup of the experiment and the task to be performed.

A.1. Experiment Goal

The primary goal of the experiment is to evaluate the usage of an adapted attitude indicator display.

A.2. Experiment Task

The primary task of the participant is to roll the aircraft back to wings-level as soon as the AI is shown again. The experiment aims to simulate a short period of inattention, followed by a sudden display of the AI showing a bank angle. This will be done for both the 'regular' AI and the 'adapted' AI, which are shown in Figure A.1 and Figure A.2 respectively.

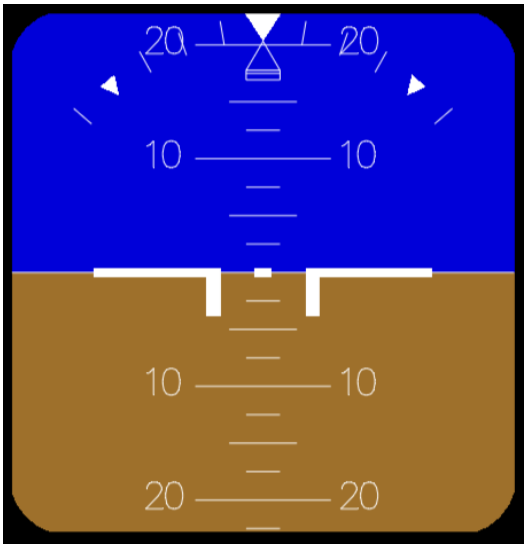

Figure A.1: Regular AI as presented in SIMONA Research Simulator

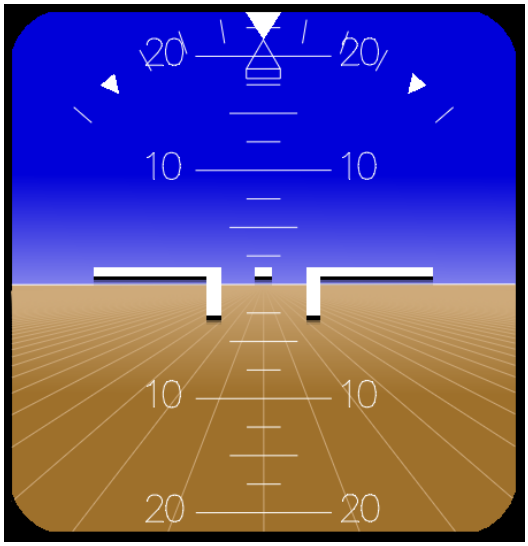

Figure A.2: Adapted AI as presented in SIMONA Research Simulator

A.3. Apparatus

The experiment will be conducted in the SIMONA Research Simulator (SRS), where motion will be enabled. You will be seated in the left seat of the cockpit and use a control column to control the roll angle. Autothrottle will be on the entire time. You can only control roll when an input is desired.

A.4. Experiment Procedure

You will get a short practice run to get familiar with the simulator dynamics. You will also get to practice the different experiment runs. After the experiment, you will be asked some questions in a questionnaire. The whole experiment will last approximately two and a half hours.

A.5. Participant Rights

Participation in the experiment is voluntary. This means that you can decide to stop the experiment at any time.
The data that will be collected during the experiment will remain confidential and anonymous. It will be treated such that only the experimenter can link the results to a particular participant. This means that none of the results can ever be traced back to you or any other participant. By participating in this experiment you agree that this anonymous data may be published by the experimenter. Lastly, we ask you ***not*** to discuss any further details of the experiment with anyone until the complete experiment has finished. This is done to prevent participant bias.

To make sure you have understood all of the above, you are asked to sign an informed consent form at the end of the experiment briefing.

B

Informed Consent Form

B.1. Opening Statement

You are invited to participate in a Master's thesis research study looking into the effect of enhancing the attitude indicator on pilot performance. This study is being done by Chloë Van Droogenbroeck (Master student), Annemarie Landman, Rene van Paassen, Olaf Stroosma, and Max Mulder from the TU Delft.

The purpose of this research study is to see if adaptations to the attitude indicator display lead to a better interpretation of the display compared to the conventional attitude indicator. The experiment will consist of two parts with a break in between. Your task is to interpret the attitude indicator display and roll the simulator back to level. Afterward, you will be asked to fill in a questionnaire. In total (incl. breaks and a questionnaire) the experiment will take around two and a half hours. All data will be anonymized and saved on a dedicated project storage drive, which only the research team can access. The anonymized data will be used for the Master thesis, and a published article, and can be used for future research. The data that was used to contact you to plan the experiment is only available for the student and will be destroyed afterward. Your name or any other information that can be used to identify you will never be used in reports or any other publications.

Participation in this study is entirely voluntary and you can withdraw anytime. You are free to omit any questions. Your data can be removed at any time. One person in the research team has the ability to de-anonymize the data via the informed consent forms for data removal purposes only.

B.2. Informed Consent Form

After being briefed and having read the opening statement, the participants had to thoroughly read, fill in, and sign the informed consent form.

PLEASE TICK THE APPROPRIATE BOXES	Yes	No
1. I have read and understood the experiment briefing or it has been read to me. I have been able to ask questions about the study and my questions have been answered to my satisfaction.	☐	☐
2. I consent voluntarily to be a participant in this study and understand that I can refuse to answer questions and I can withdraw from the study at any time (including in the period between the experiment and publication of the experiment's results), without having to give a reason.	☐	☐
3. I understand that taking part in the study involves performing tasks in the SIMONA Research Simulator, where I have to ensure the aircraft performs a level flight. I understand my control inputs and answers to a short post-experiment questionnaire are logged.	☐	☐
4. I understand that the total experiment will take approximately two and a half hours.	☐	☐
5. I understand that taking part in the study involves the risks of motion sickness or fatigue. I understand that these risks will be mitigated by taking breaks or terminating the experiment at any time desired by me.	☐	☐
6. I understand that specific personally identifiable information (name and email address) are only collected for contacting me during the planning phase, and will not be used for the study itself.	☐	☐
7. I understand that the following steps will be taken to minimize the threat of a data breach and protect my identity in the event of such a breach: contact details are destroyed after the planning phase of the experiment, all of which are stored in a dedicated project storage drive. Names and signatures are used for de-anonymization of the data to remove these if requested by the participant and are stored in a restricted drive which can only be accessed by the SIMONA Lab Manager (Olaf Stroosma).	☐	☐
8. I understand that personal information collected about me that can identify me, such as my name and contact details, will not be shared beyond the study team.	☐	☐
9. I understand that the (identifiable) personal data I provide will be destroyed immediately after use: contact details after the planning phase.	☐	☐
10. I understand that after the research study, the anonymized information I provide will be used for a master thesis report and possibly for publication in a scientific journal.	☐	☐
11. I give permission for the de-identified (simulator data and questionnaire answers) that I provide to be archived in a dedicated project storage drive so it can be used for future research and learning.	☐	☐
12. I understand that access to this repository is only available to the research team: Chloë Van Droogenbroeck, Annemarie Landman, Olaf Stroosma, Rene van Paassen, and Max Mulder.	☐	☐

Signatures

_____	_____	_____
Name of participant	Signature	Date

I, as researcher, have accurately read out the information sheet to the potential participant and, to the best of my ability, ensured that the participant understands to what they are freely consenting.

Chloë Van Droogenbroeck	_____	_____
Researcher name	Signature	Date

Study contact details for further information:

Chloë Van Droogenbroeck, [phone number], c.vandroogenbroeck@student.tudelft.nl

C

Experiment Setup

Figure C.1 shows the experiment setup with the participant sitting in the left-side seat, using a control column and the tablet on the right-hand side. The distraction task was an online numerical sequence test (`https://www.nibcode.com/en/psychometric-training/test-of-numerical-sequence`).

Figure C.1: Experiment setup

D

Post-Experiment Questionnaire Responses

1. Which AI display (regular or adapted) do you prefer and why?

P1: Adapted. The converging lines give a better awareness of the bank angle. I suspect that this could have additional value, especially for extremer attitudes (which was not a part of the runs) where the nose is very low or very high and the horizon line is practically invisible.
P2: No preference.
P3: Adapted. With the adapted AI a third bank angle indication is available besides the roll index and the ”wing bars” in the middle. This makes it more intuitive.
P4: Adapted. It looks better but I do not think it will significantly improve the functionality.
P5: Regular. Less clutter.
P6: Adapted. Clearer indication, and quicker to interpret.
P7: Adapted. For a big part because it looks more modern, a matter of taste too. The aircraft symbol is a lot nicer to look at because of the ”shadow”.
P8: Adapted. Gives more clues. The lines show a pattern on the ground that you can also see in real life. This gives an extra cue that brown means ”Earth” (*Participant mentioned that sometimes in extreme cases, people can get confused on what part of the display is ”Earth” and ”sky”*)
P9: Adapted. Gives more sense of roll rate and depth.
P10: No preference.
P11: Regular. More simple. Added features (particularly the aircraft symbol enhancement) don’t improve awareness. The same for the colors of the horizon.
P12: Adapted. More representative of the actual world.
P13: Regular. 1. I did not perceive any added value of the adapted display, of course, if the experiment results show better performance, I would reconsider. 2. If there is no added value, decluttering is preferred. (*Participants mentioned that in real life, the AI passes down more information than the one used in the experiment.*)
P14: Adapted. Looks more intuitive and clear, also more modern.
P15: Adapted. Bit more dynamic presentation.
P16: Adapted. It provides a bit of depth perception, which makes it somewhat easier to interpret.
P17: Regular. Less clutter.
P18: Adapted. More visual reference regarding ground versus air and regarding bank.
P19: Regular. The color difference between blue and brown is ”harsher” in the regular display. Clearer difference in blue/white/brown.
P20: Regular. Adapted AI is better to look at however the visual representation of wins level is more clear on the regular AI (due to the shadow below the aircraft symbol).
P21: Adapted. For some reason, it felt like I reacted more intuitively with the adapted AI.
P22: Regular. Less clutter. The line between brown and blue is more clear. The attitude pointer is more precise (no shadow).
P23: Adapted. The depth makes it feel more intuitive to use.
P24: Regular. More definition.
P25: Regular. Probably due to more than 35 years of use of the regular display. Adapted display is good and in a way also good for situational awareness. I remarked a slight over-correction through 0° bank with the adapted display and a slight under-correction with the regular display.

2. Did the adapted AI give you a sense of depth?

P1: Yes
P2: No
P3: Yes
P4: Yes
P5: Yes
P6: Yes
P7: Yes
P8: Yes
P9: Yes
P10: No
P11: Yes
P12: Yes
P13: No
P14: Yes
P15: Yes
P16: Yes
P17: No
P18: No
P19: Yes
P20: Yes
P21: Yes
P22: Yes
P23: Yes
P24: Yes
P25: Yes

3. Did this perceived depth last throughout the experiment?

P1: Yes
P2: No
P3: Yes
P4: Yes
P5: Yes
P6: Yes
P7: Yes
P8: Yes
P9: Yes
P10: No
P11: No
P12: No
P13: N/A.
P14: Yes
P15: Yes
P16: Yes
P17: No
P18: No
P19: No
P20: Yes
P21: Yes
P22: Yes
P23: Yes
P24: No
P25: Yes

4. Was the bank angle of the adapted AI easier to read than the bank angle of the regular AI? Indicate 1 to 5 with 1 being ”much easier” and 5 being ”much harder”. Please explain your answer.

P1: 2. See answer for question 1. For a couple of runs, I tried to just use the converging lines. This alone (even though the horizon line stayed visible) was enough for me to roll back to wings-level. I suspect that I would give a ”1” to this question in case of extreme attitudes.
P2: 3. No difference.
P3: 2. It is easier to establish when a bank angle is still present with the adapted AI. Especially due to the central vertical line (*participant refers to the central line of the converging lines*).
P4: 3. No difference noticed.
P5: 3. I liked that the shade is brighter near the horizon, like in real life. The extra lines to create depth made the display a bit harder to read (the bank angle as well), but I think you get used to it over time.
P6: 2. After getting used to it (initially it was a bit harder), it was easier to get a picture of the aircraft’s attitude.
P7: 3. No difference.
P8: 3. No difference.
P9: 2. Depth and linens give a sense of roll rate more than the regular AI.
P10: 3. No difference.
P11: 3. No difference.
P12: 3. Similar. During the experiment with upset recovery, I mainly focused on the top of the AI.
P13: 3. I mainly (or fully) use the sky pointer to determine which direction I have to give a roll input, not the lower part of the display.
P14: 2. The aircraft symbol seemed more defined, better contrast with the background.
P15: 3. No difference.
P16: 2/3. The value of the bank angle was equally easy to read, however, the orientation (LH/RH) was a bit easier with the adapted AI.
P17: 4. Too much information.
P18: 3. No difference.
P19: 4. For the reason mentioned in question 1.
P20: 3. Did not make a difference.
P21: 3. The bank angle interpretation felt the same.
P22: 3. Top scale (bank angle) is equal.
P23: 2. The bank angle was easier to pick up intuitively because of the depth. It better resembles the picture one would see outside.
P24: 3. I didn’t experience any difference.

P25: 3. No difference.

5. Which of the adaptations (converging lines, color gradient, shadow around aircraft symbol) to the AI were the most helpful/did you appreciate the most and why?

P1: Converging lines. Gives extra awareness of the bank angle.
P2: Color gradient and shadow around aircraft symbol. *The participant did not give any explanation.*
P3: Converging lines. Same answer as question 4.
P4: Converging lines. *The participant did not give any explanation.*
P5: Color gradient. Because it looks like a real horizon.
P6: Converging lines. Gives a sense of depth.
P7: Converging lines and shadow around aircraft symbol. I did not notice the color gradient. The shadow gives an illusion of depth and that makes it more clear because it makes the aircraft symbol seem like it is in front of everything else.
P8: Converging lines and color gradient. Gave the most depth.
P9: Converging lines and color gradient. Lines aid most in the sense of depth.
P10: Converging lines. It's the only thing that stood out for me every once in a while.
P11: Converging lines. Gave a sense of depth when focusing on it. The other features made no difference.
P12: Converging lines and color gradient. Real-life visual.
P13: N/A.
P14: Color gradient and shadow around aircraft symbol. They provided the most definition of the foreground and background (contrast).
P15: Converging lines. It created depth.
P16: Converging lines. To me, the lines added the most perspective.
P17: Color gradient. Color makes it clearer, a clearer definition.
P18: Converging lines. More 3D.
P19: Converging lines. Looks nicer but I question the functionality of the adapted display.
P20: All three. They were all pleasant adaptations whereas the shadow around the aircraft symbol was necessary to distinguish between horizon.
P21: Converging lines and color gradient. Shadow actually felt a little distracting. The other two felt a lot more pleasing to the eye.
P22: Converging lines. They may help at greater bank angles but that was not tested here.
P23: Converging lines. This was the best indicator of depth and the biggest change.
P24: Converging lines and color gradient. It gives you a more in-depth experience.
P25: Converging lines. It gave a sense of depth perception which was nice to interpret the side of angle of bank.

6. Do you see any issues with the adaptation of the AI if it were to be used in commercial aviation? Please explain.

P1: This seems to be easy to implement without too much additional training and familiarization for the crew.
P2: No. Different aircraft have different AIs. Just a matter of getting used to it.
P3: Not really. The only issue I can think of could be that some pilots prefer a ”clean” AI and they might find the converging lines ”too much”.
P4: No.
P5: No.
P6: It will need a short training session to get used to.
P7: No. Does not seem like it would be an issue.
P8: No.
P9: The lines could perhaps clutter the screen a bit.
P10: No, just minor changes.
P11: No. Can be used without problems.
P12: No.
P13: Yes. *If* there is no better roll performance of pilots (as measured in the experiments), then a decluttered display would prevail.

P14: No, it would be beneficial and simple to integrate.
P15: No, but more data is required (high pitch/low pitch simulations).
P16: Yes. It could add clutter to the display. In the experiment, a bare AI was presented but an actual PFD also shows flight director, radio altitude, etc.
P17: Not really. Whatever one is trained for, one gets used to.
P18: No, no additional training is needed. Easy to interpret.
P19: No, differences are minimal.
P20: Not really although the contrast between the aircraft symbol and horizon line could be more clear.
P21: See the answer to the previous question. The shadow of the aircraft symbol is distracting/obscuring the horizon.
P22: No, not really. I think we will all get used to it. Although I prefer less clutter instead of more.
P23: No.
P24: No, they both work nicely.
P25: Not in the range up to 30° bank. It would be interesting to see what influence the adapted display has on situational awareness when performing upset recovery training.

7. Was either of the two procedures (first and second part of the experiment) more confusing and /or disorienting? Please explain which one and why.

P1: Hard to say. The long runs resulted in a higher reaction time (I suspect).
P2: The second because the runs were quicker after one another.
P3: After noticing for the first time that the simulator movement did not match the bank angle (for this participant, this was the third run of the short runs), I tried to disregard my spatial sensations and focused on the AI alone.
P4: No.
P5: The first procedure was more demanding because I kept thinking about the answer to the numerical sequence.
P6: No. (*Participant stated that neither was really disorienting*)
P7: No.
P8: No, both were disorienting.
P9: Both felt very similar.
P10: The same for me.
P11: Not really. Sticking to and focusing on the task did the trick.
P12: Not really, the first part is more realistic.
P13: I had the impression that the pre-run simulator roll motion sometimes gave a clue as to in which direction I needed to give a roll input, maybe less so in the second part. (*Participant did later on stated that he realized that this was not always the case and that he could not rely on the simulator motion.*)
P14: The second part as it called for a more swift response. With the AP-disconnect sound, there was more of a warning.
P15: Disorientation happened when I solely trusted my senses.
P16: Not really. The tablet provided a realistic distraction but because the autopilot disconnect sign warned me about the upcoming recovery, I was equally ready when the AI turned back on.
P17: Not really.
P18: The second part as the motion was not always aligned with the PFD presentation. (*This was also not the case for the first part, which could indicate that the pilot did not notice this.*)
P19: No difference.
P20: No.
P21: Not one in particular. However, I did realize at some point that I shouldn't rely on my motion senses.
P22: Second part. The motion was random and thus not always consistent with the visual picture which was shown later. (*Participant did not really notice motion as much during the long runs.*)
P23: Not really but in the short runs it was more obvious that the motion was sometimes in the wrong direction.
P24: No. For the second part I was maybe more distracted/tired.
P25: No. Both were very good and neither was more confusing than the other.

8. What was your strategy to get the aircraft back to wings-level? What part of the display did you use to ensure the aircraft was level again?

P1: At first only the horizon, and later on the converging lines as well. Sky pointer was less used.
P2: Roll pointer.
P3: Initial reaction based on the wing bars. Transitioning to bank angle indication at the top (*participant is referring to the roll index*), followed by scanning back to the middle and lower part of the AI. For the final ”fine-tuning” scanning up again to the top of the AI.
P4: Only the horizon line was used.
P5: The aircraft symbol (wings) and horizon.
P6: The brown/black for initial correction. Aircraft symbol and sky pointer for fine-tuning.
P7: Firstly the sky pointer and secondly the aircraft symbol.
P8: First I determine the bank based on the horizon line and then I use the sky pointer to get to wings-level.
P9: A combination of the center of the AI and top to ensure level.
P10: I just look at the bank angle of the ground compared to the sky (blue/brown).
P11: Roll index worked better than the aircraft symbol when it comes to precise roll. I tried both strategies (roll index + aircraft + combined). Little roll first to see if the direction was correct.
P12: First observe and decide on the direction to roll. Then mostly the top part of the display.
P13: The sky pointer, top of the display: bring the solid triangle (aircraft) to the open triangle (earth-related).
P14: I tried to focus on the aircraft symbol but I noticed that I also used the bank angle arrow (sky pointer) at the top of the AI. Usually, I started in the middle of the AI, and during the return to wings-level I shifted more toward the top of the AI.
P15: 1, analyze the situation. 2, turn back using horizon. 3, check the bank angle indicator to ensure level flight.
P16: 1, focus on the center of the screen. 2, use the aircraft symbol to determine orientation. 3, roll wings level. 4, use the sky pointer during the last part for exact wings-level.
P17: Just the aircraft symbol with relation to the horizon.
P18: First general overview then roll index.
P19: The wings and the horizon.
P20: Disconnect feeling and just react to visual cues. I used the horizon.
P21: The aircraft symbol to judge direction. Instinct to judge the amount of initial input.
P22: The line between brown and blue and its surroundings.
P23: I initially looked at the wings in the middle for the first reaction. Then at the top to fine-tune.
P24: I tried the aircraft symbol first. Later I used the skypointer. Both worked fine.
P25: Mostly used the plane symbol.

9. Please leave any other comments in case you have any.

P1: The addition of the shadow did nothing for me. The color gradients could become interesting if we start working more with the flight path director (path in space) instead of the traditional FD.
P2: Since I could only control the roll in the simulator, I only focused on the roll pointer. Maybe if control over all axes was possible I could have used more of the AI.
P3: In the case of bank angle only, I think the adapted AI is an improvement but it might be interesting to try and analyze/research if it works better in unusual attitude situations as well.
P4: No further comments.
P5: No further comments.
P6: No further comments.
P7: Mostly a more modern look and feel. Shadow is pleasant.
P8: A 30-degree bank angle is relatively small to get a difference in reaction time. I think more extreme bank angles that are outside people’s ”comfort zone” would show bigger differences and would make them really have to interpret the display.
P9: The color gradient did not aid me personally. (*Participant mentioned they did not notice the shadow around the aircraft symbol so perhaps they were referring to that since they indicated ”color gradient” in Q5*)
P10: No further comments.
P11: No further comments.

P12: No further comments.
P13: The aircraft model in free fight returns back to wings-level when releasing the control column whereas the aircraft model during the experiment remains present bank angle when releasing the control column.
P14: To invoke more disorientation, I think the start of the simulator motion and showing the PFD should be closer to each other. Once you feel the motion of the simulator, you know that soon the PFD will turn on and that you have to do something, which gives you time to prepare.
P15: Nice presentation which could be helpful during commercial operation.
P16: The fact that the motion system rolled left or right just prior to the AI coming on, made the moment of recovery predictable. I consciously tried to ignore the roll direction of the sim as it seemed to be random and not related to the AI. However, I had a wrong initial reaction at least twice.
P17: No further comments.
P18: This PFD did not include the flight director which can sometimes cause more confusion. When in extreme attitudes, the flight director can do weird things. A pilot has to both interpret the PFD and the flight director. When the flight director does something weird, it confuses the pilot.
P19: No further comments.
P20: No further comments.
P21: No further comments.
P22: The adapted AI looks more modern, but as written before, during these exercises I did not really notice added value. This may change in other scenarios. Design is very refreshing.
P23: No further comments.
P24: No further comments.
P25: Interesting new display that might aid in better situational awareness.

E

Overview Errors

E.1. Long Runs

Table E.1: Overview errors long runs (MM = motion matching, MO = motion opposite)

Display	Motion	Error Severity [deg]	Error Duration [s]	Max Control Column Input [deg]
Baseline	MM	0.053619501	0.240234375	-2.321079003
Baseline	MM	0.066061083	0.220214844	-3.405742084
Baseline	MM	0.294657921	0.280273438	6.555064219
PDCM	MM	0.022403399	0.190185547	-1.374606486
PDCM	MM	5.052653734	0.540527344	-34.47783559
PDCM	MM	0.071009093	0.280273438	2.222353975
Baseline	MO	4.090357117	0.570556641	17.49298171
Baseline	MO	0.03030237	0.200195313	-2.078958721
PDCM	MO	1.076425218	0.370361328	-14.69310941
PDCM	MO	0.084790616	0.240234375	2.668325393

E.2. Short Runs

Table E.2: Overview errors short runs (MM = motion matching, MO = motion opposite)

Display	Motion	Error Severity [deg]	Error Duration [s]	Max Control Column Input [deg]
Baseline	MM	0.042775091	0.350341797	2.383102145
Baseline	MM	0.040005388	0.210205078	4.852291578
Baseline	MM	0.047125694	0.270263672	3.171970669
Baseline	MM	-0.014931304	0.230224609	-1.328557081
Baseline	MM	0.432322404	0.260253906	-11.46491786
Baseline	MM	-0.010699108	0.170166016	1.617075378
Baseline	MM	-0.011138171	0.149917603	1.153259427
Baseline	MM	3.8429E-05	0.210205078	-2.649248583
Baseline	MM	0.308295941	0.290283203	8.279601338
PDCM	MM	-0.015203822	0.180175781	1.082049681
PDCM	MM	1.288367294	0.470458984	12.00436602
PDCM	MM	2.386223133	0.569904327	-19.1988213
PDCM	MM	-0.010024947	0.16015625	-1.742235062
PDCM	MM	0.040956534	0.230224609	4.331149833
PDCM	MM	0.017730185	0.270263672	2.583756945
PDCM	MM	0.065367579	0.190185547	5.464732154
PDCM	MM	0.023463381	0.220214844	-4.252348926
PDCM	MM	0.099809332	0.260253906	-5.428895952
Baseline	MO	2.040843372	0.410400391	-16.73201935
Baseline	MO	0.353584469	0.300292969	8.529511219
Baseline	MO	0.131573856	0.290283203	-4.912700126
Baseline	MO	0.058881745	0.270263672	-3.690286175
Baseline	MO	-0.012748755	0.190185547	1.361182624
Baseline	MO	8.864775709	0.810791016	53.71958859
Baseline	MO	7.732892121	0.730712891	-36.44804759
Baseline	MO	7.270554485	0.389785767	-5.14159226
Baseline	MO	0.18691019	0.290283203	-5.186584471
Baseline	MO	-0.017981241	0.260253906	1.401470403
Baseline	MO	0.844690247	0.440429688	-8.73020541
Baseline	MO	0.192109414	0.290283203	5.875547772
Baseline	MO	0.138974005	0.300292969	-5.024078465

Display	Motion	Error Severity [deg]	Error Duration [s]	Max Control Column Input [deg]
Baseline	MO	0.777113345	0.330322266	-15.62890257
Baseline	MO	0.695139299	0.290283203	16.12998411
Baseline	MO	0.250749165	0.240234375	-10.02263358
Baseline	MO	0.086686846	0.210205078	6.875752795
Baseline	MO	0.150818476	0.240234375	-8.122645362
Baseline	MO	0.815703527	0.300292969	-16.05140367
Baseline	MO	0.208937993	0.330322266	-5.623861682
Baseline	MO	0.039923678	0.280273438	2.973623478
Baseline	MO	1.240706112	0.350341797	17.39143512
Baseline	MO	0.181237919	0.290283203	-6.537109062
Baseline	MO	-0.014546025	0.180175781	1.171021362
Baseline	MO	-0.013183228	0.210205078	-1.83438385
Baseline	MO	0.712674693	0.340332031	11.39086639
Baseline	MO	0.967368146	0.370361328	-14.00231728
Baseline	MO	0.881366243	0.38993454	-13.05169041
Baseline	MO	0.077348167	0.259857178	5.005861734
Baseline	MO	0.051440967	0.270263672	2.999243053
Baseline	MO	0.057846089	0.309947968	-2.876641028
Baseline	MO	0.059878207	0.240234375	-5.629884102
Baseline	MO	0.72674257	0.410400391	-8.839585513
PDCM	MO	0.013746946	0.230224609	2.456781815
PDCM	MO	-0.010788015	0.230224609	1.569723243
PDCM	MO	0.520578758	0.340332031	-8.231705349
PDCM	MO	1.178945117	0.380371094	-13.54059633
PDCM	MO	2.24656138	0.510498047	-17.2944262
PDCM	MO	0.033852169	0.230005264	3.431368821
PDCM	MO	0.385611105	0.4500103	8.516146055
PDCM	MO	0.00539575	0.210205078	-3.272693933
PDCM	MO	14.33169984	0.680664063	-57.52432317
PDCM	MO	0.027068739	0.220214844	2.998002758
PDCM	MO	0.626845465	0.270263672	15.26376579
PDCM	MO	-0.011878564	0.16015625	1.302050181
PDCM	MO	0.315178166	0.270263672	10.1774652
PDCM	MO	0.32626448	0.340332031	6.736694056
PDCM	MO	3.613930228	0.580566406	-22.05875588
PDCM	MO	0.041429488	0.3203125	2.712693876
PDCM	MO	-0.009077306	0.190185547	-2.276611652

Display	Motion	Error Severity [deg]	Error Duration [s]	Max Control Column Input [deg]
PDCM	MO	0.901911882	0.350341797	13.24029492
PDCM	MO	0.421355966	0.350341797	-8.80633017
PDCM	MO	0.000379967	0.230224609	-2.388788724
PDCM	MO	4.008170036	0.460449219	-35.83161584
PDCM	MO	0.036175727	0.190185547	-4.684216857
PDCM	MO	0.051858491	0.220214844	4.916242891
PDCM	MO	0.062209798	0.240234375	2.841370012
PDCM	MO	3.950272562	0.420410156	36.01498638
PDCM	MO	0.834535124	0.349941254	13.55728597
PDCM	MO	0.035318208	0.250244141	3.635588339

F

Analysis Error Severity

An error was defined as a roll input away from level flight after the AI presentation that caused the control column to exceed 1° of roll deflection. While all errors found, as shown in Table E.1 and Table E.2, fulfill this condition, many result in a very small error severity. From Figure F.1, F.2, F.3, and F.4, it can be seen that these small error severities are a result of a low error duration combined with a small control input.

Figure F.1: Regular AI as presented in SIMONA Research Simulator

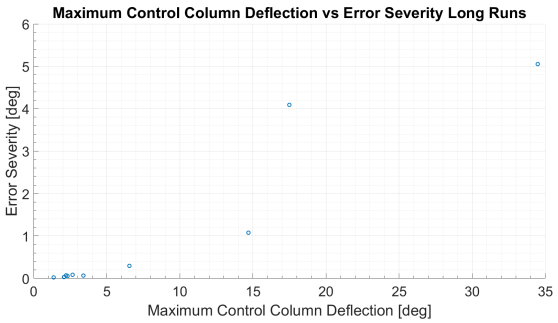

Figure F.2: Adapted AI as presented in SIMONA Research Simulator

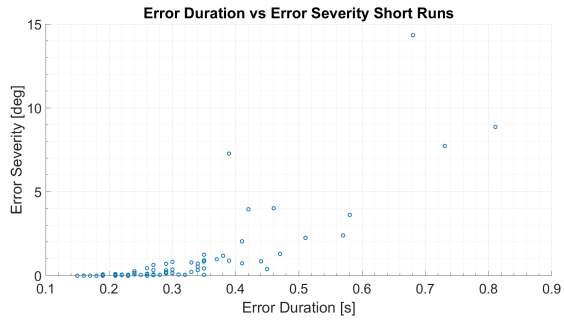

Figure F.3: Regular AI as presented in SIMONA Research Simulator

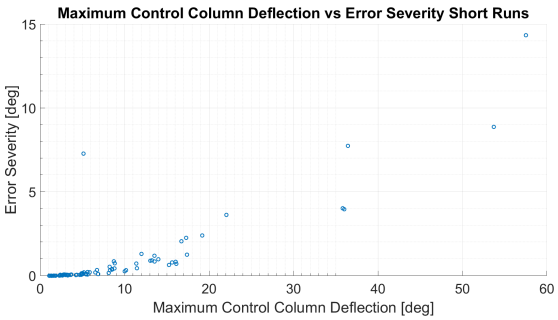

Figure F.4: Adapted AI as presented in SIMONA Research Simulator

Some of the errors are negative, which at first glance does not make sense. The autopilot is used to show a bank angle on the PFD. It controls the aircraft model which then influences what is shown on the PFD. The autopilot is set to be quite ”aggressive” to make sure the AI is not visibly moving anymore by the time the participant sees it. However, it is still slightly moving, which is also why the error severity is defined as the difference between the bank angle at the moment of the first input and the maximum bank angle after an incorrect control input is given. The autopilot first causes an overshoot in the bank angle and then returns. However, as it takes a bit of time for the aircraft model to respond to the input given, the autopilot is still slightly moving the aircraft model while a control input has already been given. If this control input is not large enough, the bank angle does not surpass the bank angle at the moment of the first input, which causes it to be negative. The decision was made to keep these errors in as they were still errors.

Figure F.5 shows what a run with a negative error severity looks like. The negative error severity is caused by the ”maximum” bank angle being smaller than the bank angle at first input. It is clear this participant

made an error since there is a second ”peak”, which is not present in the run without an error, as can be seen in Figure F.6.

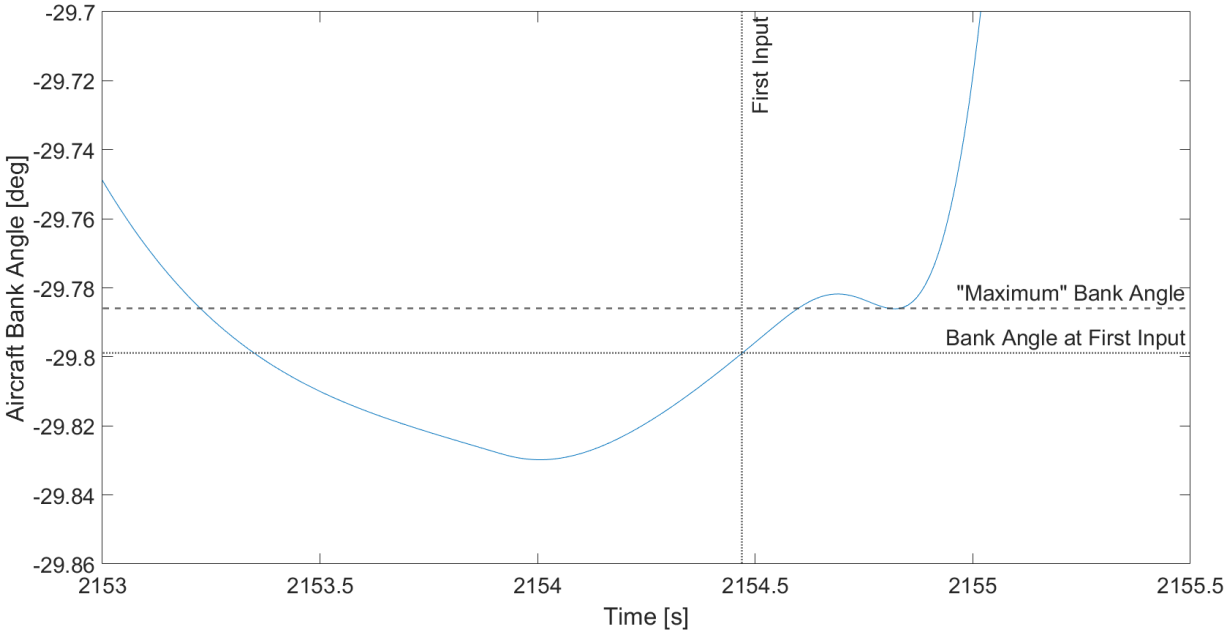

Figure F.5: Example of a run with a negative error severity

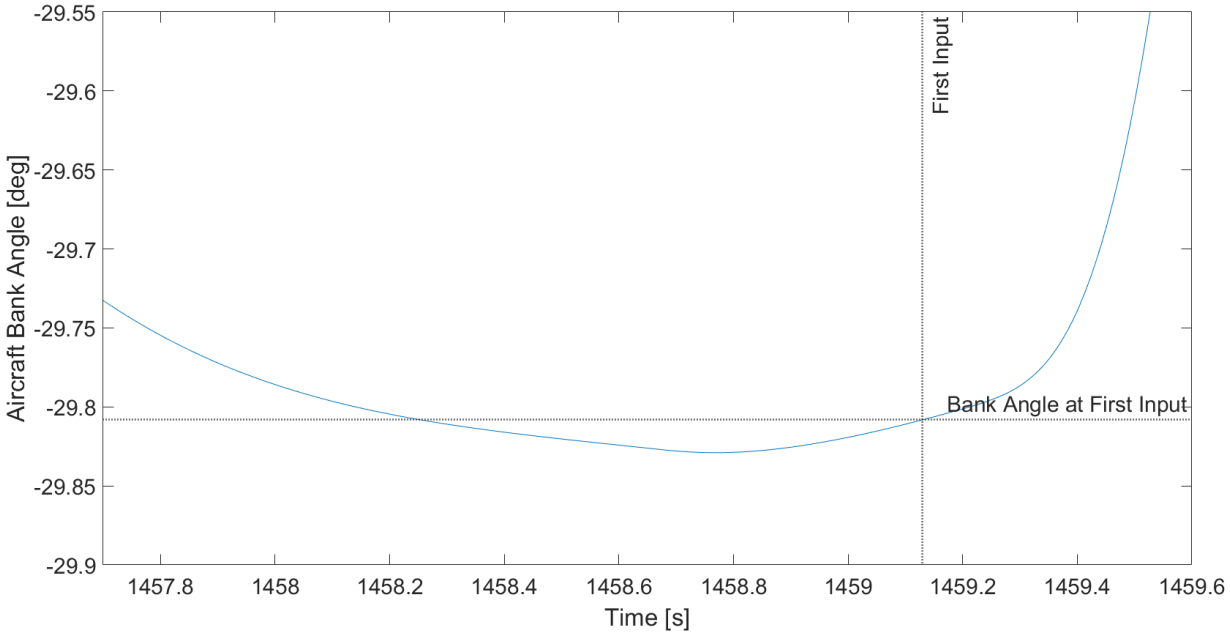

Figure F.6: Example of a run with no error

G

Influence of Age and Experience on Reaction Time

Participants ranged between the ages of 30 and 62, with experience between 2,500 and 22,500 flight hours. Figure G.1 and Figure G.2 show that neither age nor experience had an influence on a participant's average reaction time.

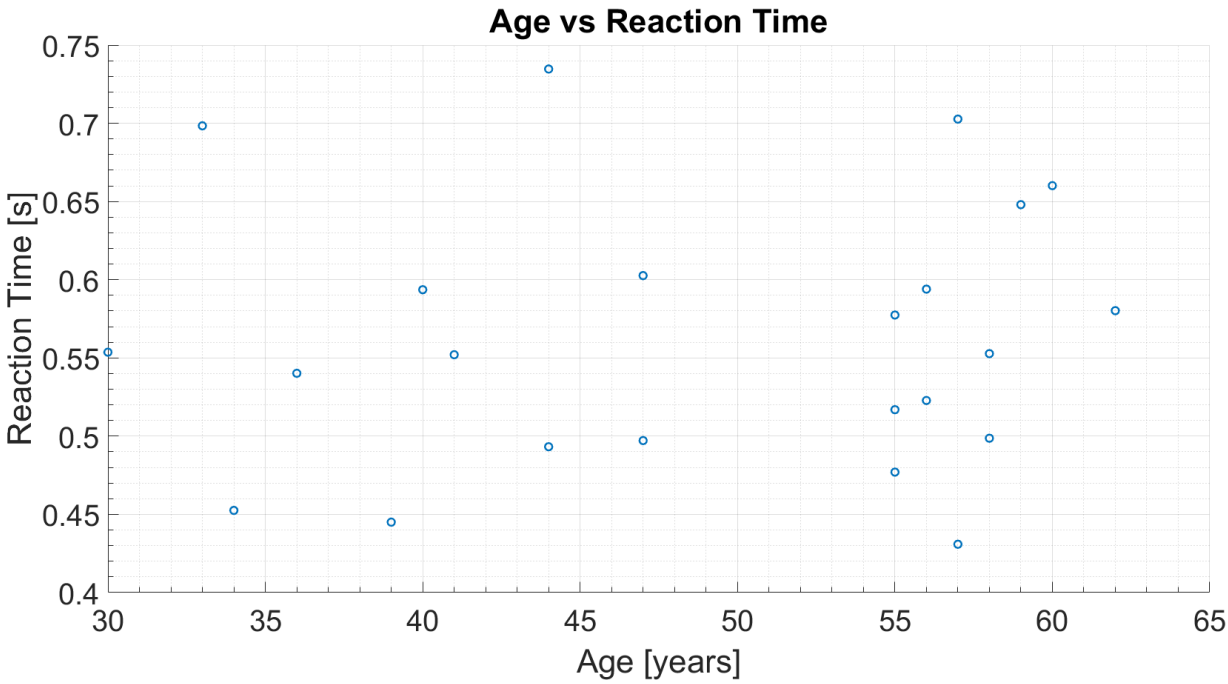

Figure G.1: Average reaction time of each participant compared to their age

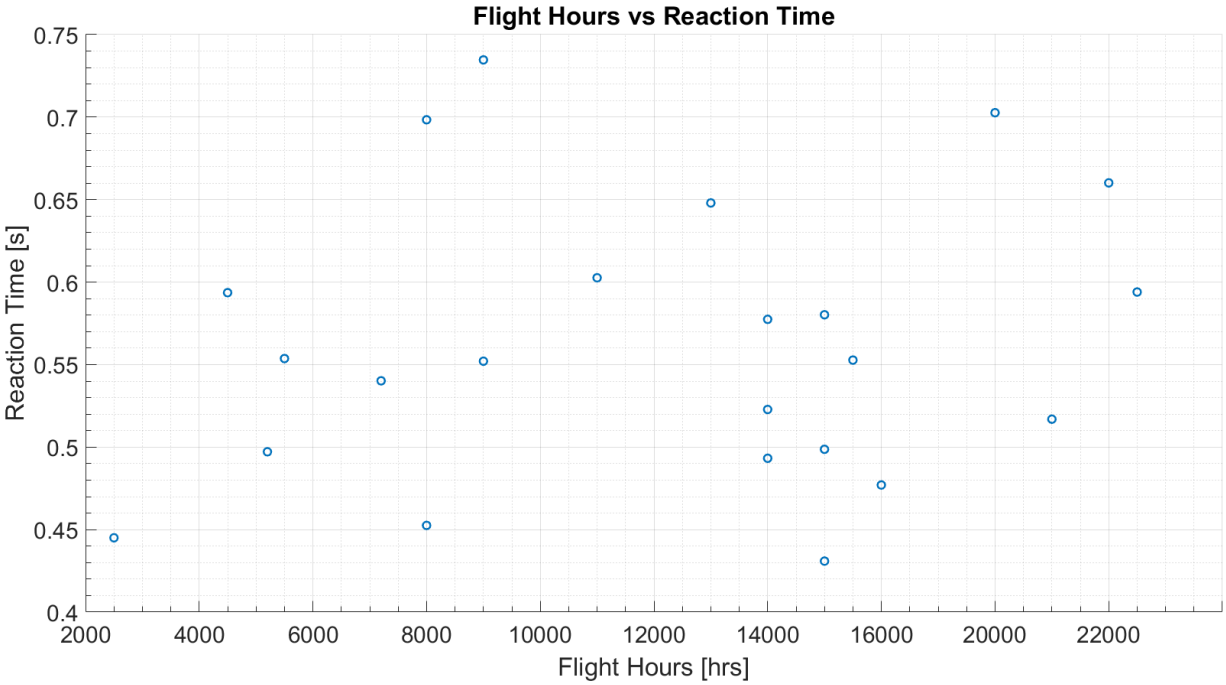

Figure G.2: Average reaction time of each participant compared to their experience

Modifications to PDCM AI

Figure H.1 shows the baseline and PDCM AIs used in the experiment.

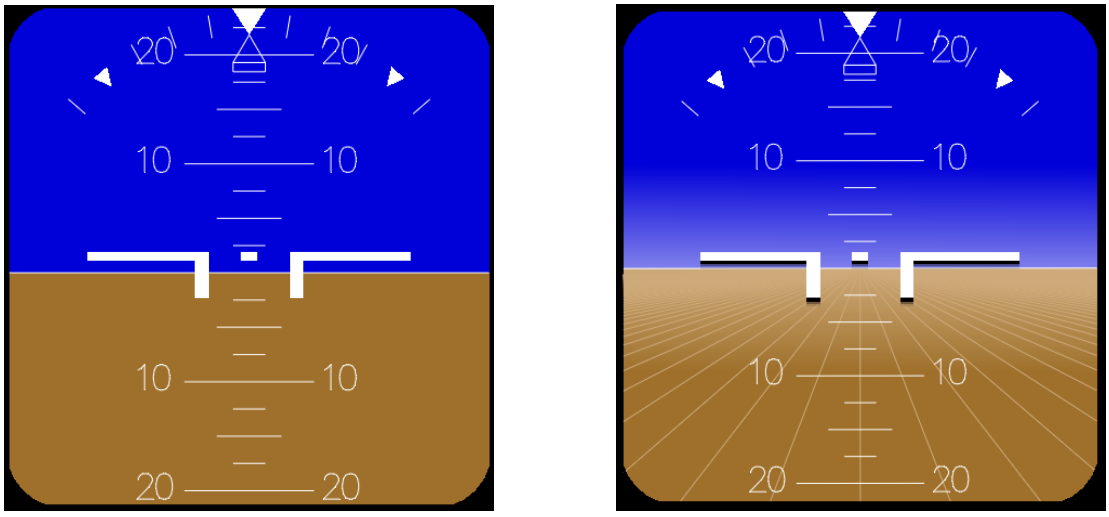

(a) Baseline AI **(b)** PDCM AI

Figure H.1: Attitude indicators used in the experiment

One of the main points of feedback given by participants was that the the modifications can add to the clutter of the PFD used in flight, which is much more cluttered than the baseline AI used in the experiment. To solve this issue, the linear perspective lines (and thus also the color gradient) could be changed to a color that is closer to the original ground color, as can be seen in Figure H.2.

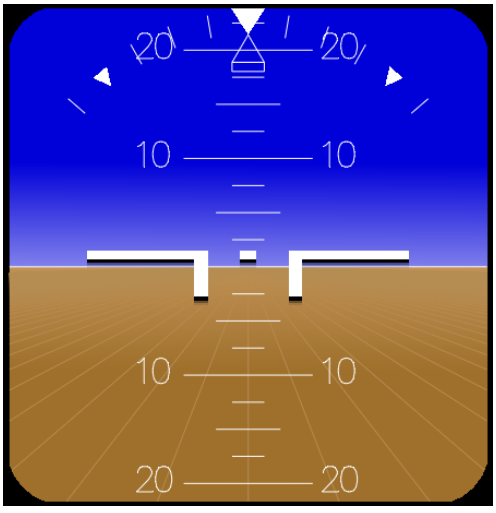

Figure H.2: PDCM AI with more subtle color gradient and converging lines

A second point of feedback was that, due to the shadow added below the aircraft symbol, the amount of pitch was harder to assess by only looking at the aircraft symbol. The shadow took away the blue color of the sky which is usually still visible below the aircraft symbol when the aircraft is pitching. This could be solved in two ways: One, applying a shadow only below the center of gravity symbol and the vertical bars of the aircraft symbol, as can be seen in Figure H.3. Two, make the shadow thinner and place it “on top” of the aircraft symbol instead of below it. Both options leave the same amount of sky visible below the horizontal bars of the aircraft symbol as with the baseline AI. The second option would be easier to apply to different aircraft symbol shapes and also looks more realistic.

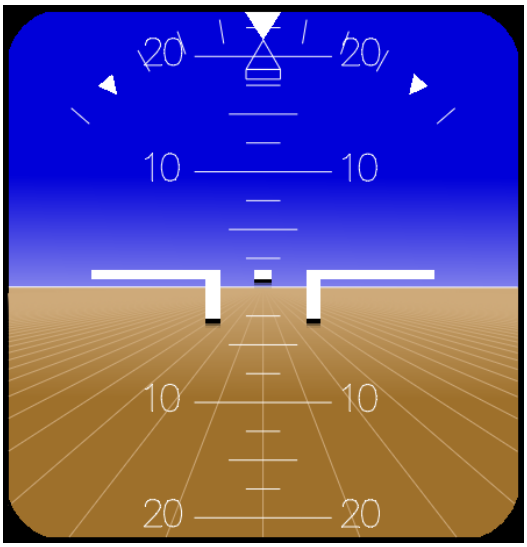

Figure H.3: PDCM AI with shadow only below center of gravity and vertical part of the aircraft symbol

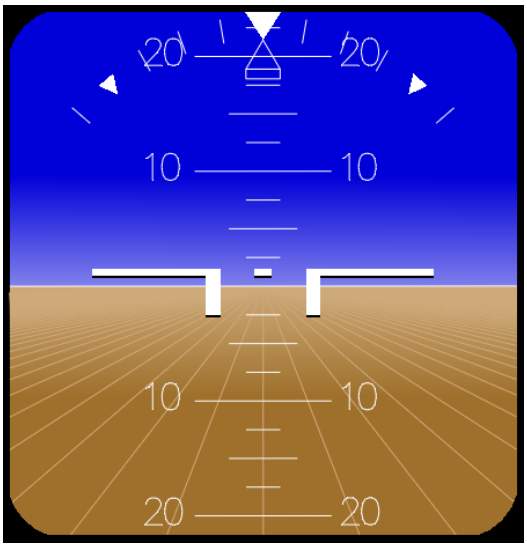

Figure H.4: PDCM AI with a smaller shadow that sits on top of aircraft symbol

Additional Information DUECA

I.1. Modifications to the AI

- To modify the AI, additional code was written in **attitude_indicator.cxx**, found in the following directory: *SDLeansPerception/SDLeansPerception/PFDB747*.
- To switch from the baseline AI to the modified version “stocks” are used. If these stocks end in “new”, they are used for the modified AI, e.g., m_att_stock1new
- Initially, the idea was to add a “window” around the AI, as can be seen in Figure I.1. The code for this is still present, part of it is in **attitude_indicator.cxx** and part of it in **pfd_frame.cxx**.

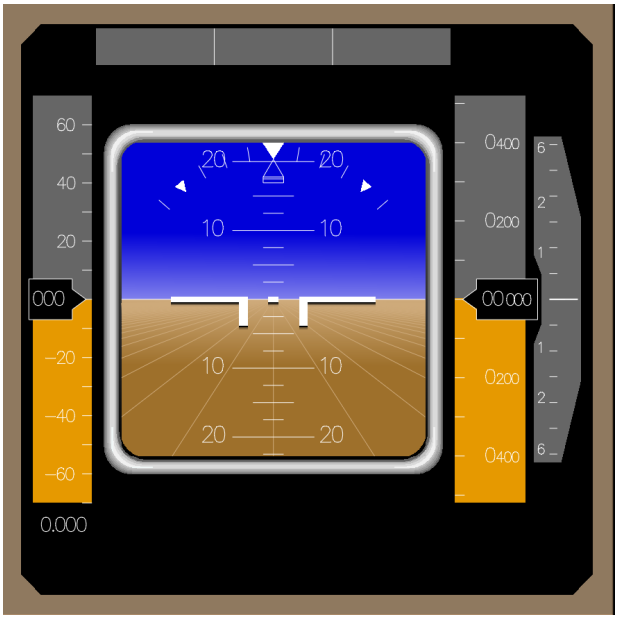

Figure I.1: PFD with window

I.2. The experiment conditions

- Usually, the aircraft model dictates the movements made by the simulator. However, in this experiment, this is overruled by the “motion confuser” to get the simulator in the correct position. When the motion confuser turns off, the pilot can take over the simulator’s motion again. The code for this is found in **MotionConfuser.cxx** (*SDLeansPerception/SDLeansPerception/MotionConfuser*).
- To choose which experiment condition should be run on the simulator, an ECI module is present (see Figure I.2). The settings for the ECI module are found in **ECIModule.cxx** (*SDLeansPerception/SDLeansPerception/ECI*)

I.3. Experiment procedure

To replicate the experiment used in this study and ensure everything works as intended, the following procedure should be followed:

I.3.1. Free flight

- While in *hold* in DUSIME, select Initial Flight Condition “TEST_SAVE_STATE.txt”
- Click Apply
- Click RESET to turn on outside visuals in the simulator
- Go to *advance* in DUSIME
- Click DISENGAGE switch in MCP737 **twice**. This ensures that the autopilot is turned off so that the pilot is flying the aircraft. Otherwise, the aircraft model will not react the same way as it will in the experiment.

I.3.2. Long runs

- Click DISENGAGE switch in MCP737. If you forget this, the autopilot disconnect warning will not produce noise.
- Click RESET
- Select the wanted scenario (left/right turn, normal/adapted AI, motion-matching/-opposite)
- Click Start Scenario
- Next run: click RESET **!IMPORTANT!***, select the wanted scenario, click Start Scenario

*Click RESET **BEFORE** starting the next long run. The RESET button is not only for turning on the outside visuals but also impacts the Motion Confuser. If you click RESET after you already started the run, the Motion Confuser will not be running and the simulator will not move the way you want it to but instead move like the aircraft model. If you already started the run, click RESET and click Start Scenario again.

I.3.3. Short Runs

- Select scenario (left/right turn, normal/adapted AI, short-matching/-opposite)
- Click Start Scenario
- Next run: select scenario, click Start Scenario (no need to click RESET between runs)

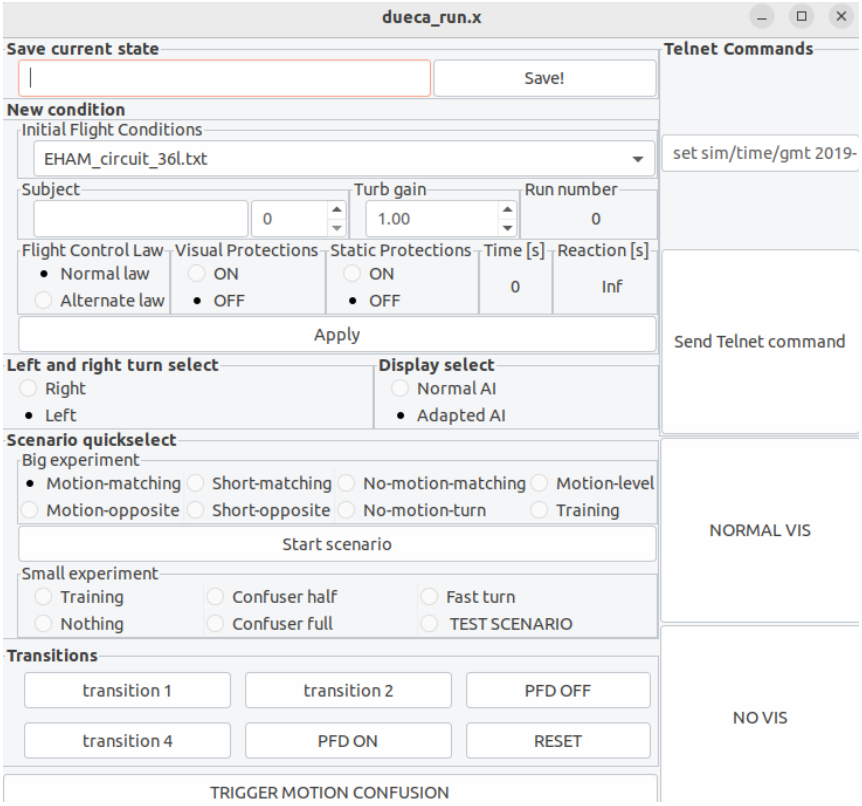

Figure I.2: ECI

J

Code Dependent Measures

```
% Import all files, use .mat files

filenames = {'Participant3', 'Participant3_1', 'Participant4' '
    Participant4_1', 'Participant5', 'Participant5_1', ...
              'Participant6', 'Participant6_1', 'Participant7', '
                 Participant7_1', 'Participant8', 'Participant8_1', ...
              'Participant9', 'Participant9_1', 'Participant10', '
                 Participant10_1', 'Participant11', 'Participant11_1', ...
              'Participant12', 'Participant12_1', 'Participant13', '
                 Participant13_1', 'Participant14', 'Participant14_1', ...
              'Participant15', 'Participant15_1', 'Participant16', '
                 Participant16_1', 'Participant17', 'Participant17_1', ...
              'Participant18', 'Participant18_1', 'Participant19', '
                 Participant19_1', 'Participant20', 'Participant20_1', ...
              'Participant21', 'Participant21_1', 'Participant22', '
                 Participant22_1', 'Participant23', 'Participant23_1', ...
              'Participant24', 'Participant24_1', 'Participant25', '
                 Participant25_1'};

% Start and end times of long and short runs for files where both are logged
    t_long_start = [390, NaN, 490, NaN, 600, NaN,...
                    410, NaN, 460, NaN, 800, NaN,...
                    380, NaN, 530, NaN, 350, NaN,...
                    480, NaN, 480, NaN, 410, NaN,...
                    480, NaN, 660, NaN, 600, NaN,...
                    480, NaN, 520, NaN, 400, NaN,...
                    400, NaN, 250, NaN, 360, NaN, ...
                    400, NaN, 430, NaN];
    t_long_end = [1150, NaN, 1250, NaN, 1280, NaN,...
                  1150, NaN, 1210, NaN, 1600, NaN,...
                  1150, NaN, 1320, NaN, 1100, NaN,...
                  1200, NaN, 1250, NaN, 1150, NaN,...
                  1240, NaN, 1450, NaN, 1350, NaN,...
                  1220, NaN, 1240, NaN, 1150, NaN,...
                  1130, NaN, 970, NaN, 1070, NaN,...
                  1120, NaN, 1170, NaN];
    t_short_start = [1290, 0, 1410, 0, 1450, 0,...
                     1300, 0, 1330, 0, 1760, 0,...
                     1280, 0, 1490, 0, 1250, 0,...
                     1360, 0, 1380, 0, 1280, 0,...
                     1360, 0, 1590, 0, 1490, 0,...
                     1370, 0, 1380, 0, 1300, 0,...
                     1270, 0, 1110, 0, 1210, 0,...
                     1260, 0, 1320, 0];

```

```
% Runs that need to be removed (incorrect motion or extra run), manually
% found by looking at the data

remove_long = {0, 0, [2, 5], 0, 1, 0,...
               0, 0, 0, 0, 5, 0,...
               0, 0, 2, 0, 0, 0,...
               0, 0, 0, 0, 0, 0,...
               0, 0, 0, 0, 0, 0,...
               0, 0, 0, 0, 0, 0,...
               0, 0, 0, 0, 0, 0,...
               0, 0, 0, 0};
remove_short = {0 [3, 18] 0 0 37 0,...
                9 0 0 0 0 0,...
                0 0 0 0 0 15,...
                0 19 0 0 0 0,...
                0 0 0 0 0 0,...
                0 0 0 0 0 0,...
                6 0 0 6 0 0,...
                0 0 0 0};

% Start of loop to get dependent measures
for pp=1:numel(filenames)
    tic;
    log.data = load(filenames{pp});
    log.data = log.data.log.data;   % Uncomment this after initial run
    elapsedTime = toc;
    %fprintf('Time elapsed for loading %s: %f seconds\n', filenames{pp},
        elapsedTime)

    % Save to a faster file format, only have to do this once to generate
    % the files
    %save(sprintf('%s.mat', filenames{pp}));

    log.timeStamp = log.data(:,1);
    log.sim_time = log.data(:,2);
    log.trigger = log.data(:,3);
    log.ux = log.data(:,4);
    log.uy = log.data(:,5);
    log.uz = log.data(:,6);
    log.uc = log.data(:,7);
    log.phi = log.data(:,8);
    log.theta = log.data(:,9);
    log.psi = log.data(:,10);
    log.p = log.data(:,11);
    log.q = log.data(:,12);
    log.r = log.data(:,13);
    log.der_p = log.data(:,14);
    log.der_q = log.data(:,15);
    log.der_r = log.data(:,16);
    log.fx_sim = log.data(:,17);
    log.fy_sim = log.data(:,18);
    log.fz_sim = log.data(:,19);
    log.xdotdot_sim = log.data(:,20);
    log.ydotdot_sim = log.data(:,21);
    log.zdotdot_sim = log.data(:,22);
    log.xdot_sim = log.data(:,23);
```

```
93      log.ydot_sim = log.data(:,24);
94      log.zdot_sim = log.data(:,25);
95      log.p_sim = log.data(:,26);
96      log.q_sim = log.data(:,27);
97      log.r_sim = log.data(:,28);
98      log.pfd_config = log.data(:,29);
99      log.motion_condition = log.data(:,30);
100     log.sanity = log.data(:,31);
101
102     log.ux_rad = log.ux/0.342719; %necessary due to column-roll-gain factor
103     log.ux_rad_dot = gradient(log.ux_rad); % column deflection RATE
104
105
106 %% Making distinction between long and short runs %%
107
108 % Moment PFD turns on %
109 [APdisc] = find(log.trigger == 1);
110 t_APdisc = log.sim_time(APdisc);
111
112 t_PFDonlong = [];
113 t_PFDonshort = [];
114 PFDonlong_idx = [];
115 PFDonshort_idx = [];
116
117 for i = 1:length(APdisc)
118     if (t_APdisc(i) > t_long_start(pp)) & (t_APdisc(i) < t_long_end(pp))
119         t_PFDonlong = [t_PFDonlong, t_APdisc(i) + 6];
120         PFDonlong_idx = [PFDonlong_idx, find(log.sim_time == t_APdisc(i))
               +600];
121     end
122 end
123
124 for j = 1:length(APdisc)
125    if (t_APdisc(j) > t_short_start(pp))
126        t_PFDonshort = [t_PFDonshort, t_APdisc(j) + 0.1];
127        PFDonshort_idx = [PFDonshort_idx, find(log.sim_time == t_APdisc(j))
              +10];
128     end
129 end
130
131 %% Dependent Measures %%
132
133 % Reaction time: time between PFD turning on and first moment control rate >
      0
134
135 % Error detection: control input > 1deg in wrong direction
136
137 % Error severity: difference bewteen bank angle when pilot first reacted
138 % (as this is what they "saw" when they responded, cannot use bank angle
139 % when PFD turned on because PFD was still very slightly moving when it
     turned on)
140
141 % Error duration: time between first reaction (when an error was made) and
     moment the direction of the input changes %
142
143 % Setting up control arrays %
```

```
beta = 300;
mini_control_array = [];
controlarrayinput1 = [];

%% Long Runs %%

% Moment of first control input %
firstinputs_globalidx_long = [];

% Reaction time %
t_firstreaction_long = [];
reactiontime_long = [];

% First input > 1deg %
firstinput1_globalidx_long = [];

% Error rate, severity and duration %
errors_long = [];
peakux_globalidx_long = [];
peakux_long = [];
t_peakux_long = [];
errorseverity_long = [];
errorduration_long = [];

for ii = 1:length(PFDonlong_idx)
    mini_control_array = log.ux_rad_dot(PFDonlong_idx(ii):PFDonlong_idx(ii)+
        beta);
    firstinputs_long = find(abs(mini_control_array) > 0, 1,'first');
    firstinputs_globalidx_long = [firstinputs_globalidx_long, PFDonlong_idx(
        ii) + firstinputs_long - 1];
    t_firstreaction_long = [t_firstreaction_long, log.sim_time(
        firstinputs_globalidx_long(ii))];
    reactiontime_long = [reactiontime_long, t_firstreaction_long(ii) -
        t_PFDonlong(ii)];
    reactiontime_long(reactiontime_long<0.1) = NaN; % Get rid of runs where
        pp reacted before PFD turned on
    controlarrayinput1 = rad2deg(log.ux_rad(PFDonlong_idx(ii):PFDonlong_idx(
        ii)+beta));
    firstinput1_long = find(abs(controlarrayinput1) > 1, 1,'first');
    firstinput1_globalidx_long = [firstinput1_globalidx_long, PFDonlong_idx(
        ii) + firstinput1_long - 1];
    if isnan(reactiontime_long) % No error detected when pp reacted before
        PFD turned on
        errors_long = [errors_long, NaN];
        peakux_globalidx_long = [peakux_globalidx_long, NaN];
        peakux_long = [peakux_long, NaN];
        t_peakux_long = [t_peakux_long, NaN];
        errorseverity_long = [errorseverity_long, NaN];
        errorduration_long = [errorduration_long, NaN];
    elseif any(cellfun(@(x)ismember(ii,x),remove_long(pp))) == 1 % Get rid
        of incorrect/extra runs (manually found), 0 when no runs to be
        removed, place somewhere else so reactiontime also removed
        reactiontime_long(ii) = NaN;
        errors_long = [errors_long, NaN];
        peakux_globalidx_long = [peakux_globalidx_long, NaN];
        peakux_long = [peakux_long, NaN];
```

```
190         t_peakux_long = [t_peakux_long, NaN];
191         errorseverity_long = [errorseverity_long, NaN];
192         errorduration_long = [errorduration_long, NaN];
193     elseif (rad2deg(log.phi(PFDonlong_idx(ii))) > 0) & (rad2deg(log.ux_rad(
            firstinput1_globalidx_long(ii))) < 0 ) % right bank error
194         errors_long = [errors_long, 1];
195         controlarrayerror = rad2deg(log.ux_rad_dot(
                firstinput1_globalidx_long(ii):firstinput1_globalidx_long(ii)+
                beta));
196         peakux_long_idx = find(controlarrayerror >= 0, 1, 'first');
197         peakux_globalidx_long = [peakux_globalidx_long,
                firstinput1_globalidx_long(ii) + peakux_long_idx - 1];
198         peakux_long = [peakux_long, rad2deg(log.ux_rad(peakux_globalidx_long
                (ii)))];
199         t_peakux_long = [t_peakux_long, log.sim_time(peakux_globalidx_long(
                ii))];
200         max_bank_long = max(abs(rad2deg(log.phi(firstinput1_globalidx_long(
                ii):firstinput1_globalidx_long(ii)+beta))));
201         errorseverity_long = [errorseverity_long, max_bank_long - abs(
                rad2deg(log.phi(firstinputs_globalidx_long(ii))))];
202         errorduration_long = [errorduration_long, t_peakux_long(ii) -
                t_firstreaction_long(ii)];
203     elseif (rad2deg(log.phi(PFDonlong_idx(ii))) < 0) & (rad2deg(log.ux_rad(
            firstinput1_globalidx_long(ii))) > 0 ) % left bank error
204         errors_long = [errors_long, 1];
205         controlarrayerror = rad2deg(log.ux_rad_dot(
                firstinput1_globalidx_long(ii):firstinput1_globalidx_long(ii)+
                beta));
206         peakux_long_idx = find(controlarrayerror <= 0, 1, 'first');
207         peakux_globalidx_long = [peakux_globalidx_long,
                firstinput1_globalidx_long(ii) + peakux_long_idx - 1];
208         peakux_long = [peakux_long, rad2deg(log.ux_rad(peakux_globalidx_long
                (ii)))];
209         t_peakux_long = [t_peakux_long, log.sim_time(peakux_globalidx_long(
                ii))];
210         max_bank_long = max(abs(rad2deg(log.phi(firstinput1_globalidx_long(
                ii):firstinput1_globalidx_long(ii)+beta))));
211         errorseverity_long = [errorseverity_long, max_bank_long - abs(
                rad2deg(log.phi(firstinputs_globalidx_long(ii))))];
212         errorduration_long = [errorduration_long, t_peakux_long(ii) -
                t_firstreaction_long(ii)];
213     else
214         errors_long = [errors_long, 0];
215         peakux_globalidx_long = [peakux_globalidx_long, NaN];
216         peakux_long = [peakux_long, NaN];
217         t_peakux_long = [t_peakux_long, NaN];
218         errorseverity_long = [errorseverity_long, NaN];
219         errorduration_long = [errorduration_long, NaN];
220     end
221 end
222
223 % Matching vs Opposite vs Normal vs Adapted %
224
225 reactiontime_long_match_norm = [];
226 reactiontime_long_match_adapt = [];
227 reactiontime_long_opp_norm = [];
```

```
reactiontime_long_opp_adapt = [];

errors_long_opp = [];
errors_long_match = [];
errors_long_match_norm = [];
errors_long_match_adapt = [];
errors_long_opp_norm = [];
errors_long_opp_adapt = [];

errorseverity_long_match_norm = [];
errorseverity_long_match_adapt = [];
errorseverity_long_opp_norm = [];
errorseverity_long_opp_adapt = [];

errorduration_long_match_norm = [];
errorduration_long_match_adapt = [];
errorduration_long_opp_norm = [];
errorduration_long_opp_adapt = [];

peakux_long_match_norm = [];
peakux_long_match_adapt = [];
peakux_long_opp_norm = [];
peakux_long_opp_adapt = [];

for a=1:length(firstinputs_globalidx_long)
    %{
    if (log.motion_condition(firstinputs_globalidx_long(a)) ~= 0.0)
        errors_long_opp = [errors_long_opp, errors_long(a)];
    elseif (log.motion_condition(firstinputs_globalidx_long(a)) == 0.0)
        errors_long_match = [errors_long_match, errors_long(a)];
    %}
    if (log.motion_condition(firstinputs_globalidx_long(a)) == 0.0) & (log.
       pfd_config(firstinputs_globalidx_long(a)) == 0.0)
        reactiontime_long_match_norm = [reactiontime_long_match_norm,
           reactiontime_long(a)];
        errors_long_match_norm = [errors_long_match_norm, errors_long(a)];
        errorseverity_long_match_norm = [errorseverity_long_match_norm,
           errorseverity_long(a)];
        errorduration_long_match_norm = [errorduration_long_match_norm,
           errorduration_long(a)];
        peakux_long_match_norm = [peakux_long_match_norm, peakux_long(a)];
    elseif (log.motion_condition(firstinputs_globalidx_long(a)) == 0.0) & (
       log.pfd_config(firstinputs_globalidx_long(a)) == 1.0)
        reactiontime_long_match_adapt = [reactiontime_long_match_adapt,
           reactiontime_long(a)];
        errors_long_match_adapt = [errors_long_match_adapt, errors_long(a)];
        errorseverity_long_match_adapt = [errorseverity_long_match_adapt,
           errorseverity_long(a)];
        errorduration_long_match_adapt = [errorduration_long_match_adapt,
           errorduration_long(a)];
        peakux_long_match_adapt = [peakux_long_match_adapt, peakux_long(a)];
    elseif (log.motion_condition(firstinputs_globalidx_long(a)) ~= 0.0) & (
       log.pfd_config(firstinputs_globalidx_long(a)) == 0.0)
        reactiontime_long_opp_norm = [reactiontime_long_opp_norm,
           reactiontime_long(a)];
        errors_long_opp_norm = [errors_long_opp_norm, errors_long(a)];
```

```
274         errorseverity_long_opp_norm = [errorseverity_long_opp_norm,
                errorseverity_long(a)];
275         errorduration_long_opp_norm = [errorduration_long_opp_norm,
                errorduration_long(a)];
276         peakux_long_opp_norm = [peakux_long_opp_norm, peakux_long(a)];
277     elseif (log.motion_condition(firstinputs_globalidx_long(a)) ~= 0.0) & (
            log.pfd_config(firstinputs_globalidx_long(a)) == 1.0)
278         reactiontime_long_opp_adapt = [reactiontime_long_opp_adapt,
                reactiontime_long(a)];
279         errors_long_opp_adapt = [errors_long_opp_adapt, errors_long(a)];
280         errorseverity_long_opp_adapt = [errorseverity_long_opp_adapt,
                errorseverity_long(a)];
281         errorduration_long_opp_adapt = [errorduration_long_opp_adapt,
                errorduration_long(a)];
282         peakux_long_opp_adapt = [peakux_long_opp_adapt, peakux_long(a)];
283     end
284 end
285
286 %% Short Runs %%
287
288 % Moment of first control input %
289 firstinputs_globalidx_short = [];
290
291 % Reaction time %
292 t_firstreaction_short = [];
293 reactiontime_short = [];
294
295 % First input > 1deg %
296 firstinput1_globalidx_short = [];
297
298 % Error rate, severity and duration %
299 errors_short = [];
300 peakux_globalidx_short = [];
301 peakux_short = [];
302 t_peakux_short = [];
303 errorseverity_short = [];
304 errorduration_short = [];
305
306 for jj = 1:length(PFDonshort_idx)
307     mini_control_array = log.ux_rad_dot(PFDonshort_idx(jj):PFDonshort_idx(jj
            )+beta);
308     firstinputs_short = find(abs(mini_control_array) > 0, 1,'first');
309     firstinputs_globalidx_short = [firstinputs_globalidx_short,
            PFDonshort_idx(jj) + firstinputs_short - 1];
310     t_firstreaction_short = [t_firstreaction_short, log.sim_time(
            firstinputs_globalidx_short(jj))];
311     reactiontime_short = [reactiontime_short, t_firstreaction_short(jj) -
            t_PFDonshort(jj)];
312     reactiontime_short(reactiontime_short<0.1) = NaN; % Get rid of runs
            where pp reacted before PFD turned on
313     controlarrayinput1 = rad2deg(log.ux_rad(PFDonshort_idx(jj):
            PFDonshort_idx(jj)+beta));
314     firstinput1_short = find(abs(controlarrayinput1) > 1, 1,'first');
315     firstinput1_globalidx_short = [firstinput1_globalidx_short,
            PFDonshort_idx(jj) + firstinput1_short - 1];
```

```
316     if isnan(reactiontime_short) % No error detected when pp reacted before
            PFD turned on
317         errors_short = [errors_short, NaN];
318         peakux_globalidx_short = [peakux_globalidx_short, NaN];
319         peakux_short = [peakux_short, NaN];
320         t_peakux_short = [t_peakux_short, NaN];
321         errorseverity_short = [errorseverity_short, NaN];
322         errorduration_short = [errorduration_short, NaN];
323     elseif any(cellfun(@(x)ismember(jj,x),remove_short(pp))) == 1 % Get rid
            of incorrect/extra runs (manually found), 0 when no runs to be
            removed
324         reactiontime_short(jj) = NaN;
325         errors_short = [errors_short, NaN];
326         peakux_globalidx_short = [peakux_globalidx_short, NaN];
327         peakux_short = [peakux_short, NaN];
328         t_peakux_short = [t_peakux_short, NaN];
329         errorseverity_short = [errorseverity_short, NaN];
330         errorduration_short = [errorduration_short, NaN];
331     elseif (rad2deg(log.phi(PFDonshort_idx(jj))) > 0) & (rad2deg(log.ux_rad(
            firstinput1_globalidx_short(jj))) < 0 ) % right bank error
332         errors_short = [errors_short, 1];
333         controlarrayerror = rad2deg(log.ux_rad_dot(
                firstinput1_globalidx_short(jj):firstinput1_globalidx_short(jj)+
                beta));
334         peakux_short_idx = find(controlarrayerror >= 0, 1, 'first');
335         peakux_globalidx_short = [peakux_globalidx_short,
                firstinput1_globalidx_short(jj) + peakux_short_idx - 1];
336         peakux_short = [peakux_short, rad2deg(log.ux_rad(
                peakux_globalidx_short(jj)))];
337         t_peakux_short = [t_peakux_short, log.sim_time(
                peakux_globalidx_short(jj))];
338         max_bank_short = max(abs(rad2deg(log.phi(firstinput1_globalidx_short
                (jj):firstinput1_globalidx_short(jj)+beta))));
339         errorseverity_short = [errorseverity_short, max_bank_short - abs(
                rad2deg(log.phi(firstinputs_globalidx_short(jj))))];
340         errorduration_short = [errorduration_short, t_peakux_short(jj) -
                t_firstreaction_short(jj)];
341     elseif (rad2deg(log.phi(PFDonshort_idx(jj))) < 0) & (rad2deg(log.ux_rad(
            firstinput1_globalidx_short(jj))) > 0 ) % left bank error
342         errors_short = [errors_short, 1];
343         controlarrayerror = rad2deg(log.ux_rad_dot(
                firstinput1_globalidx_short(jj):firstinput1_globalidx_short(jj)+
                beta));
344         peakux_short_idx = find(controlarrayerror <= 0, 1, 'first');
345         peakux_globalidx_short = [peakux_globalidx_short,
                firstinput1_globalidx_short(jj) + peakux_short_idx - 1];
346         peakux_short = [peakux_short, rad2deg(log.ux_rad(
                peakux_globalidx_short(jj)))];
347         t_peakux_short = [t_peakux_short, log.sim_time(
                peakux_globalidx_short(jj))];
348         max_bank_short = max(abs(rad2deg(log.phi(firstinput1_globalidx_short
                (jj):firstinput1_globalidx_short(jj)+beta))));
349         errorseverity_short = [errorseverity_short, max_bank_short - abs(
                rad2deg(log.phi(firstinputs_globalidx_short(jj))))];
350         errorduration_short = [errorduration_short, t_peakux_short(jj) -
                t_firstreaction_short(jj)];
```

```
    else
        errors_short = [errors_short, 0];
        peakux_globalidx_short = [peakux_globalidx_short, NaN];
        peakux_short = [peakux_short, NaN];
        t_peakux_short = [t_peakux_short, NaN];
        errorseverity_short = [errorseverity_short, NaN];
        errorduration_short = [errorduration_short, NaN];
    end
end

% Matching vs opposite vs normal vs adapted %

reactiontime_short_match_norm = [];
reactiontime_short_match_adapt = [];
reactiontime_short_opp_norm = [];
reactiontime_short_opp_adapt = [];

errors_short_opp = [];
errors_short_match = [];
errors_short_match_norm = [];
errors_short_match_adapt = [];
errors_short_opp_norm = [];
errors_short_opp_adapt = [];

errorseverity_short_match_norm = [];
errorseverity_short_match_adapt = [];
errorseverity_short_opp_norm = [];
errorseverity_short_opp_adapt = [];

errorduration_short_match_norm = [];
errorduration_short_match_adapt = [];
errorduration_short_opp_norm = [];
errorduration_short_opp_adapt = [];

peakux_short_match_norm = [];
peakux_short_match_adapt = [];
peakux_short_opp_norm = [];
peakux_short_opp_adapt = [];

for b=1:length(firstinputs_globalidx_short)
    %{
    % Uncomment for only opposite and matching motion
    if (log.motion_condition(firstinputs_globalidx_short(b)) ~= 12.0)
        errors_short_opp = [errors_short_opp, errors_short(b)];
    elseif (log.motion_condition(firstinputs_globalidx_short(b)) == 12.0)
        errors_short_match = [errors_short_match, errors_short(b)];
    %}
    if (log.motion_condition(firstinputs_globalidx_short(b)) == 12.0) & (log
        .pfd_config(firstinputs_globalidx_short(b)) == 0.0)
        reactiontime_short_match_norm = [reactiontime_short_match_norm,
            reactiontime_short(b)];
        errors_short_match_norm = [errors_short_match_norm, errors_short(b)
            ];
        errorseverity_short_match_norm = [errorseverity_short_match_norm,
            errorseverity_short(b)];
```

```
402         errorduration_short_match_norm = [errorduration_short_match_norm,
                errorduration_short(b)];
403         peakux_short_match_norm = [peakux_short_match_norm, peakux_short(b)
                ];
404     elseif (log.motion_condition(firstinputs_globalidx_short(b)) == 12.0) &
            (log.pfd_config(firstinputs_globalidx_short(b)) == 1.0)
405         reactiontime_short_match_adapt = [reactiontime_short_match_adapt,
                reactiontime_short(b)];
406         errors_short_match_adapt = [errors_short_match_adapt, errors_short(b
                )];
407         errorseverity_short_match_adapt = [errorseverity_short_match_adapt,
                errorseverity_short(b)];
408         errorduration_short_match_adapt = [errorduration_short_match_adapt,
                errorduration_short(b)];
409         peakux_short_match_adapt = [peakux_short_match_adapt, peakux_short(b
                )];
410     elseif (log.motion_condition(firstinputs_globalidx_short(b)) ~= 12.0) &
            (log.pfd_config(firstinputs_globalidx_short(b)) == 0.0)
411         reactiontime_short_opp_norm = [reactiontime_short_opp_norm,
                reactiontime_short(b)];
412         errors_short_opp_norm = [errors_short_opp_norm, errors_short(b)];
413         errorseverity_short_opp_norm = [errorseverity_short_opp_norm,
                errorseverity_short(b)];
414         errorduration_short_opp_norm = [errorduration_short_opp_norm,
                errorduration_short(b)];
415         peakux_short_opp_norm = [peakux_short_opp_norm, peakux_short(b)];
416     elseif (log.motion_condition(firstinputs_globalidx_short(b)) ~= 12.0) &
            (log.pfd_config(firstinputs_globalidx_short(b)) == 1.0)
417         reactiontime_short_opp_adapt = [reactiontime_short_opp_adapt,
                reactiontime_short(b)];
418         errors_short_opp_adapt = [errors_short_opp_adapt, errors_short(b)];
419         errorseverity_short_opp_adapt = [errorseverity_short_opp_adapt,
                errorseverity_short(b)];
420         errorduration_short_opp_adapt = [errorduration_short_opp_adapt,
                errorduration_short(b)];
421         peakux_short_opp_adapt = [peakux_short_opp_adapt, peakux_short(b)];
422     end
423 end
424
425 %% Saving dependent measures
426 % Turn rows into colums, easier to plug into excel
427
428 reactiontime_long = reactiontime_long.';
429 errors_long = errors_long.';
430 errorseverity_long = errorseverity_long.';
431 errorduration_long = errorduration_long.';
432 peakux_long = peakux_long.';
433
434 reactiontime_long_match_norm = reactiontime_long_match_norm.';
435 reactiontime_long_match_adapt = reactiontime_long_match_adapt.';
436 reactiontime_long_opp_norm = reactiontime_long_opp_norm.';
437 reactiontime_long_opp_adapt = reactiontime_long_opp_adapt.';
438
439 errors_long_match_norm = errors_long_match_norm.';
440 errors_long_match_adapt = errors_long_match_adapt.';
441 errors_long_opp_norm = errors_long_opp_norm.';
```

```
442 errors_long_opp_adapt = errors_long_opp_adapt.';
443
444 errorseverity_long_match_norm = errorseverity_long_match_norm.';
445 errorseverity_long_match_adapt = errorseverity_long_match_adapt.';
446 errorseverity_long_opp_norm = errorseverity_long_opp_norm.';
447 errorseverity_long_opp_adapt = errorseverity_long_opp_adapt.';
448
449 errorduration_long_match_norm = errorduration_long_match_norm.';
450 errorduration_long_match_adapt = errorduration_long_match_adapt.';
451 errorduration_long_opp_norm = errorduration_long_opp_norm.';
452 errorduration_long_opp_adapt = errorduration_long_opp_adapt.';
453
454 peakux_long_match_norm = peakux_long_match_norm.';
455 peakux_long_match_adapt = peakux_long_match_adapt.';
456 peakux_long_opp_norm = peakux_long_opp_norm.';
457 peakux_long_opp_adapt = peakux_long_opp_adapt.';
458
459
460 reactiontime_short = reactiontime_short.';
461 errors_short = errors_short.';
462 errorseverity_short = errorseverity_short.';
463 errorduration_short = errorduration_short.';
464 peakux_short = peakux_short.';
465
466 reactiontime_short_match_norm = reactiontime_short_match_norm.';
467 reactiontime_short_match_adapt = reactiontime_short_match_adapt.';
468 reactiontime_short_opp_norm = reactiontime_short_opp_norm.';
469 reactiontime_short_opp_adapt = reactiontime_short_opp_adapt.';
470
471 errors_short_match_norm = errors_short_match_norm.';
472 errors_short_match_adapt = errors_short_match_adapt.';
473 errors_short_opp_norm = errors_short_opp_norm.';
474 errors_short_opp_adapt = errors_short_opp_adapt.';
475
476 errorseverity_short_match_norm = errorseverity_short_match_norm.';
477 errorseverity_short_match_adapt = errorseverity_short_match_adapt.';
478 errorseverity_short_opp_norm = errorseverity_short_opp_norm.';
479 errorseverity_short_opp_adapt = errorseverity_short_opp_adapt.';
480
481 errorduration_short_match_norm = errorduration_short_match_norm.';
482 errorduration_short_match_adapt = errorduration_short_match_adapt.';
483 errorduration_short_opp_norm = errorduration_short_opp_norm.';
484 errorduration_short_opp_adapt = errorduration_short_opp_adapt.';
485
486 peakux_short_match_norm = peakux_short_match_norm.';
487 peakux_short_match_adapt = peakux_short_match_adapt.';
488 peakux_short_opp_norm = peakux_short_opp_norm.';
489 peakux_short_opp_adapt = peakux_short_opp_adapt.';
490
491 % Save dependent measures after each for loop
492 save(['DM','_', filenames{pp}, '.mat'], "reactiontime*", "error*","peakux*")
493
494 end
```